DESIGN AND ANALYSIS OF EBG-BASED LOW-PROFILE MICROSTRIP ANTENNAS FOR WIRELESS COMMUNICATIONS

BY

FAHAD AHMED AL-KHURAISH

A Thesis Presented to the
DEANSHIP OF GRADUATE STUDIES

KING FAHD UNIVERSITY OF PETROLEUM & MINERALS

DHAHRAN, SAUDI ARABIA

In Partial Fulfillment of the
Requirements for the Degree of

MASTER OF SCIENCE

In

ELECTRICAL ENGINEERING

09 JUNE, 2010

KING FAHD UNIVERSITY OF PETROLEUM & MINERALS

DHAHRAN 31261, SAUDIA ARABIA

DEANSHIP OF GRADUATE STUDIES

This thesis written by:

FAHAD AHMED AL-KHURAISH

Under the supervision of his thesis Advisor and approved by his thesis Committee, has been presented to and accepted by the Dean of Graduate Studies, in partial fulfillment of the requirements for the degree of

MASTER OF SCIENCE IN ELECTRICAL ENGINEERING

Thesis Committee

Dr. Mohammed A. Alsunaidi (Chairman)

Dr. Ahmad M. Yamani (Member)

Sheikh Shariff Iqbal

Dr. Sheikh S. Iqbal (Member)

Dr. Samir H. Abdul-Jauwad
Department Chairman

Dr. Salam A. Zumoo
Dean of Graduate Studies
Date:

I would like to dedicate my thesis to

My Parents,

My Family

&

My Teachers

ACKNOWLEDGMENT

"**Knowledge and ability are power**", I do thank Allah Almighty for giving me the knowledge as well as the ability to complete this work.

"**Support and guidance are successful factors**", I would like to thank also my advisor for his guidance, patience and dedication throughout my master. The considerable amount of time he dedicated for this work is greatly appreciated and I do ask Allah to reward him for this. I would like to thank my thesis committee members for their advice and support to have this work done.

"**Encouragement and motivation are fuel**", I am also grateful and thankful to my parents, my wife, my brothers and sisters who encouraged and motivated me throughout this work. Without their support, I would not have been able to complete my work.

TABLE OF CONTENTS

ACKNOWLEDGMENT IV
LIST OF FIGURES ..... VI.
LIST OF TABLES ..... XI.
THESIS ABSTRACT (ENGLISH) ..... XII.
THESIS ABSTRACT (ARABIC) ..... XIII.
CHAPTER 1 1
INTRODUCTION 1
1.1 MICROSTRIP ANTENNAS 1
1.2 ELECTROMAGNETIC BAND GAP (EBG) 3
1.3 NUMERICAL TECHNIQUES 5
1.3.1 METHOD OF MOMENT (MOM) 5
1.3.2 FINITE ELEMENT METHOD (FEM) 6
1.3.3 FINITE DIFFERENCE TIME DOMIN (FDTD) METHOD 6
1.4 THESIS OBJECTIVES 10
1.5 THESIS ORGANIZATION 11
CHAPTER 2 12
APPLYING EBG CONCPET IN MICROSTRIP ANTENNAS 12
2.1 LITERATURE REVIEW 12
2.2 DERIVATION OF THE THEORETICAL MODEL 13
CHAPTER 3 24
THE FINITE DIFFERENCE TIME DOMAIN (FDTD) METHOD 24
3.1 INTRODUCTION TO FDTD METHOD 24
3.2 ABSORBING BOUNDARY CONDITIONS: THE PML 29
3.3 NUMERICAL DISPERSION AND STABILITY 34
3.4 PARAMETERS CALCUATIONS 35
CHAPTER 4 41
SIMULATION RESULTS OF EBG-BASED ANTENNA STRUCTURES 41
4.1 EBG ON GROUND PLANE RESULTS 41
4.2 EBG ON PATCH RESULTS 51
4.3 OBSERVATIONS 54
CHAPTER 5 69
ANALYSIS OF PROPOSED ANTENNAS MODELS 69
5.1 FDTD SOLUTIONS 69
5.2 EXPERIMENTAL RESULTS 84
CHAPTER 6 93
CONCLUSION AND FUTURE WORK 93
6.1 SUMMARY AND CONCLUSION 93
6.2 FUTURE WORK 94
REFERENCES 95
VITAE 101

LIST OF FIGURES

Figure 1.1 : A rectangular microstrip (patch) antenna 2

Figure 1.2: EBG construction for one (1-D) or more dimensions (2-D & 3-D)....4

Figure 1.3: EBG periodic in one direction (one dimension).....5

Figure 1.4: Needed memory size and CPU solution time for three numerical methods 7

Figure 2.1: (a) 4 elements of Mushroom like EBG (MEG) structure and (b) overall structure of Mushroom like EBG (MEBG) structure with feeding network [23] 14

Figure 2.2: (a) 4 elements of slotted patch EBG (SPEBG) structure and (b) overall structure of slotted patch EBG (SPEBG) structure with feeding network [4] 15

Figure 2.3: A 2 by 2 microstrip array antenna with and without the modified slotted patch EBG [4] 16

Figure 2.4: (a) slot loaded EBG structure and (b) A low profile antenna over a finite EBG ground plane [24] 16

Figure 2.5: The dumbbell like EBG [34] 17

Figure 2.6: Flow of current and equivalent circuit model for dumbbell like EBG [34].....17

Figure 2.7: (a) Configuration of the fork-like EBG (b) Details of one unit of the fork-like EBG lattice [26] 18

Figure 2.8: Configuration of the F-like EBG structure [32].....18

Figure 2.9: Geometry of the proposed EBG backed antenna [30] 19

Figure 2.10: Prospective view of spiral-fan shaped EBG [22] 19

Figure 2.11: Topologies of SRR configurations and their equivalent circuits models [34] 20

Figure 2.12: Topologies of different SRR configurations and their equivalent circuits for the topologies are depicted in the second column, while the circuit models for the complementary counterparts are represented in the third columns

[34] 20
Figure 2.13: (a) lumped-element equivalent circuit for the basic cell of the SRR loaded transmission line. (b) Simplified circuit with series branch replaced by its equivalent impedance [35] 21
Figure 2.14: Layout of the fabricated SRR loaded structure [35].....21
Figure 2.15: The geometry configuration of the individual SRR, and the electric charge and current distribution in it as well as the individual SRR equivalent circuit model [35].....21
Figure 3.1: Space-time chart of the Yee algorithm for a one-dimensional wave propagation 25
Figure 3.2: Unit cell of Yee's mesh positioning of various field components 26
Figure 3.3: Transverse Electric (TE) case 31
Figure 3.4: The PML technique Frame [42].....33
Figure 3.5: Excitation Input Voltage as a Gaussian pulse 36
Figure 3.6: Transient current for the basic patch antenna 37
Figure 3.7: Transient voltage for the basic patch antenna 37
Figure 3.8: Frequency response for input impedance (real) for the basic patch antenna 39
Figure 3.9: Frequency response for input impedance (imaginary) for the basic patch antenna 39
Figure 3.10: Frequency response for S_{11} Parameter for the basic patch antenna 40
Figure 4.1: Patch antenna basic design as a reference layout 42
Figure 4.2: Patch antenna basic design as a reference layout S_{11} Parameter 42
Figure 4.3: Patch antenna EBG case 1 layout 43
Figure 4.4: Patch antenna EBG case 1 S_{11} parameter 43
Figure 4.5: Patch antenna EBG case 2 layout 44
Figure 4.6: Patch antenna EBG case 2 S_{11} parameter 44
Figure 4.7 Patch antenna EBG case 3 layout 45

Figure 4.8 Patch antenna EBG case 3 S_{11} parameter 45
Figure 4.9: Patch antenna EBG case 4 layout 46
Figure 4.10 Patch antenna EBG case 4 S_{11} parameter 46
Figure 4.11: Patch antenna EBG case 5 layout 47
Figure 4.12: Patch antenna EBG case 5 S_{11} parameter.....47
Figure 4.13: Patch antenna EBG case 6 layout 48
Figure 4.14: Patch antenna EBG case 6 S_{11} parameter 48
Figure 4.15: Patch antenna EBG case 7 layout. 49
Figure 4.16: Patch antenna EBG case 7 S_{11} parameter 49
Figure 4.17: Patch antenna EBG case 8 layout 50
Figure 4.18: Patch antenna EBG case 8 S_{11} parameter 50
Figure 4.19: Patch antenna EBG case 9 layout 51
Figure 4.20: Patch antenna EBG case 9 S_{11} parameter 51
Figure 4.21: Patch antenna EBG case 10 layout 52
Figure 4.22: Patch antenna EBG case 10 S11 parameter 52
Figure 4.23: Patch antenna EBG case 11 layout.....53
Figure 4.24: Patch antenna EBG case 11 S_{11} parameter 53
Figure 4.25: Patch antenna EBG case 12 layout 53
Figure 4.26: Patch antenna EBG case 12 S_{11} parameter 54
Figure 4.27: New basic design Patch antenna layout 55
Figure 4.28: New Patch antenna design S_{11} parameter 56
Figure 4.29: Patch antenna EBG case 13 S_{11} layout 56
Figure 4.30: Patch antenna EBG case 13 S_{11} parameter 57
Figure 4.31: Patch antenna EBG case 14 S_{11} layout 57
Figure 4.32: Patch antenna EBG case 14 S_{11} parameter 58
Figure 4.33: Patch antenna EBG case 15 S_{11} layout 58
Figure 4.34: Patch antenna EBG case 15 S_{11} parameter 59
Figure 4.35: Patch antenna EBG case 16 S_{11} layout 59
Figure 4.36: Patch antenna EBG case 16 S_{11} parameter 60

Figure 4.37: Patch antenna EBG case 16 S_{11} parameter 61

Figure 4.38: S_{11} parameter for new patch antenna reference design 62

Figure 4.39: S_{11} parameter for the reference design with step size 0.95 mm 63

Figure 4.40: S_{11} parameter for the reference design with step size 0.85 mm 63

Figure 4.41: S_{11} parameter for the reference design with step size 0.78 mm 64

Figure 4.42: S_{11} parameter for the reference design with step size 0.75 mm 64

Figure 4.43: S_{11} parameter for the reference design with step size 0.72 mm 65

Figure 4.44: S_{11} parameter for the reference design with step size 0.70 mm 65

Figure 4.45: S_{11} parameter for the reference design with step size 0.65 mm 66

Figure 4.46: S_{11} parameter for the reference design with step size 0.60 mm 66

Figure 5.1: Basic Patch Antenna without EBG 70

Figure 5.2: Reference Structure without EBG S11 Parameter 70

Figure 5.3: Patch Antenna with EBG (SRR on the patch).....71

Figure 5.4: Reference Structure with EBG (SRR only).....72

Figure 5.5: Design No.1, Patch Antenna with EBG (a) Top view and (b) Bottom View 73

Figure 5.6: Design No. 1 S11 Parameter 74

Figure 5.7: Design No. 2, Patch Antenna with EBG (a) Top View and (b) Bottom View 75

Figure 5.8: Design No. 2 S11 Parameter 76

Figure 5.9: Design No. 3, Patch Antenna with EBG (a) Top View and (b) Bottom View 77

Figure 5.10: Design No. 3 S11 Parameter 78
Figure 5.11: Design No.4, Patch Antenna with EBG (a) Top View and (b) Bottom View 79
Figure 5.12: Design No. 4 S11 Parameter 80
Figure 5.13: Design No.5, Patch Antenna with EBG (a) Top View and (b) Bottom View 81
Figure 5.14: Design No. 5 S11 Parameter 82
Figure 5.15: Fabricated patch antenna before SRR and EBG etching (a) Top view and (b) Bottom view.....85
Figure 5.16: Experimental result of structure has neither SRR nor EBG on the ground plane 86
Figure 5.17: Theoretical & Experimental results of structure has neither SRR nor EBG on the ground plane.....87
Figure 5.18: Etched SRR only on the fabricated patch antenna without EBG on the ground plane (a) Top view and (b) Bottom view.....88
Figure 5.19: Theoretical & Experimental results of structure that has only SRR. 89
Figure 5.20: Etched antenna with SRR and EBG on the ground plane (a) Top view and (b) Bottom view. 90
Figure 5.21: Theoretical & Experimental result of structure having both SRR as well as EBG on the ground plane.....91
Figure 5.22: The Azimuthal radiation pattern (H plane) – Dashed line for structure without SRR and EBG on the ground plane while bold and continuous line is for the structure with SRR and EBG.....92
Figure 5.23: The elevation radiation pattern (E plane) – Dashed line for structure without SRR and EBG on the ground plane while bold and continuous line is for the structure with SRR and EBG.....92

LIST OF TABLES

Table 1.1: Performance values for three numerical methods taken at resonance.. 7

Table 4.1: Calculated Patch Size Reduction and Area Saving 67

Table 5.1: A summary of the features of the five proposed designs 83

THESIS ABSTRACT

Name: FAHAD AHMED AL-KHURAISH

Title: DESIGN AND ANALYSIS OF EBG-BASED LOW-PROFILE MICROSTRIP ANTENNAS FOR WIRELESS COMMUNICATIONS

Major Field: ELECTRICAL ENGINEERING

Date of Degree: JUNE 2010

Users of portable wireless devices like mobile phones always desire such devices to have small volume, light weight (or low-profile) and low cost. With the dramatic reduction in overall size, the antennas used in such portable devices have become one of their largest components. Therefore, much effort has been devoted to miniaturizing the size of antennas to meet the demand for devices with smaller volume and low profile.

The objective of this research work is to design and analyze Electromagnetic Band Gap (EBG) based low-profile antennas for wireless communications. To satisfy that, the EBG concept was employed in the ground plane as well as the patch antenna. Electromagnetic model for the wave propagation in EBG-based structures was carried out and mathematical model was solved numerically using the full-wave Finite Difference Time Domain (FDTD) method.

Some novel models were proposed and significant reduction in microstrip antennas sizes applying EBG concept was achieved. Experimental verifications on antenna models were performed and compared to simulated results.

خلاصة الرسالة

الاسم: فهد بن أحمد الخريش

العنوان: تصميم وتحليل الهوائيات من نوع المطبوعات المصغرة وذات المساحة الصغيرة والمعتمدة على زمر الفجوات الكهرومغناطيسية للاتصالات اللاسلكية

التخصص: الهندسة الكهربائية

تاريخ الدرجة: يونيو 2010

يحب دائما مستخدمي الأجهزة اللاسلكية المتنقلة كالهواتف المتنقلة ونحوها ، أن تكون تلك الأجهزة صغيرة الحجم، خفيفة الوزن وأن تكون قليلة التكلفة. وحتى يتم تصغيرها بالأحجام المثيرة ، أصبحت الهوائيات المستخدمة في تلك الأجهزة من أكبر أجزائها. لذا فقد كرس العمل لتصغير أحجام الهوائيات حتى تلبي رغبة الحصول على أجهزة لاسلكية متنقلة وبحجم أصغر ووزن أقل.

هدف هذا البحث تصميم وتحليل هوائيات من نوع المطبوعات المصغرة وذات المساحة الصغيرة التي تعتمد على زمر الفجوات الكهرومغناطيسية لتطبيقات الاتصالات اللاسلكية. وحتى يتم ذلك ، فان مبدأ زمر الفجوات الكهرومغناطيسية جرى تطبيقه على السطح الأرضي وعلى قمة رقعة الهوائيات من نوع المطبوعات المصغرة. جرى القيام بعمل النموذج الكهرومغناطيسي لانتشار الموجه للهياكل المعتمدة على زمر الفجوات الكهرومغناطيسية وتم حل الهيكل الرياضي عدديا باستخدام طريقة "الفروق المحدودة في المجال الزمني" (FDTD) للموجه الكاملة.

تم اقتراح نماذج جديدة والتي قللت مساحات هائلة كانت مطلوبة للهوائيات من نوع المطبوعات المصغرة ووفرت مساحات الرقع بتطبيق مبدأ زمر الفجوات الكهرومغناطيسية. جرى القيام بالتجربة العملية على التصاميم المقترحة وقورنت نتائجها بالنتائج النظرية.

CHAPTER 1

INTRODUCTION

This chapter introduces the microstrip antenna, electromagnetic Band Gap (EBG) and numerical techniques used popularly in solving electromagnetic problems.

1.1 MICROSTRIP ANTENNA

A radiating element or an antenna is defined by Webster's encyclopedia as "a usually metallic device (as a rod or wire) for radiating or receiving radio waves" [1] and according to the IEEE standard definitions, the antenna or Arial is defined as "a means of radiating or receiving radio waves (RF)".

In wireless communications, the antenna is considered as a key component that plays a vital role in the overall system performance. This concept resulted in exploring means and ways to develop many types of antenna structures or geometries that serve different applications. Therefore, there are so many types of antennas like: wire antenna (such as straight wire, or dipole, loop and helix), aperture antennas (for instance pyramidal horn, conical horn, rectangular waveguide), array antennas (such as Yag-Uda array, aperture array, microstrip patch array, slotted waveguide array), Reflector antennas (for example, parabolic reflector with front feed, parabolic reflector with cassegrain feed, corner reflector) and Lens antenna (convex-plane, convex-convex, concave-plane, concave-convex) as well as microstrip antennas. The major characteristics that guide a user in selecting an antenna are radiation pattern or antenna pattern, radiation power density, radiation intensity and directivity, gain, antenna efficiency, bandwidth, resonant frequency, polarization and input impendence. Explanation for used characteristics in this thesis will be given later.

The microstrip (or patch) antennas have a history of 60 years, where they were used primarily for space applications at the beginning. Then, they were become used for government and commercial applications as of today such as wireless communication applications like Global Positioning System (GPS) receivers, Wireless Local Area Network (WLAN), Paging systems, handheld mobile telephones, radar systems and biomedical applications [2] and [3]. Every microstrip antenna consists of a metallic strip or patch printed on a thin-grounded dielectric substrate as in figure 1.1.

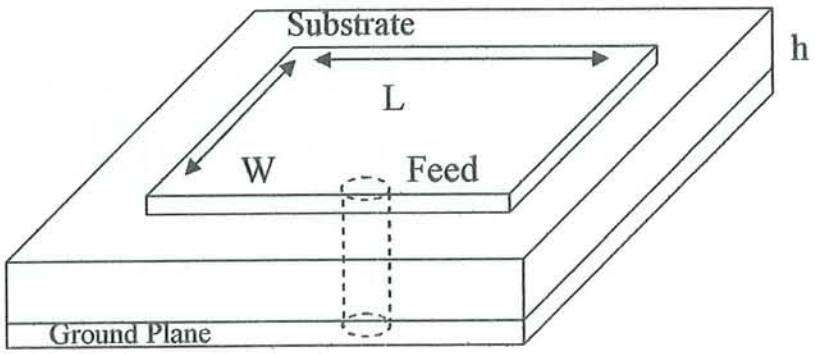

Figure 1.1 : A rectangular microstrip (patch) antenna

Coaxial line or probe placed on the bottom of the substrate, microstrip line, aperture coupling and proximity coupling are the major feeding methods of the microstrip antenna. In general, selection of one way of feeding method or another depends on the antenna user who pays a close attention to the antenna efficiency and fabrication simplicity. The microstrip antenna could come in different configurations; square, thin strip (dipole), elliptical, triangular as well as rectangular and circular which are the most popular ones due to their simple analysis and fabrication reasons.

Simply, the patch antenna radiates when the fringing effect takes place in the edges of the patch due to the charges distribution and movement when an excitation is fed. The patch antenna has some advantages like the low profile (size); of course, its size depends on the chosen frequency band of operation, light

in weight and cost little during the manufacturing [3]. Moreover, possibility of giving a linear or circular polarization and easy coupling or integration with microwave Integrated Circuits (ICs) are also advantages of microstrip patch antenna. On the other hand, narrow bandwidth, dielectric and conductor losses for thin antenna patches, sensitivity to environmental factors (like temperature and humidity) and poor polarization, low efficiency, limited power capacity are disadvantages of the patch antenna [4].

Several ideas were suggested to improve the patch antenna performance. Removing patch antenna ground plane edges and using isolated soft surface structure within the bare substrate was suggested in [5]. This suggestion was one of proposed ideas to overcome surface wave issue and ground plane limitation as other methods cannot solve which results in improving the patch antenna gain. Moreover, there are several methods to enhance the patch antenna bandwidth. Inserting a small dielectric resonator loaded patch antenna was mentioned in [6] and designing microstrip antenna with a notch was elaborated in [7]. In addition to that, compensating rectangular microstrip antenna with negative capacitor and negative inductor was explained in [8] and modeling the patch antenna with E-shaped was suggested in [9] and U-shaped was proposed in [10].

1.2 ELECTROMAGNETIC BAND GAP (EBG)

Electromagnetics is a branch of physics or electrical engineering in which electric and magnetic phenomena are studied. The Electromagnetic Band Gap (EBG) materials or Photonic Band Gap (PBG) materials or Photonic Crystals are periodic arrangements of atoms or moleculars (crystal lattice if it is small or building block of atoms or moleculars, if it is big) made artificially. Since EBG materials discovery, they have created new possibilities for controlling and manipulating the propagation of electromagnetic fields. Utilization of EBG structures is becoming attractive in the electromagnetic community and is

resulting in many promising applications such as perfect dielectric mirror that reflects electromagnetic waves, resonant cavity which traps electromagnetic waves. In additional to that, waveguide that transports electromagnetic waves through localizing defects in photonic crystals as well as beam splitters, high quality lasers, couplers, channel add-drop filters, (de)-multiplexers, and antennas in [11-13] are applying the EBG concept.

Generally, the terminology EBG is used to denote the structure that produces an absence of a response in either frequency or wave number (or band gap) for some polarization or angle of incidence or vector orientation (electromagnetic properties). In short words, structure or lattice that introduces gaps into its energy band and prevents electromagnetic from propagating with certain energy in certain direction is called EBG taking in the consideration that the gap might extend to all directions where it is denoted as complete EBG. So, an appropriate design of EBG structure could forbid the electromagnetic waves propagation, permit the electromagnetic propagation in a defined direction, or localize the electromagnetic waves in certain areas.

By employment of dielectric, the EBG can be constructed in one, two and three dimensions where in each case, the alternating layers with different dielectric constants spaced by a distance, are placed periodically in one or more orthogonal directions as figure 1.2 presents. For example, in the one dimension case, layers or materials including the dielectric are periodic in one direction (for instance, Z direction) and homogeneous in the other two orthogonal directions (by plane) as figure 1.3 highlights [14].

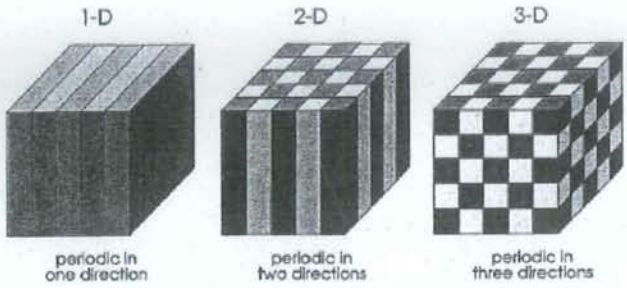

Figure 1.2: EBG construction for one (1-D) or more dimensions (2-D & 3-D)

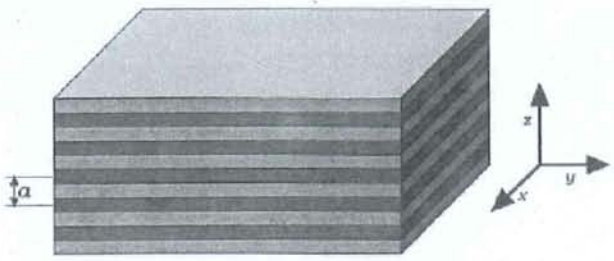

Figure 1.3: EBG periodic in one direction (one dimension)

1.3 NUMERICAL TECHNQUES

A question might arise, why numerical techniques are used. It is simply because electromagnetic problems usually involve partial differential equations or integral equations and their solution would be difficult in complicated configurations. Therefore, numerical techniques that give approximate and fast-calculated solutions are approached especially with availability of modern computers that reduce the computational time. The mostly used methods in solving microwave problems are:

1.3.1 METHOD OF MOMENT (MOM)

The Method Of Moment (MOM or sometime, it is called MoM), has long been the corner-stone in the analysis of electromagnetic problems that have arbitrary shaped objects and best suited for structures with homogenous dielectric materials and perfect element conductors and with use of other technique, this method was extended to solve inhomogeneous dielectric materials structures [15-16].

MOM suits multilayer substrates structures and therefore is frequently used to model the patch antenna. MOM technique requires that the current density on the structure is approximated by an appropriate set of basis functions both in the patch itself and in the probe [17] & [9].

To solve electromagnetic problems using MOM numerically, matrix equation requires higher operations and higher memory size to store the matrix elements as well as longer time to compute and therefore, consider being expensive at the end. In the literature, several techniques such as Impendence Matrix Localization (IML), Fast Multiple Method (FMM), the Conjugate Gradient Fast Fourier Transform Method (CG-FFTM) and others were developed to speed up the matrix-vector multiplication so that, MOM will be efficient [5].

1.3.2 FINITE ELEMENT METHOD (FEM)

Finite Element Method (FEM) is commonly used in modeling electromagnetic problems at low frequencies (static, quasi-static electric and magnetic fields at DC and at lower than 1 KHz frequencies) as well as at higher frequencies for enclosed systems (waveguide and cavity etc). On the other hand, this method has some limitations as it requires large memory for updating the equivalent surface current and it cannot be extended to analyze high frequencies problems involving scattering and radiation. However, it gives higher accuracy during boundaries approximation [18].

1.3.3 FINITE DIFFERENCE TIME DOMIN (FDTD) METHOD

Finite Difference Time Domain (FDTD) method is widely used by researchers and it is a powerful method to analyze and solve the electromagnetic problems numerically including the complicated ones. Originally, FDTD was initiated by Yee [19] for electromagnetic scattering and absorption problems and then it has been adopted for the last 45 years from its existence to analyze antenna and other electromagnetic problems, regardless if they are uniform or non-uniform geometry [10] & [20]. Detailed explanation of this method will be presented in chapter 3.

Performance of these three numerical methods was investigated in [16] during designing a linearly polarized probe-fed patch antenna having same dimensions and parameters in each case. It was reported by that study, among the above numerical methods, FEM requires the highest memory capacity to discretize the given structure while FDTD relatively need higher memory capacity than MOM as six components of electrical (E) and magnetic (H) fields vectors, three for each, are needed to be computed for each cell and requires therefore longer time too.

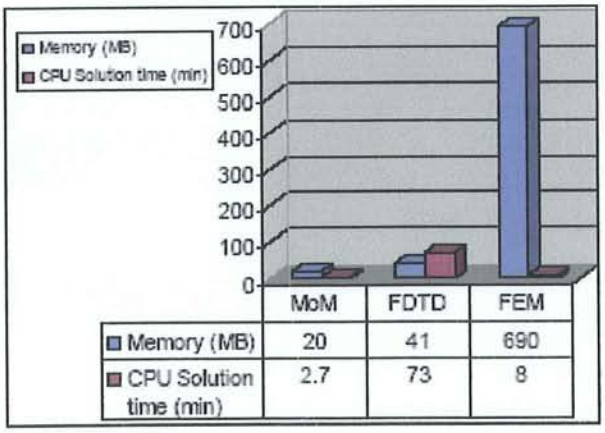

Figure 1.4: Needed memory size and CPU solution time for three numerical methods.

	MOM	FDTD	FEM	MEASUREMENT
f_0 (GHz)	1.5676	1.568	1.555	**1.562**
S11 (dB)	-24.6	-26.6	-28.7	**-30.3**
VSWR	1.13	1.1	1.12	**1.1**
Zin (Ω)	47.1	45.9	53.4	**46.4**
BW (%)	2.6	2.2	2.2	**3.1**

Table 1.1: Performance values for three numerical methods taken at resonance.

It would be better, if some definitions are given before explaining the above table. The general definition of resonant frequency is the frequency, which the system tends to oscillate at maximum amplitude. For microstrip patch antenna, the resonance frequency is given by:

$$f_r = \frac{1}{2L_{eff}\sqrt{\varepsilon_{reff}}\sqrt{\mu_o\varepsilon_o}} = \frac{1}{2(L+2\Delta L)\sqrt{\varepsilon_{reff}}\sqrt{\mu_o\varepsilon_o}} \tag{1.1}$$

Return loss (S_{11}) parameter is one of the most indicators of the performance of an antenna. The return loss describes how much energy is reflected in the incident wave and reveals the mismatch between the antenna and transmission line with characteristic impedance Z_o.

VSWR (denoted also as s) is the ratio of maximum magnitude of voltage over minimum magnitude of voltage and is given by:

$$s = \frac{V_{\max}}{V_{\min}} \tag{1.2}$$

Input impedance is defined as the impedance presented by an antenna at its terminals and it is usually represented by:

$$Z_A = \mathrm{R}_\mathrm{A} + jX_A \tag{1.3}$$

$$R_A = \mathrm{R}_\mathrm{r} + R_L \tag{1.4}$$

here, **A** is antenna port. (R_A) is antenna resistance and X_A is antenna reactance, (R_r) is radiation resistance and (R_L) is loss resistance.

Bandwidth (denoted as BW) of the antenna is the range of frequencies within which the performance of the antenna, with respect to some characteristics, conforms to a specified standard. The radiation pattern is a graphical representation of the radiated power from antenna.

Now, table 1.1, lists electromagnetic parameters: resonance frequency (f_o), return loss parameter (S_{11}), Voltage Standing Wave Ratio (VSWR), input

impedance (Z_{in}) and Bandwidth (BW) calculated by each numerical method and compare them with the measured values. It is observed that the three numerical techniques give parameters values which match approximately with the measured values but with little differences. Now, it is end user turn, to select a method among these three methods that suits his application and gives an acceptable accuracy for him.

In general and based on the above results, FDTD was selected as numerical technique to carry out this work mainly for two reasons. It gives nearly matching values for electromagnetic parameters values when compared to the measured data and it is simpler than other numerical techniques highlighted previously.

On the other hand, there are many commercial software packages such as High Frequency Structure Simulator (HFSS), IE3D and CST that can solve and analyze electromagnetic problems. However, one of the objectives of this work is to learn one numerical method and to develop special-purpose simulator.

1.4 THESIS OBJECTIVES

The thesis goal is to formulate an accurate theoretical full-wave model to numerically analyze designed microstrip patch antennas with Electromagnetic Band Gap (EBG) structures. The designs should be novel, low profile and suitable and compatible for wireless communications.

It is also the objective of this thesis to verify the features of the novel EBG-based microstrip antennas theoretically to prove patch antennas size reduction and ability to shift or control resonance frequency with EBG-based structures.

Simplest design among proposed novel EBG-based antennas that does resonate at 0.9 GHz and 1.8 GHz will be selected, fabricated and subjected for laboratory experiment to validate the simulated theoretical results.

1.5 THESIS ORGANIZATION

This thesis is organized into six chapters. In **Chapter 1,** an overview of microstrip antenna is summarized and EBG and well as numerical techniques are briefly described.

In **Chapter 2,** the concept of applying the EBG on microstrip antenna is explained. Then, the derivations of the theoretical model are presented.

In **Chapter 3,** a detailed description of the Finite Difference Time Domain (FDTD) Method that is used in solving the EBG problem is given.

In **Chapter 4,** FDTD simulation results for some novel designs applying EBG on the ground plane and on patch are presented.

In **Chapter 5,** Split Ring Resonator (SRR) model and the application of FDTD method on this developed model are discussed. Moreover, experimentally obtained results are presented and compared to simulation results at the of this chapter.

In **Chapter 6,** summary and conclusion of this thesis as well as the proposed future work that can enhance the design of the EBG-based low profile microstrip antenna are given.

CHAPTER 2

APPLYING EBG CONCEPT IN MICROSTRIP ANTENNA

This chapter explains applying the EBG concept in microstrip patch antenna after giving a brief literature overview.

2.1 LITERATURE REVIEW

In the literature, several techniques for applying the EBG concept on microstrip antenna were suggested. Utilizing two-layers patch antennas with high impendence EBG substrate was proposed in [2]. This technique was proved to improve the performance of microstrip patch antenna. Having a microstrip patch antenna with EBG structure sandwiched between the patch and the ground plane was initiated in [21] and it showed a bandwidth improvement. Additionally, [22] suggested using spiral fan-shape EBG patch structure between narrowband patch antenna and its ground plane and showed at the end, a bandwidth enhancement of a narrow band rectangular microstrip antenna, because of excellent return loss and good impedance matching.

Designing dual Bandgap below 10 GHz, which is dependable on patch width and inner patch width, using slotted patch EBG (double L slot in original Mushroom EBG patch) structure, was recommended in [23]. Similarly, [24] obtained a low profile dual band patch antenna using inverted L antenna with slotted EBG structure. Moreover, [4] suggested modifying the slotted patch EBG structure and got improvement in the radiation pattern.

A 2-D EBG structure in microstrip antenna was suggested in [25] to improve the radiation pattern and to reduce the mutual coupling between elements due to surface waves reduction. One more idea to reduce the mutual coupling was illustrated in [26] where another EBG structure in a fork-like-shape inserted as patch array was presented. In [27] designing suspended patch antenna with fork-

like EBG substrate was highlighted. In last two cases, the antenna performance was observed improved. Applying EBG technology on a patch antenna with vias guaranteed good radiation pattern for patch antenna [28-29].

As the EBG principle can be implemented in the top layer of a patch antenna, it was suggested, changing the way, EBG Structure is etched. Etching the EBG structure on the ground plane proved that the microstrip antenna bandwidth and gain got improved [30]. Designing and obtaining a wider operating bandwidth for a single layer coaxially fed rectangular microstrip patch antenna by cutting a U shape slot on the patch was explained in [6].

Directivity also, of microstrip patch antenna can be enhanced with EBG using Frequency Selective Surfaces (FSS). This technique is commonly used to protect the antenna from the weather while letting the desired electromagnetic waves pass within a narrow band as Superstrate with octagonal aperture was explained [31].

Adding additional gaps into EBG structure and stacked EBG utilization through placing EBG lattice in a coplanar position were two advanced methods presented in [32] to improve compactness in EBG design and utilization through slot-strip EBG design. These methods could achieve 40 % reduction of the normal EBG structure area.

2.2 DERIVATION OF THE THEORETICAL MODEL

Sievenpiper suggested in [33] implementing EBG as periodic structure (periodic structure known as High Impedance Surface) in the ground plane of microstrip antenna. This technique, allows electromagnetic waves for some frequencies ranges to propagate. [23] presented that each EBG configuration can be expressed theoretically by an equivalent circuit consisting of Inductor, L and Capacitor, C. Initially EBG structures were widely designed based on Mushroom EBG (MEBG) structure that is simply square patch elements placed in a periodical manner in the ground plane with vias as shown in figure 2.1.

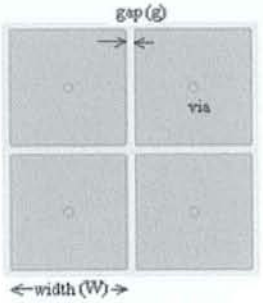

(a)

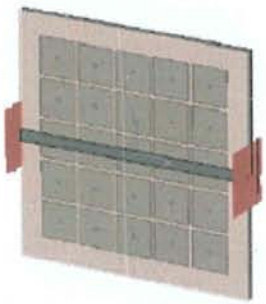

(b)

Figure 2.1: (a) 4 elements of Mushroom like EBG (MEG) structure and (b) overall structure of Mushroom like EBG (MEBG) structure with feeding network [23].

This EBG configuration has two merits. It improves the antenna gain and enhances the bandwidth [2] & [29]. However, it has a demerit as it does resonate below 10 GHz with only one resonance frequency. The equivalent Inductor, L and Capacitor, C circuit of this structure can be determined as follows [23]:

$$L = \mu_o h \qquad (2.1)$$

$$C = W\varepsilon_o \frac{(\varepsilon_r + 1)}{\pi} \cosh^{-1}\left(\frac{2W}{g}\right) \qquad (2.2)$$

where, $\mu_o, h, W, \varepsilon_o, \varepsilon_r, g$: are respectively permeability in free space, thickness of the substrate, patch width of the EBG structure, permittivity of free space, relative permittivity of the substrate and gap between elements in EBG structure.

Later, researchers have modified MEBG and come up with other EBG structures. One of these is Slotted Patch EBG (SPEBG) as shown in figure 2.2 that is similar to MEBG structure. However, L slots, which have defined thickness, were used instead of square patch elements. Modified SPEBG structure as shown in figure 2.3 was examined in detail in one paper [4] and found giving good performance to antenna radiation pattern compared with SPEBG as surface wave effect was reduced.

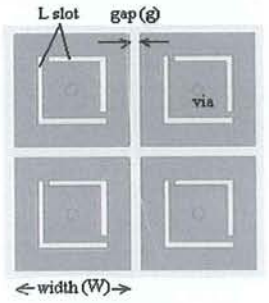

(a)

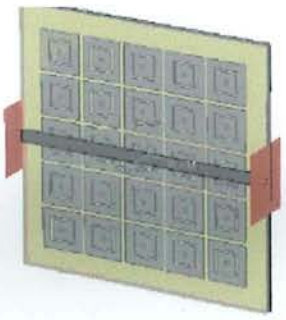

(b)

Figure 2.2: (a) 4 elements of slotted patch EBG (SPEBG) structure and (b) overall structure of slotted patch EBG (SPEBG) structure with feeding network [4].

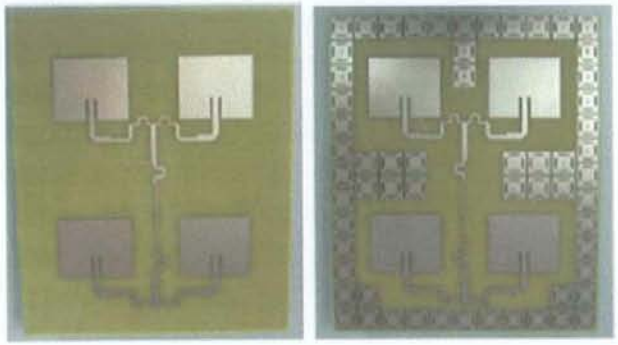

Figure 2.3: A 2 by 2 microstrip array antenna with and without the modified slotted patch EBG [4].

SPEBG structure will have a dual Bandgap below 10 GHz, if the patch width and identical slots on the patch near the edges is implemented [24] as illustrated in figure 2.4.

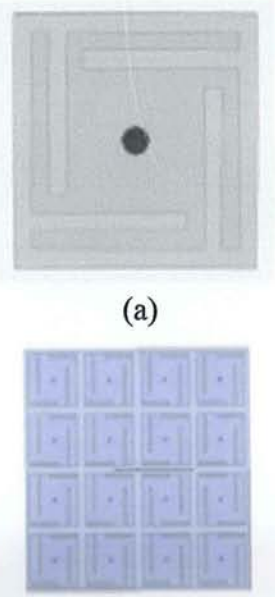

(a)

(b)

Figure 2.4: (a) slot loaded EBG structure and (b) A low profile antenna over a finite EBG ground plane [24].

A dumbbell-like EBG as depicted in figure 2.5 is another EBG design which has no vias at all. It was developed in [34] to improve the antenna radiation property and bandwidth thru enhancing the mutual coupling between elements. The dumbbell-like EBG equivalent circuit is shown in Figure 2.6.

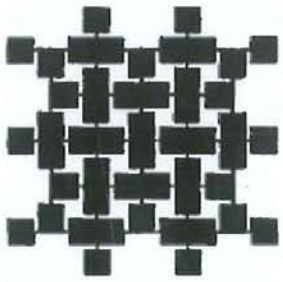

Figure 2.5: The dumbbell like EBG [34]

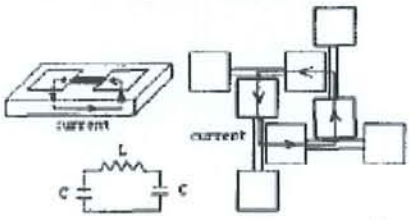

Figure 2.6: Flow of current and equivalent circuit model for dumbbell like EBG [34]

A fork-like EBG structure as well as F-like EBG structure in [26] and in [32] as shown in figure 2.7 and figure 2.8 respectively are also EBG configurations that apply vias technique. These configurations were tested and proven that they can reduce the mutual coupling and antenna size by around 40%, besides controlling the band gap of the EBG structure.

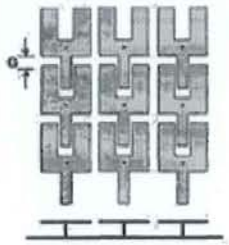

(a)

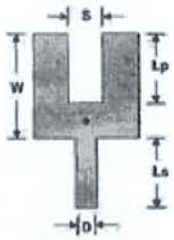

(b)

Figure 2.7: (a) Configuration of the fork-like EBG (b) Details of one unit of the fork-like EBG lattice [26].

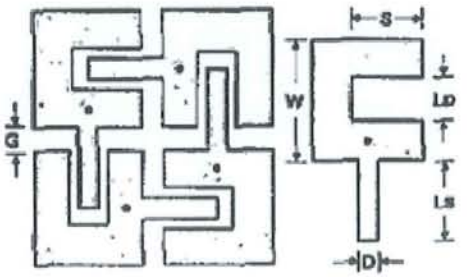

Figure 2.8: Configuration of the F-like EBG structure [32].

A cross-shaped EBG that has no vias at all, as illustrated in the figure 2.9 was investigated and the gain and bandwidth of the structure were reported enhanced [30].

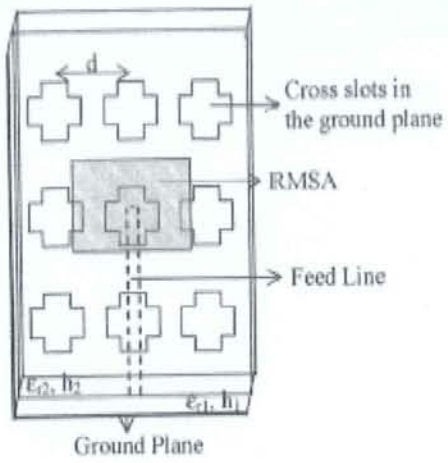

Figure 2.9: Geometry of the proposed EBG backed antenna [30].

A spiral-fan shaped EBG that has no vias at all, as sketched below in figure 2.10 was studied thoroughly in [22] and found that such structure gives excellent return loss and good impedance matching as well as antenna bandwidth.

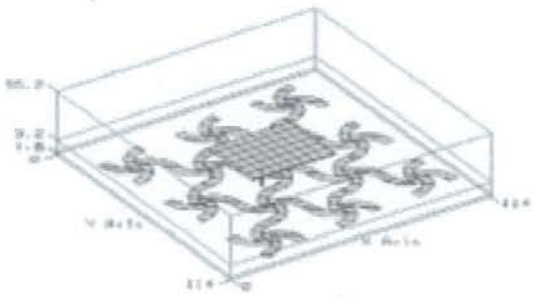

Figure 2.10: Prospective view of spiral-fan shaped EBG [22].

Equivalent circuits models for different circular Spilt Rings Resonators (SRR) was illustrated and presented in [34] and in [35]. By achieving experimentally the negative value of effective permeability, using array of metallic artificial atoms or simply SRR, facilitated to researchers to come up with a good and practical tool to design and fabricate artificial media [34]. Such modeling will help estimating some structure characteristics like resonance frequency and effective permeability.

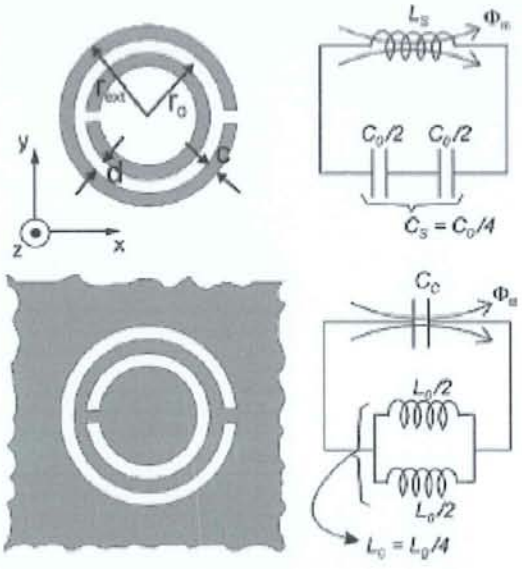

Figure 2.11: Topologies of SRR configurations and their equivalent circuits models [34].

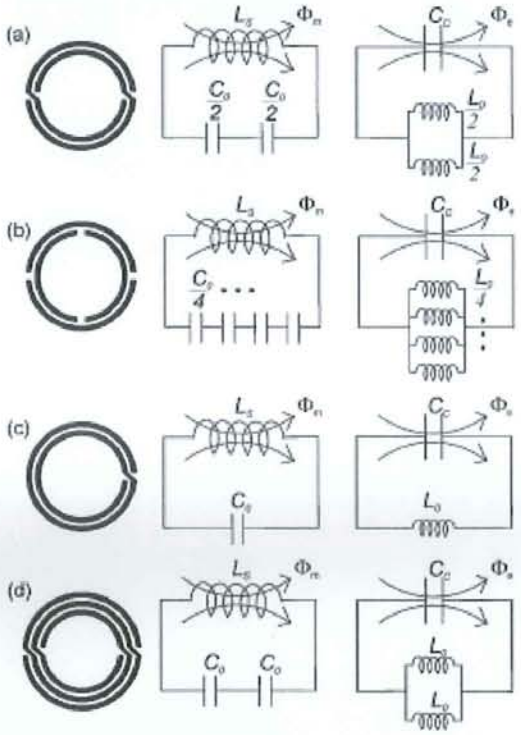

Figure 2.12: Topologies of different SRR configurations and their equivalent circuits for the topologies are depicted in the second column, while the circuit models for the complementary counterparts are represented in the third columns [34].

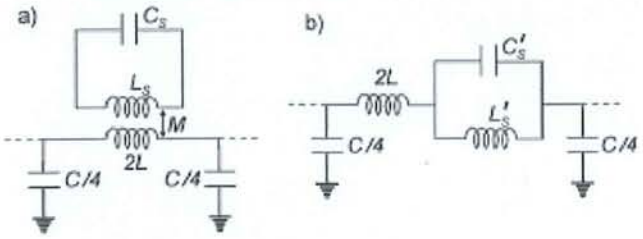

Figure 2.13: (a) lumped-element equivalent circuit for the basic cell of the SRR loaded transmission line. (b) Simplified circuit with series branch replaced by its equivalent impedance [35].

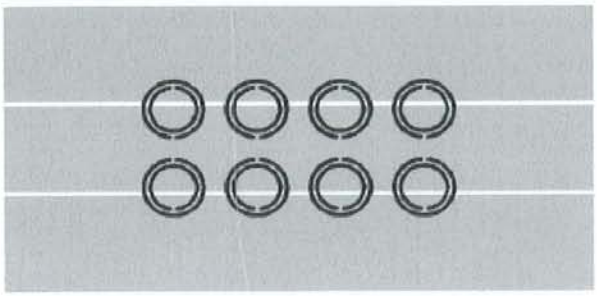

Figure 2.14: Layout of the fabricated SRR loaded structure [35].

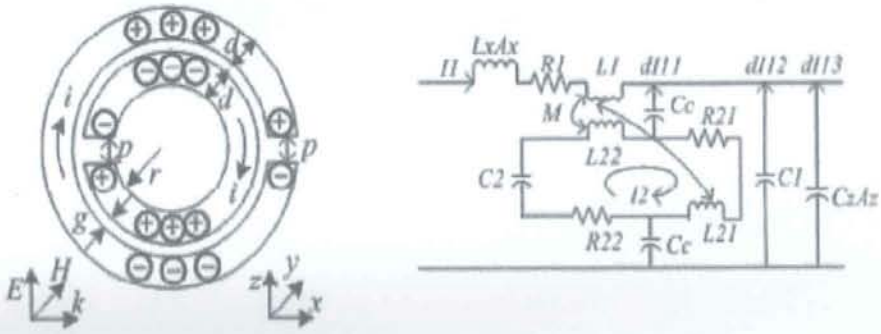

Figure 2.15: The geometry configuration of the individual SRR, and the electric charge and current distribution in it as well as the individual SRR equivalent circuit model [35].

In the literature, placing different structures of an embedded Spilt Ring Resonator (SRR) on the antenna substrate was investigated. Some improvement of the antenna characteristics such as gain, antenna efficiency, dual frequency of operation compared to the simple or classical antenna were shown improved [36]. In addition to that, many EBG structures and materials were used as antenna substrate. Two kinds of dielectric EBG antenna, using either EBG reflector or defect EBG materials associated with a metallic plate, were developed. A study of EBG materials, using 2-D cylindrical dielectric rods with a certain relative dielectric constant on antenna, was proposed and studied. Some useful advantages such as directivity increase, higher bandwidth and low profile structure were reported [37].

Because of EBG structure can control and manipulate the propagation of electromagnetic waves, many EBG structures studies were made and some of these studies were to enlarge the defect bands using parameters such as thickness, permittivity, periodicity of the layers, dimension of the defect, etc. EBG structure application on an antenna can be summarized as follows:

1. Applying EBG structures as artificial ground planes such as Perfect Magnetic Conductors (PMC), reactive surfaces or Artificial Magnetic Conductor (AMC).
2. Applying EBG structure as substrate for microstrip patch antenna such as High Impedance Surface (HIS).
3. Applying EBG structure as superstrates over the radiation sources.

A study was performed to merge applying EBG structures as artificial ground planes and EBG structure as superstrates over the radiation sources [38]. It concluded that, a compact high directive EBG resonator antenna increases the antenna directivity and allows having a compact antenna structure.

In [39], EBG material with defect was placed in the middle of structure of double layer arranged periodically in the Z direction. This created an allowed frequency band with band gap as well as it enhanced the structure resonance frequency bandwidth.

CHAPTER 3

THE FINITE DIFFERENCE TIME DOMAIN (FDTD) METHOD

This chapter is devoted to explain the Finite Difference Time Domain (FDTD) method in more detail and its requirements and to explain about its requirements such as Absorbing Boundary Condition (ABC), numerical dispersion and stability. Then, it highlights the calculated parameters out of FDTD method that were computed and obtained in this thesis work.

3.1 INTRODUCTION TO FDTD METHOD

Ever since the Finite Difference Time Domain (FDTD) method was proposed for electromagnetic scattering and absorption problems, it has been a popular numerical solution choice for the researchers doing antenna analysis, microwave engineering, bio-electromagnetic and shielding applications and in solving other electromagnetic problems in years following their existence until now.

The simplicity and efficiency of FDTD method in modeling, analyzing and studying electromagnetic structures with practical accuracy are advantages of utilizing it over other methods.

FDTD was initially proposed by Yee in 1966 to solve electromagnetic scattering and absorption problems [19]. Yee introduced a set of finite difference equations for the system of partial differential equations due to the fact that solution of time-dependent Maxwell's equations in their standard forms in most cases are unknown. He was able to achieve obtaining the solution of Maxwell's

equations in the isotropic media numerically, when the boundary conditions selected to be appropriate for a perfect conductor.

He discretized the differential form of Maxwell's equations using electrical $\vec{E}$ and magnetic $\vec{H}$ fields grids so that equations are updated to get the present fields throughout the computational domain reference to the previous fields. Then, the updated Maxwell's equations using a second-order central differencing scheme, with electric and magnetic fields interleaved in both space and time on staggered grids, are used in a leapfrog scheme to incrementally march the electrical and magnetic fields forward in time as shown in the figure 3.1.

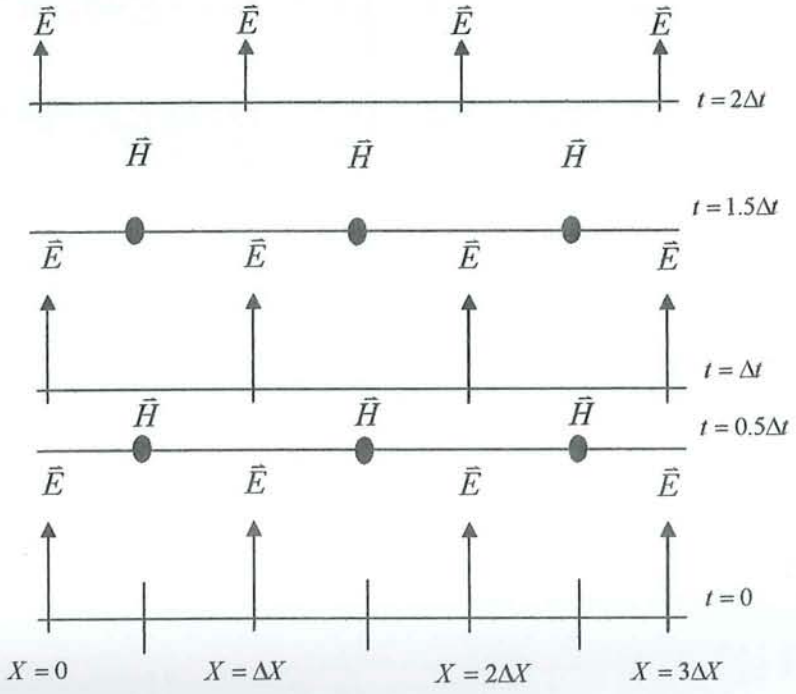

Figure 3.1: Space-time chart of the Yee algorithm for a one-dimensional wave propagation [42]

In all of finite difference equations, the components of $\vec{E}$ and $\vec{H}$ are located within a single unit cell in a three-dimensional lattice shown in figure 3.2. Each $\vec{E}$ component is surrounded by four $\vec{H}$ components, and each $\vec{H}$ component is surrounded by four $\vec{E}$ components. Further, a beautiful simple picture of 3-D

space being filled by an interlinked array of Faraday's law and Ampere's law form can be provided by the Yee arrangement. It is also very useful in specifying field boundary conditions and singularities.

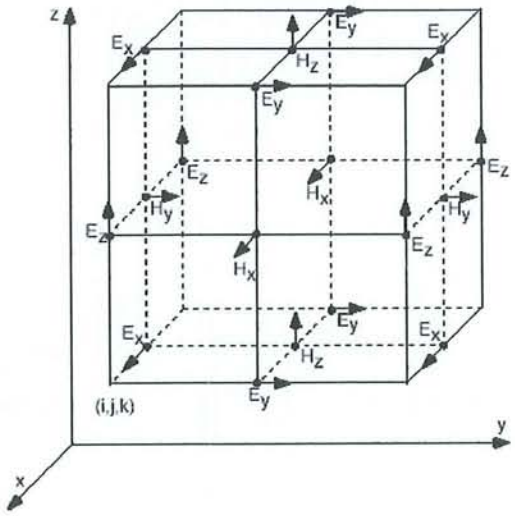

Figure 3.2: Unit cell of Yee's mesh positioning of various filed components [19]

When FDTD was suggested, it could not attract the researches attention, as the computational cost of this method was high. In addition to that, it had another limitation drawback to model any electromagnetic problems. This is because, it was able to handle only small electromagnetic problems with closed boundary conditions.

Later, almost three decades ago, usage of FDTD is strengthened and it was found to be a useful and competent method in solving large and complex electromagnetic problems because of two main reasons explained in [20]. One reason is the electromagnetic computational cost fell down due to development of very fast computers with very large memory capacity. Secondly, further enhancements and improvements on FDTD method by Taflove and others [40] in several areas and applications were published in the literature.

Yee in [19] started with Maxwell's curl equations for an isotropic media that are given by:

$$\vec{\nabla} \times \vec{E} = -\frac{\partial \vec{B}}{\partial t} \tag{3.1}$$

As $B = \mu H$, equation 3.1 can be re-written as:

$$\vec{\nabla} \times \vec{E} = -\mu \frac{\partial \vec{H}}{\partial t} \tag{3.2}$$

$$\vec{\nabla} \times \vec{H} = J + \frac{\partial \vec{D}}{\partial t} \tag{3.3}$$

As $D = \varepsilon E$ and $J = \sigma E$, equation 3.2 can be re-written as:

$$\vec{\nabla} \times \vec{H} = \sigma \vec{E} + \varepsilon \frac{\partial \vec{E}}{\partial t} \tag{3.4}$$

In the rectangular coordinate system (x, y, z), the equivalent vector components of Maxwell's curl equations 3.2 and 3.4 can be re-worked as:

$$\frac{\partial H_x}{\partial t} = \frac{1}{\mu}\left(\frac{\partial E_y}{\partial z} - \frac{\partial E_z}{\partial y}\right) \tag{3.5}$$

$$\frac{\partial H_y}{\partial t} = \frac{1}{\mu}\left(\frac{\partial E_z}{\partial x} - \frac{\partial E_x}{\partial z}\right) \tag{3.6}$$

$$\frac{\partial H_z}{\partial t} = \frac{1}{\mu}\left(\frac{\partial E_x}{\partial y} - \frac{\partial E_y}{\partial x}\right) \tag{3.7}$$

$$\frac{\partial E_x}{\partial t} = \frac{1}{\varepsilon}\left(\frac{\partial H_z}{\partial y} - \frac{\partial H_y}{\partial z} - \sigma E_x\right) \tag{3.8}$$

$$\frac{\partial E_y}{\partial t} = \frac{1}{\varepsilon}\left(\frac{\partial H_x}{\partial z} - \frac{\partial H_z}{\partial x} - \sigma E_y\right) \tag{3.9}$$

$$\frac{\partial E_z}{\partial t} = \frac{1}{\varepsilon}\left(\frac{\partial H_y}{\partial x} - \frac{\partial H_x}{\partial y} - \sigma E_z\right) \tag{3.10}$$

Yee denoted a mesh point as:

$$(i, j, k) = (\Delta i, \Delta j, \Delta k) \tag{3.11}$$

Where, Δi , Δj , and Δk are the space increments. To represent any function (F) of space and time, the following notation is used

$$F(i, j, k, n) = F(\Delta i, \Delta j, \Delta k, n\Delta t) \tag{3.12}$$

Here, Δt is the time increment.

As a continuation process, Yee used the above expressions while formulating the Maxwell's equations using derivatives of the space and time. The second-order accurate in the space and the time increments using the following finite difference expression:

$$\frac{\partial F^n(i,j,k)}{\partial x} = \frac{F^n(i+\tfrac{1}{2},j,k) - F^n(i-\tfrac{1}{2},j,k)}{\Delta x} \tag{3.13}$$

$$\frac{\partial F^n(i,j,k)}{\partial t} = \frac{F^{n+\frac{1}{2}}(i,j,k) - F^{n-\frac{1}{2}}(i,j,k)}{\Delta t} \tag{3.14}$$

At the end, Yee constructed the below six finite-difference approximation for the system of equations in 3.5 ~ 3.10, that have local truncation error of the second order in all increments. This was made after replacing the field components of $\vec{E}$ and $\vec{H}$ on the mesh in a way shown in figure 3.1 then he evaluated $\vec{E}$ and $\vec{H}$ at alternate half-time steps:

$$H_x^{n+\frac{1}{2}}(i, j+\tfrac{1}{2}, k+\tfrac{1}{2}) = H_x^{n-\frac{1}{2}}(i, j+\tfrac{1}{2}, k+\tfrac{1}{2}) + \frac{\Delta t}{\mu(i, j+\tfrac{1}{2}, k+\tfrac{1}{2})} \left[\frac{E_y^n(i, j+\tfrac{1}{2}, k+1) - E_y^n(i, j+\tfrac{1}{2}, k)}{\Delta z} + \frac{E_y^n(i, j, k+\tfrac{1}{2}) - E_y^n(i, j+1, k+\tfrac{1}{2})}{\Delta y} \right] \tag{3.15}$$

$$H_y^{n+\frac{1}{2}}\left(i+\tfrac{1}{2},j,k+\tfrac{1}{2}\right)=H_y^{n-\frac{1}{2}}\left(i+\tfrac{1}{2},j,k+\tfrac{1}{2}\right)+\frac{\Delta t}{\mu\left(i+\frac{1}{2},j,k+\frac{1}{2}\right)}\left[\begin{array}{l}\dfrac{E_z^n\left(i+1,j,k+\frac{1}{2}\right)-E_z^n\left(i,j,k+\frac{1}{2}\right)}{\Delta y}\\ +\dfrac{E_x^n\left(i+\frac{1}{2},j,k\right)-E_x^n\left(i+\frac{1}{2},j,k+1\right)}{\Delta z}\end{array}\right] \tag{3.16}$$

$$H_z^{n+\frac{1}{2}}\left(i+\tfrac{1}{2},j+\tfrac{1}{2},k\right)=H_x^{n-\frac{1}{2}}\left(i+\tfrac{1}{2},j+\tfrac{1}{2},k\right)+\frac{\Delta t}{\mu\left(i+\frac{1}{2},j+\frac{1}{2},k\right)}\left[\begin{array}{l}\dfrac{E_x^n\left(i+\frac{1}{2},j+1,k\right)-E_x^n\left(i+\frac{1}{2},j,k\right)}{\Delta x}\\ +\dfrac{E_y^n\left(i,j+\frac{1}{2},k\right)-E_y^n\left(i+1,j+\frac{1}{2},k\right)}{\Delta x}\end{array}\right] \tag{3.17}$$

$$E_x^{n+1}\left(i+\tfrac{1}{2},j,k\right)=\left[1-\frac{\sigma\left(i+\frac{1}{2},j,k\right)\Delta t}{\varepsilon\left(i+\frac{1}{2},j,k\right)}\right]E_x^n\left(i+\tfrac{1}{2},j,k\right)+\frac{\Delta t}{\varepsilon\left(i+\frac{1}{2},j,k\right)}\left[\begin{array}{l}\dfrac{H_y^{n+1/2}\left(i+\frac{1}{2},j,k-\frac{1}{2}\right)-H_y^{n+1/2}\left(i+\frac{1}{2},j,k+\frac{1}{2}\right)}{\Delta z}\\ +\dfrac{H_z^{n+1/2}\left(i+\frac{1}{2},j+\frac{1}{2},k\right)-H_z^{n+1/2}\left(i+\frac{1}{2},j-\frac{1}{2},k\right)}{\Delta y}\end{array}\right] \tag{3.18}$$

$$E_y^{n+1}\left(i,j+\tfrac{1}{2},k\right)=\left[1-\frac{\sigma\left(i,j+\frac{1}{2},k\right)\Delta t}{\varepsilon\left(i,j+\frac{1}{2},k\right)}\right]E_y^n\left(i,j+\tfrac{1}{2},k\right)+\frac{\Delta t}{\varepsilon\left(i,j+\frac{1}{2},k\right)}\left[\begin{array}{l}\dfrac{H_x^{n+\frac{1}{2}}\left(i,j+\frac{1}{2},k+\frac{1}{2}\right)-H_x^{n+\frac{1}{2}}\left(i,j+\frac{1}{2},k-\frac{1}{2}\right)}{\Delta z}+\\ \dfrac{H_z^{n+\frac{1}{2}}\left(i-\frac{1}{2},j+\frac{1}{2},k\right)-H_z^{n+\frac{1}{2}}\left(i+\frac{1}{2},j+\frac{1}{2},k\right)}{\Delta x}\end{array}\right] \tag{3.19}$$

$$E_z^{n+1}\left(i,j,k+\tfrac{1}{2}\right)=\left[1-\frac{\sigma\left(i,j,k+\frac{1}{2}\right)\Delta t}{\varepsilon\left(i,j,k+\frac{1}{2}\right)}\right]E_z^n\left(i,j,k+\tfrac{1}{2}\right)+\frac{\Delta t}{\varepsilon\left(i,j,k+\frac{1}{2}\right)}\left[\begin{array}{l}\dfrac{H_y^{n+\frac{1}{2}}\left(i+\frac{1}{2},j,k+\frac{1}{2}\right)-H_y^{n+\frac{1}{2}}\left(i-\frac{1}{2},j,k+\frac{1}{2}\right)}{\Delta x}\\ +\dfrac{H_x^{n+\frac{1}{2}}\left(i,j-\frac{1}{2},k+\frac{1}{2}\right)-H_x^{n+\frac{1}{2}}\left(i,j+\frac{1}{2},k+\frac{1}{2}\right)}{\Delta y}\end{array}\right] \tag{3.20}$$

3.2 ABSORBING BOUNDARY CONDITIONS: THE PML

An essential part used while solving electromagnetic problem numerically using FDTD is Absorbing Boundary Condition (ABC). It is used to truncate the

computation domain or to produce negligible reflection. ABC is needed when modeling an open region electromagnetic problem as the tangential component of electric field along the outer boundary of the computation domain cannot be updated using the basic Yee's algorithm [20].

Yee proposal of FDTD technique was well appreciated and used by many works however, it needs to have boundary for the computational domain. ABC is derived either from differential equations, through factoring the wave equation and permitting only outgoing waves, or applying an absorber material where the field is truncated as propagation is ongoing toward the absorber. Several studies to come up with absorber related ABC were discussed and reported in the literature, until Jean Berenger in [12] proposed the Perfectly Matched Layer (PML), which reduces boundary reflections, and become widely accepted compared with the suggested earlier ABC.

Berenger published a paper suggesting a new technique using an absorbing layer. This absorbing layer is designed artificially and placed around the outer boundary of the computational domain. It is placed in this scheme to especially absorb without reflecting the electromagnetic waves so outgoing plane wave incidents at an arbitrary angle to this layer is absorbed completely in this layer without reflecting them back [41]. On simple words, the outgoing plane wave upon this absorbing layer is passed or transmitted completely to free space.

To achieve PML principle, Berenger in his PML paper, considered a PML medium for two-dimension problems in Transverse Electric (TE) case, where electrical field using Cartesian coordinates is in x, y plane without varying along the z-axis as shown below in the figure 3.3.

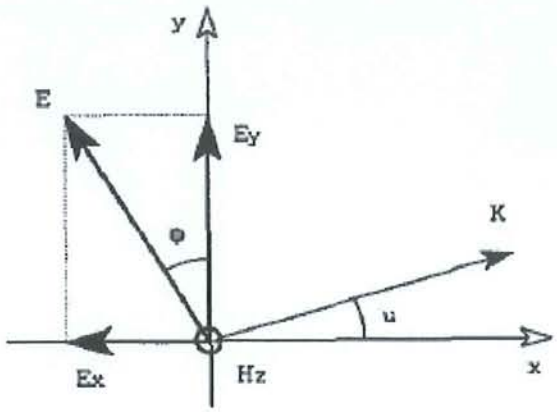

Figure 3.3: Transverse Electric (TE) case

Then, the Maxwell's equations were reduced into three equations in a medium with electric conductivity (σ) and magnetic conductivity (σ*) as follows, after deriving the three involved electromagnetic fields E_x , E_y and E_z :

$$\varepsilon_o \frac{\partial E_x}{\partial t} + \sigma E_x = \frac{\partial H_z}{\partial y} \tag{3.21}$$

$$\varepsilon_o \frac{\partial E_y}{\partial t} + \sigma E_y = -\frac{\partial H_z}{\partial x} \tag{3.22}$$

$$\mu_o \frac{\partial H_z}{\partial t} + \sigma^* H_z = \frac{\partial E_x}{\partial y} - \frac{\partial E_y}{\partial x} \tag{3.23}$$

With, the following condition satisfied,

$$\frac{\sigma}{\varepsilon_0} = \frac{\sigma^*}{\mu_0} \tag{3.24}$$

This implies that, the impedance of concerned absorbing layer or medium is equal to the free space impedance and reflection does not occur (incident plane wave is fully propagated).

In addition, the technique breaks the magnetic component H_y into two subcomponents which can be denoted as H_{yx} and H_{yz}. For TE case, the four

components of the electromagnetic field using PML medium definition can be written as follows:

$$\varepsilon_o \frac{\partial E_x}{\partial t} + \sigma_y E_x = \frac{\partial \left(H_{zx} + H_{Zy} \right)}{\partial y} \tag{3.25}$$

$$\varepsilon_o \frac{\partial E_y}{\partial t} + \sigma E_y = -\frac{\partial \left(H_{zx} + H_{zy} \right)}{\partial x} \tag{3.26}$$

$$\mu_o \frac{\partial H_{zx}}{\partial t} + \sigma_x^* H_{zx} = -\frac{\partial E_y}{\partial x} \tag{3.27}$$

$$\mu_o \frac{\partial H_{zy}}{\partial t} + \sigma_y^* H_{zy} = \frac{\partial E_x}{\partial y} \tag{3.28}$$

here, $H_z = H_{zx} + H_{zy}$

The PML technique can be visualized in a frame as in figure 3.4 that shows the absorbing PML media around the computational domain [42].

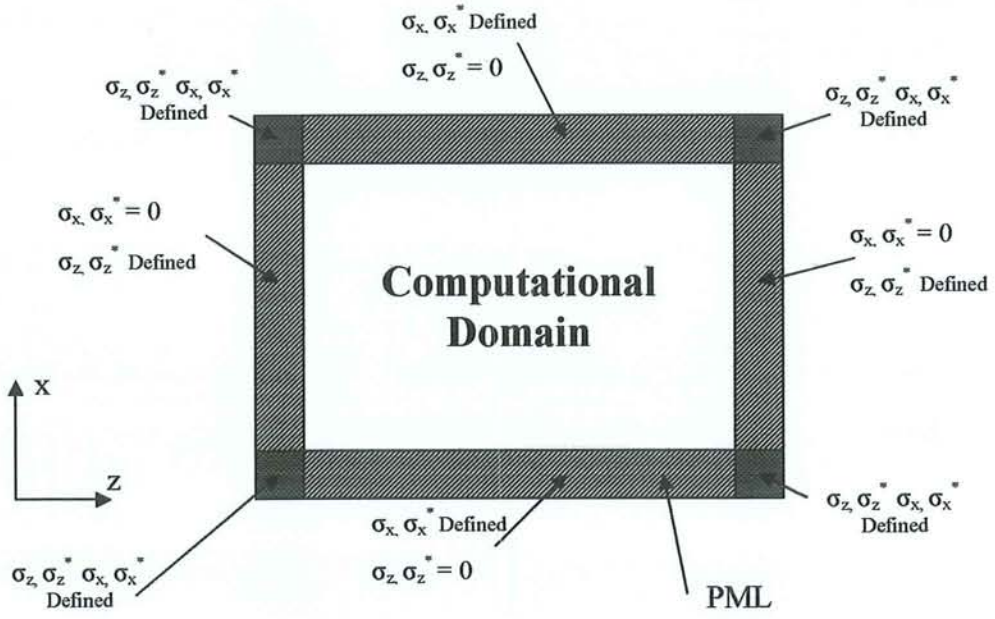

Figure 3.4: The PML technique Frame [42]

Few year later, Berenger PML absorbing boundary condition was modified by Chen, Fang, and Gao in [43] and two PML conductivity formulas have been developed as follows :

$$\sigma(\rho) = \sigma_{\max}\left(\frac{\rho}{d}\right)^{n} \tag{3.29}$$

$$\sigma_{\max} = -\frac{(n+1)\varepsilon_0 v \ln(R_0)}{2d} \tag{3.30}$$

where d denotes the thickness of the PML, n is the order, v is the light velocity, and R_0 is the reflection from the PML at normal incidence.

Similarly, in Transverse Magnetic (TM) case, PML technique breaks the magnetic component E_y into two subcomponents which can be denoted as E_{yx} and E_{yz} and the four components of the electromagnetic field using PML medium definition can be written as follows:

$$\varepsilon_o \frac{\partial E_{zx}}{\partial t} + \sigma_x E_{zx} = \frac{\partial H_y}{\partial x} \tag{3.31}$$

$$\varepsilon_o \frac{\partial E_{zy}}{\partial t} + \sigma_y E_{zy} = \frac{\partial H_x}{\partial y} \tag{3.32}$$

$$\mu_o \frac{\partial H_x}{\partial t} + \sigma_y^* H_x = \frac{\partial (E_{zx} + E_{zy})}{\partial y} \tag{3.33}$$

$$\mu_o \frac{\partial H_y}{\partial t} + \sigma_x^* H_y = \frac{\partial (E_{zx} + E_{zy})}{\partial x} \tag{3.34}$$

here, $E_z = E_{zx} + E_{zy}$

3.3 NUMERICAL DISPERSION AND STABILITY

During simulation a wave problem in the computational domain, numerical dispersion is generated from the Maxwell's curl equations (equations 3.15 ~ 3.20) as the phase velocity of the wave solved numerically in FDTD grid may differ from the actual of the light speed. The phase velocity of the numerical wave was reported in [41], depending on three factors: the direction of propagation, wavelength, and the cell size. Therefore, to control the limit of amount of the numerical dispersion, the edges of each cell must be at least ten times smaller than the shortest wavelength expected to propagate in the computational domain. The smaller the cell size used the more computational demand of the model is needed. A rule-of-thumb is that

$$\Delta x, \Delta y, \Delta z \leq \frac{\lambda_0}{10} \tag{3.35}$$

Where, λ_0 is meant for shortest wavelength.

In numerical methods context, both accuracy and stability are extremely important for reliable and useful solution. Accuracy is related to the closeness of the approximated solution to the exact solution and stability is the requirement to ensure that scheme does not diverge with the time. Otherwise, computed result for $\bar{E}$ and $\bar{H}$ fields components in an unstable model will increase without limit as the simulation progresses.

To meet computational stability requirement, the next equation known as Courant-Freidrichs-Lewy (CFL) Stability Criterion, which shows the relationship between the time increment Δt and space increment Δx, Δy and Δz, must be satisfied.

$$\Delta t \leq \frac{1}{c_{\max}\sqrt{\left(\frac{1}{(\Delta x)^2}\right)+\left(\frac{1}{(\Delta y)^2}\right)+\left(\frac{1}{(\Delta z)^2}\right)}} \tag{3.36}$$

where, c_{max} is the maximum wave velocity in the region.

3.4 PARAMETERS CALCUATIONS

Now having introduced Yee's mesh and representation of the electromagnetic fields as well as ABC and PML, time comes to put all together in one FORTAN program to compute numerically the electromagnetic fields and get needed current and voltage transient time parameters data. These obtained data will be used to calculate the input impedance and return loss parameter (S_{11}) data frequency spectrum in another FORTRAN program. Then, MATLAB software is used to re-arrange the calculated FORTRAN data and to generate plots accordingly.

The transient time response of current and voltage are the first two calculated parameters data, after exciting the structure with an input voltage as a Gaussian pulse as shown in figure 3.5. Current and voltage time response are plotted in figure 3.6 and figure 3.7 respectively. Both plots show that current and voltage time response fluctuating at the beginning of time steps and then reach

zero value (total time steps taken in the FORTAN program was 20,000 time steps).

The simulated structure is with relative dielectric 2.2 and has substrate dimensions 40x49x1.58 mm and patch dimensions 29.25x38.35 mm. The patch was fed with a coaxial line, source was placed on one third and one half of the patch x and y dimensions.

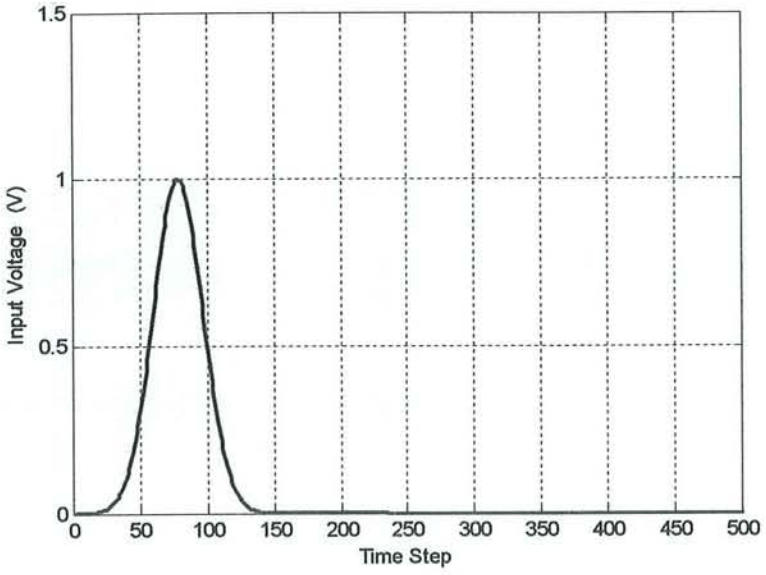

Figure 3.5: Excitation Input Voltage as a Gaussian pulse

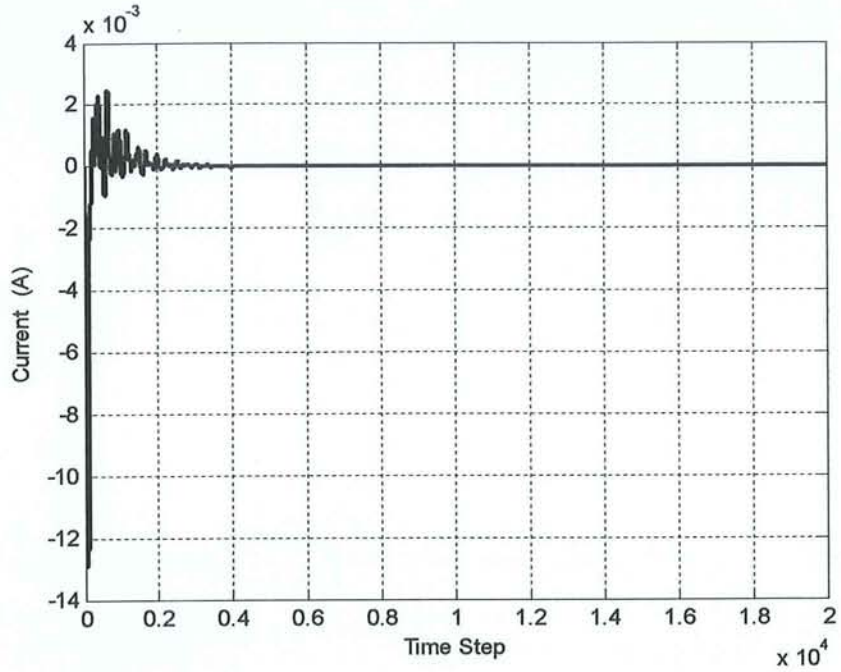

Figure 3.6: Transient current for the basic patch antenna

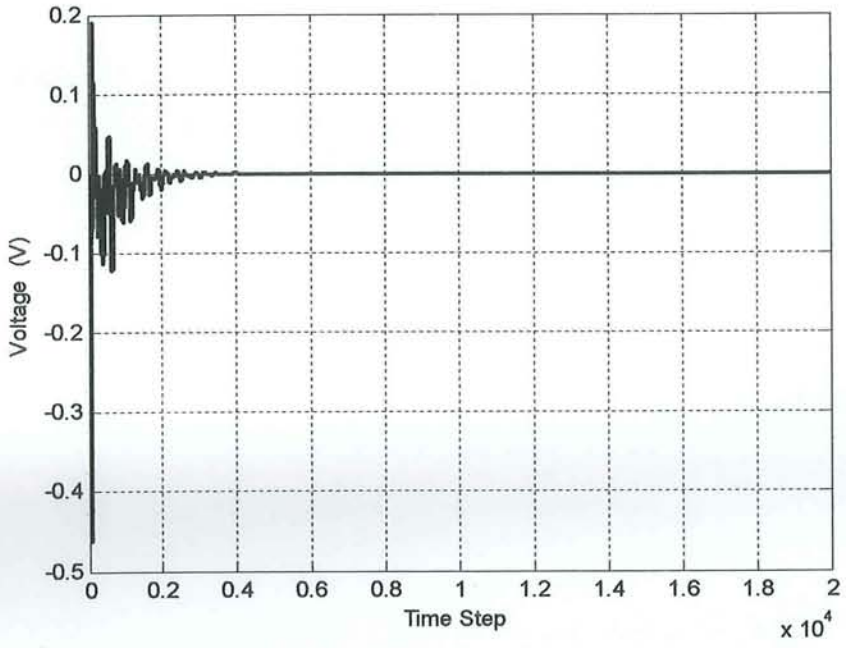

Figure 3.7: Transient voltage for the basic patch antenna

Obtaining the current and voltage time response data is not the end of the story. The current or i(t) and voltage or v(t) time response data will be saved by one FORTRAN program file and then they will retrieved back by another FORTRAN program file after taking their Fourier transformation.

After that, the second FORTRAN program file will start calculating the structure input impendence and then, the S11 parameter will be calculated as function of frequency.

The input impedance can be obtained by Fourier Transform of voltage over Fourier Transform of current and it is given by:

$$Zin = \frac{FT\{v(t)\}}{FT\{i(t)\}} \qquad (3.37)$$

Then, input impedance can be written in real (resistance) and imaginary (reactance) forms by :

$$Zin = R + jX \qquad (3.38)$$

Once the real and imaginary input values of impedance are obtained, MATLAB will be used to plot them versus frequency as shown in figure 3.8 and figure 3.9.

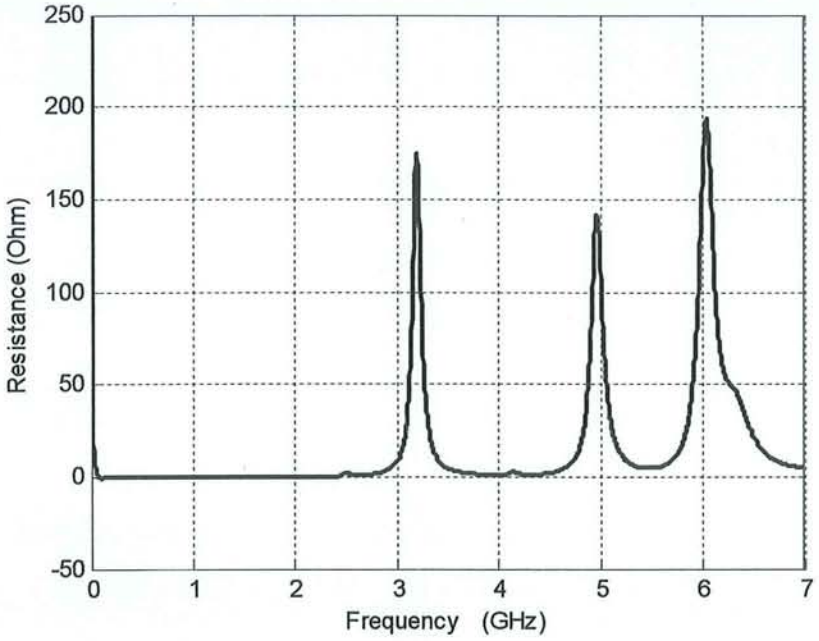

Figure 3.8: Frequency response for input impedance (real) for the basic patch antenna

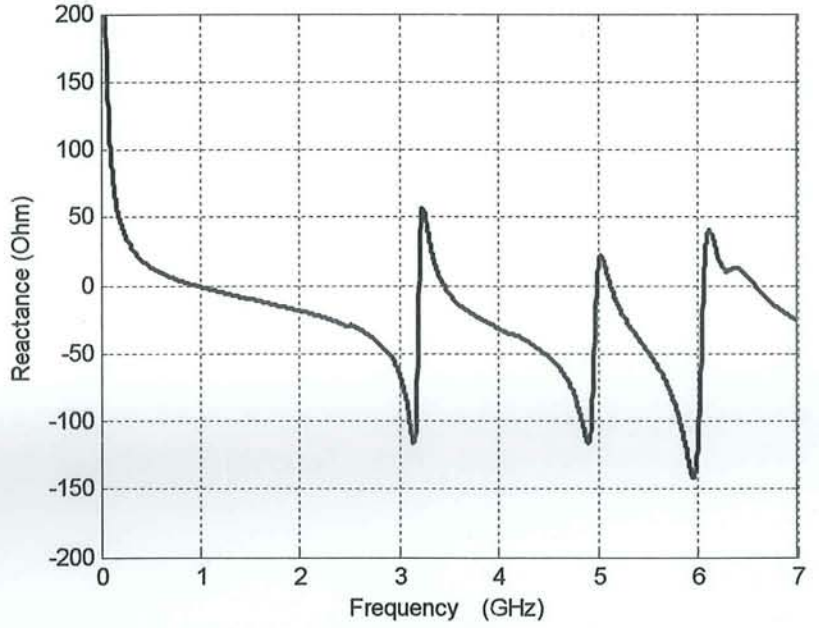

Figure 3.9: Frequency response for input impedance (imaginary) for the basic patch antenna

After that, S_{11} parameter will be calculated using equation 3.39 where Zo is the source impedance (taken as 50 Ω) and then, S_{11} parameter frequency response can be plotted as shown in figure 3.10. It is worth mentioning that the maximum taken FORTRAN frequency spectrum was chosen to be 7 GHz.

$$S11 = 20 * \log_{10}\left(\left|\frac{Zin - Zo}{Zin + Zo}\right|\right) \tag{3.39}$$

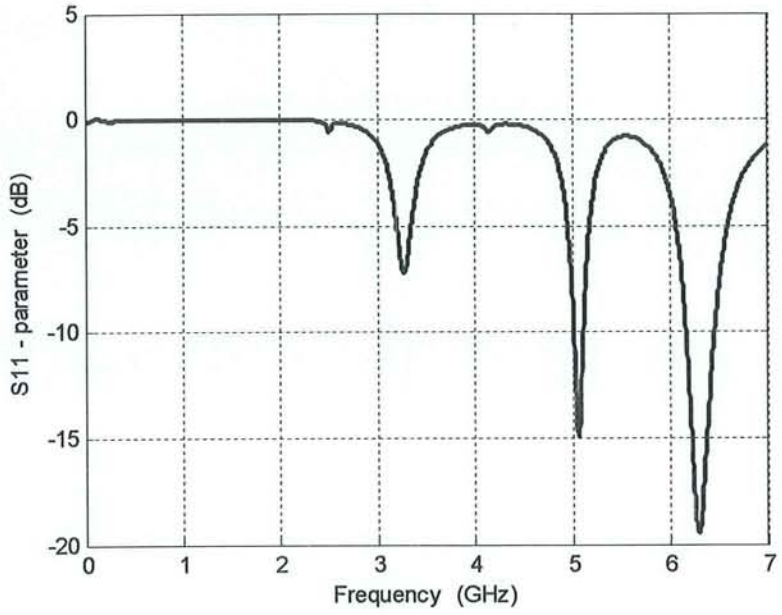

Figure 3.10: Frequency response for S_{11} Parameter for the basic patch antenna

CHAPTER 4

SIMULATION RESULTS FOR EBG-BASED ANTENNA STRCUTURES

This chapter lists all FDTD simulation results for EBG-based antenna structures where EBG was applied on the antenna ground plane and on the patch. Then, it will highlight some observations at the end of this chapter.

4.1 EBG ON GROUND PLANE RESULTS

Initially, trials were made to study the effects of placing EBG structure on the ground plane of patch antenna. FORTAN program was used as a tool to numerically represents the electromagnetic problem and calculate electromagnetic fields after introducing EBG concept. Then, MATLAB software was used to plot the generated S_{11} parameter data for each case and get it compared with a basic design problem set as a reference structure for all cases. The following paragraphs describe these trials and comment on the observations.

First of all, a patch antenna basic design as a reference with substrate dimensions 24x24x0.79 mm and patch dimensions 8x8 mm was used for the following cases. The source will be fed into the patch on one third and one half of the patch x and y patch dimensions respectively. This patch antenna basic design is resonating at 12 GHz and 17 GHz as shown in figure 4.2.

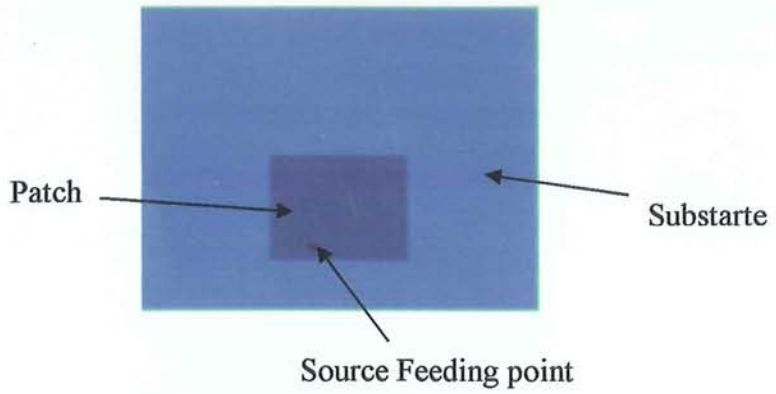

Figure 4.1: Patch antenna basic design as a reference layout

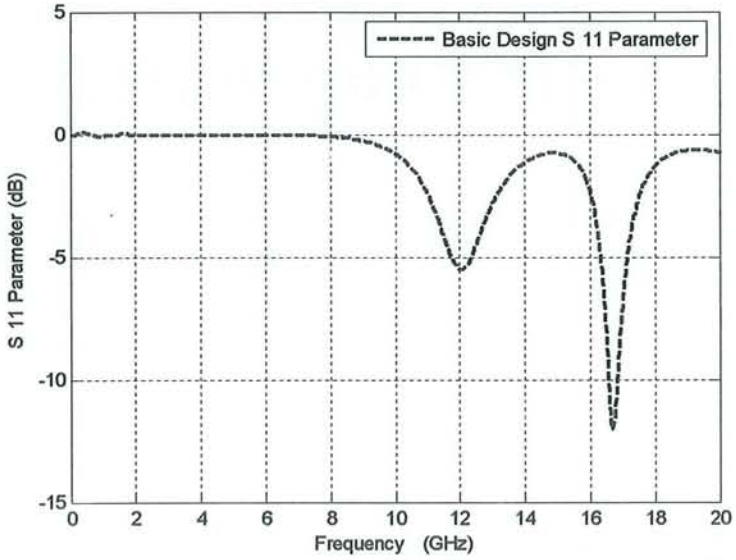

Figure 4.2: Patch antenna basic design as a reference layout S_{11} parameter

If EBG is introduced in the ground plane as depicted in figure 4.3, resonance frequency at 12 GHz starts sharpening and bandwidth starts increasing as shown in figure 4.4.

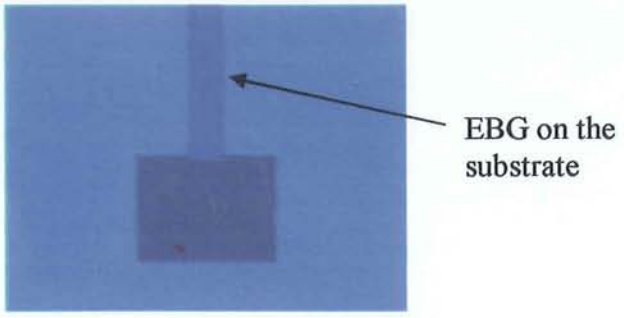

Figure 4.3: Patch antenna EBG case 1 layout

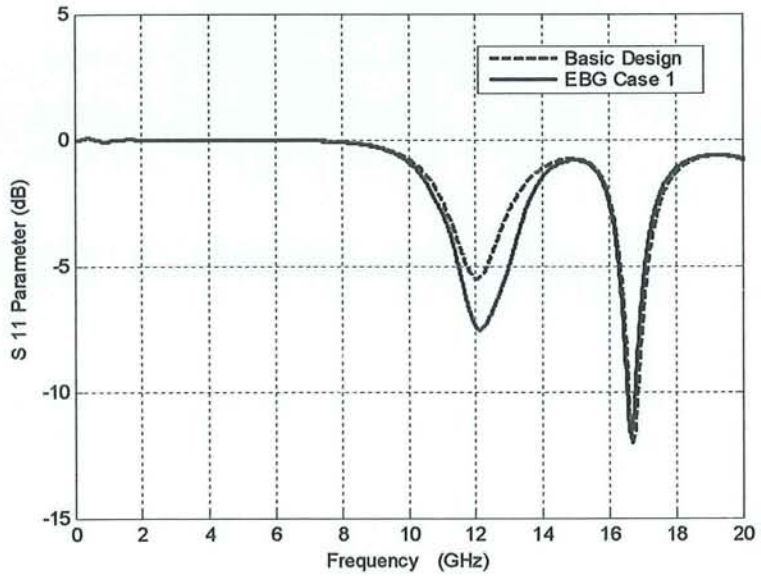

Figure 4.4: Patch antenna EBG case 1 S_{11} parameter

Now, if an EBG similar to the above case is extended on the substrate into the middle of the patch as illustrated in figure 4.5, resonance frequency at 12 GHz and 17 GHz sharpen more especially the one at 12 GHz whereas, the resonance frequency at 17 GHz is shifted to around 15 GHz. For both resonance frequencies, bandwidth increases more and one more resonant frequency at low range approximately at 8 GHz starts appearing as shown in figure 4.6.

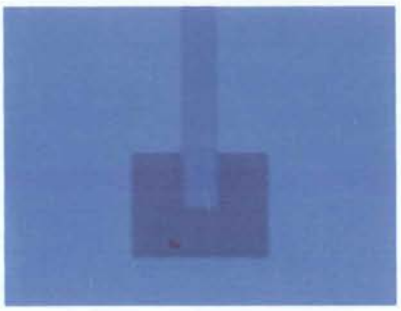

Figure 4.5: Patch antenna EBG case 2 layout

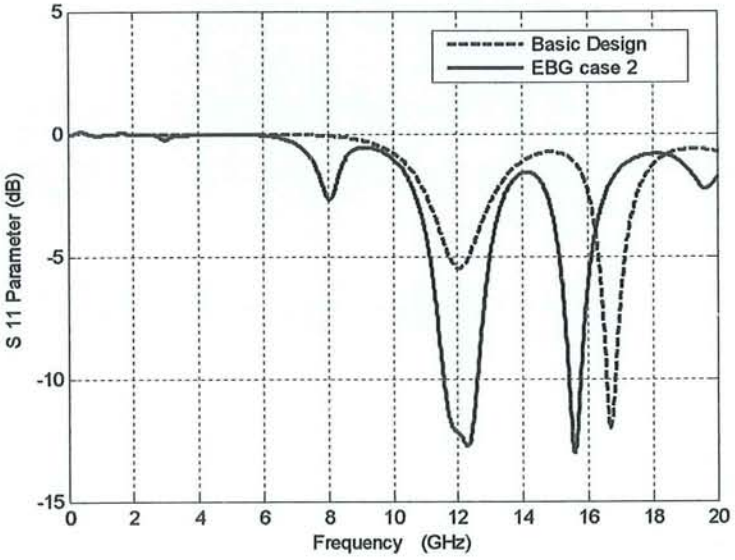

Figure 4.6: Patch antenna EBG case 2 S_{11} parameter

If the EBG concept was made as above case except EBG is widen as illustrated in figure 4.7, resonance frequencies at 12 GHz and 17 GHz continue sharpening more and shifted to lower frequency range, specifically at 11 GHz and 15 GHz as shown in figure 4.8. Consequently bandwidths at 11 GHz and 15 GHz continue increasing more in addition to that, a resonant frequency at low frequency range around 8 GHz starts appearing.

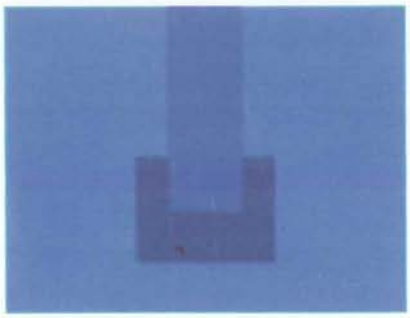

Figure 4.7 Patch antenna EBG case 3 layout

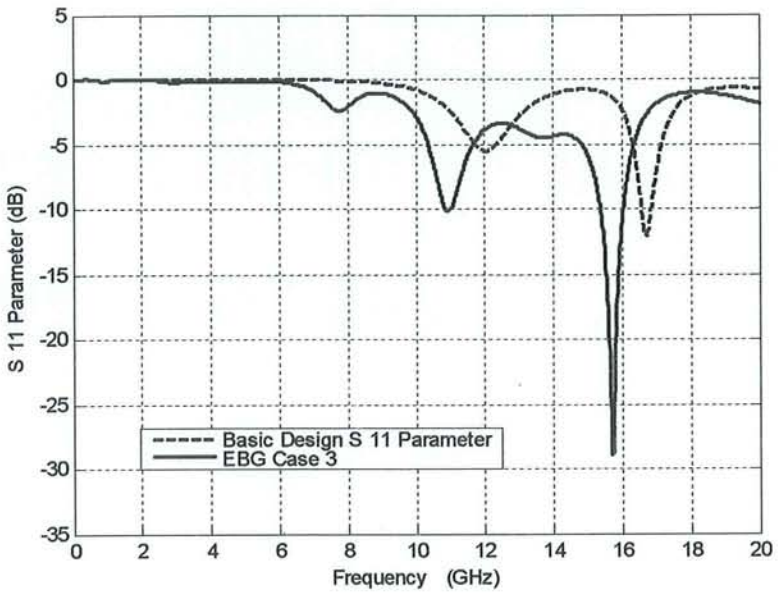

Figure 4.8 Patch antenna EBG case 3 S_{11} parameter

The case will be different, if the EBG is applied on the ground plane from substrate edge to middle of the distance to the patch as shown in figure 4.9. The resonance frequencies at 12 GHz and 17 GHz as well as their bandwidth are almost maintained unchanged as illustrated in figure 4.10

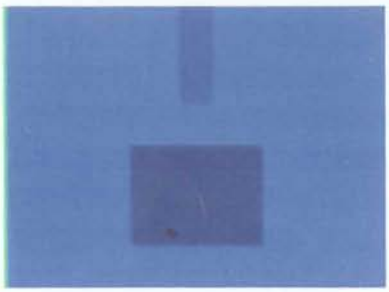

Figure 4.9: Patch antenna EBG case 4 layout

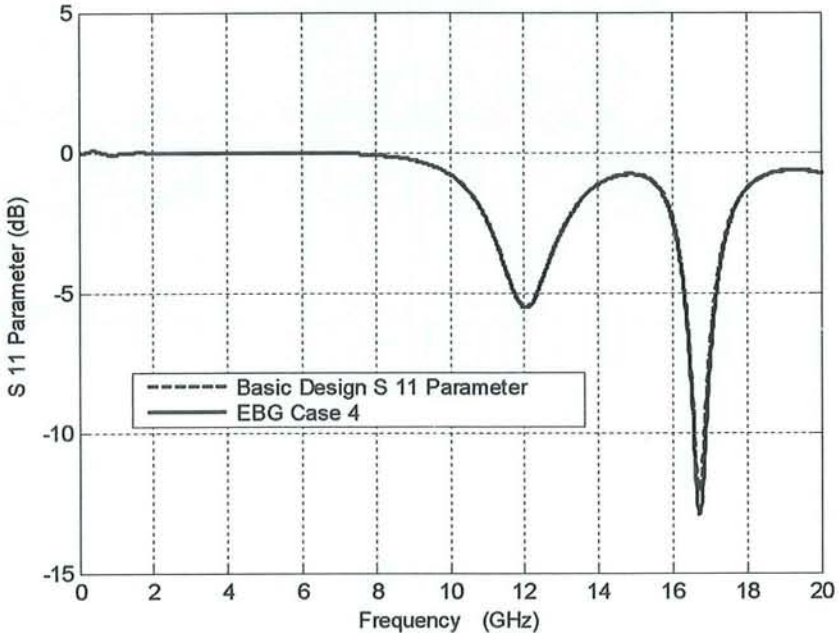

Figure 4.10 Patch antenna EBG case 4 S_{11} parameter

In the next case, EBG was placed in another location. It was placed to the right side, and extended to two thirds of the patch as shown in figure 4.11. Resonance frequencies at 12 GHz and 17 GHz sharpen more and one new resonance frequency at 15 G Hz appears while resonance frequency at 17 GHz does not become dominant. Resonance frequencies bandwidths increase more consequently. In addition to that, more resonant frequencies at lower and higher frequencies ranges start appearing specifically at nearly 3 GHz and 7 GHz as shown in figure 4.12.

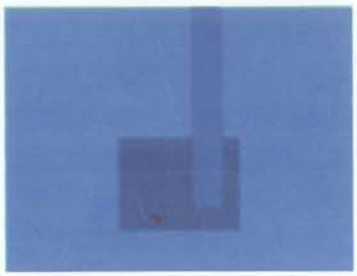

Figure 4.11: Patch antenna EBG case 5 layout

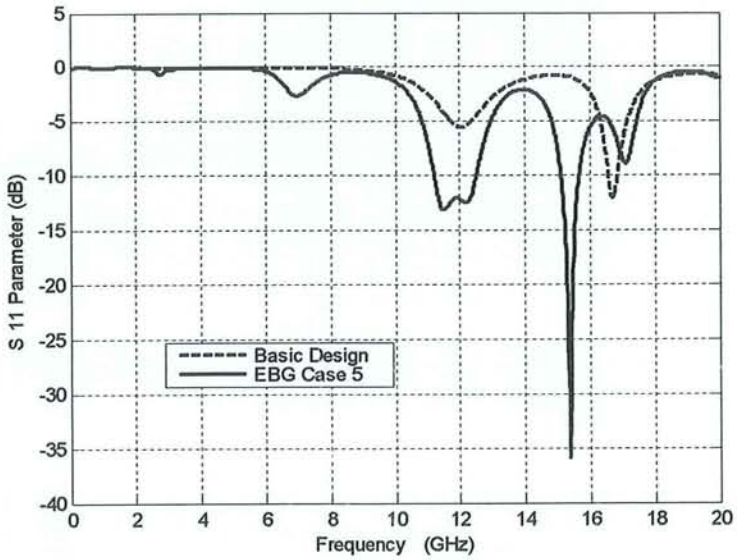

Figure 4.12: Patch antenna EBG case 5 S_{11} parameter.

In the next case, EBG was placed in the left side, extended to two thirds of the patch and then, branched inside the patch as illustrated in figure 4.13. The resonance frequencies at 12 GHz and 17 GHz are changed and multiple resonance frequencies at lower and higher frequencies range (10 GHz, 12 GHz, 14 GHz and 18 GHz) start appearing. Resonance frequencies at 10 GHz and 18 GHz are sharp and new resonance frequencies bandwidths are larger than the basic design resonance frequencies bandwidths as shown in figure 4.14.

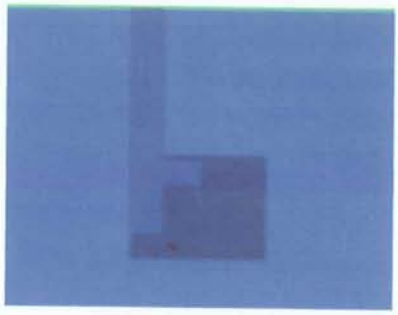

Figure 4.13: Patch antenna EBG case 6 layout

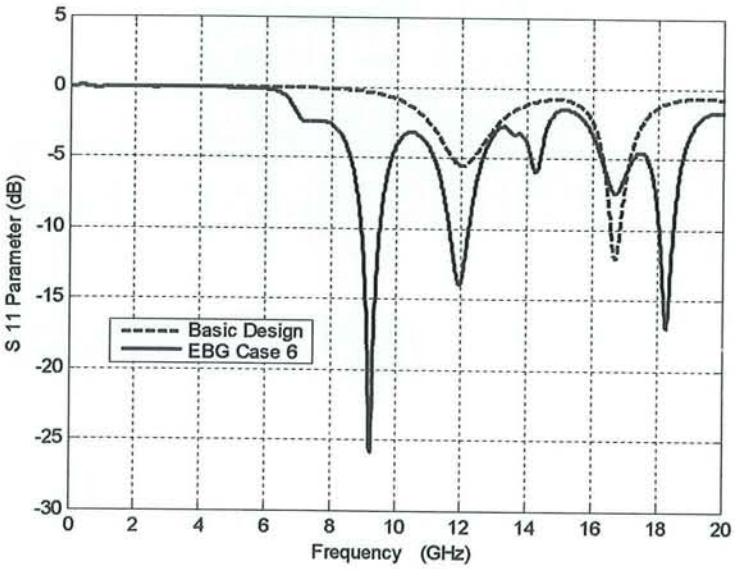

Figure 4.14: Patch antenna EBG case 6 S_{11} parameter

Adding more EBG to the structure on the ground plane as two identical lines extended to middle of the patch as illustrated in figure 4.15, sharpens resonance frequencies at 12 GHz and 17 GHz and shifts them to nearly 11 GHz and 16 GHz plus having one resonance frequency with small bandwidth at low frequency range (at 8 GHz). Consequently, resonance frequencies bandwidths at 11 GHz and 16 GHz increase as shown in figure 4.16.

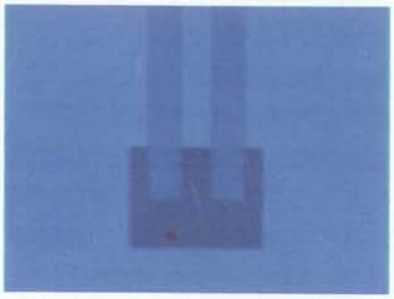

Figure 4.15: Patch antenna EBG case 7 layout.

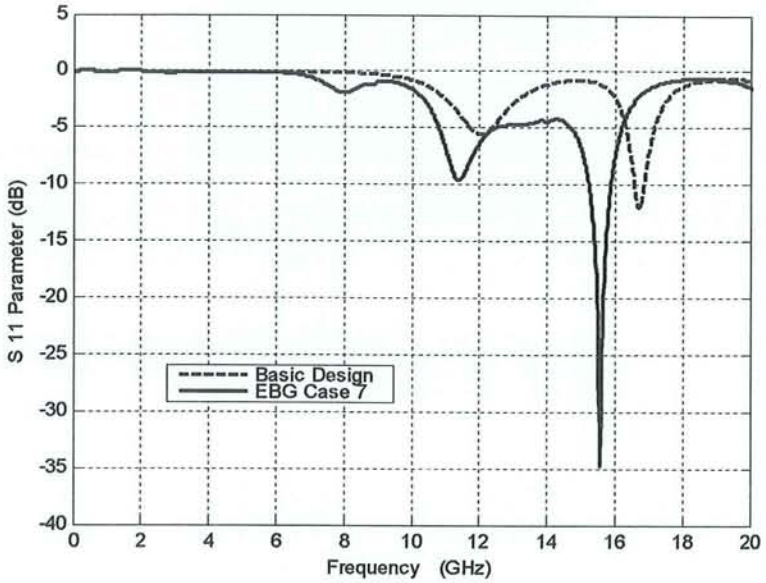

Figure 4.16: Patch antenna EBG case 7 S_{11} parameter

On the other hand, if EBG is added to the structure as two lines that are not identically extending to the middle of the patch as illustrated in figure 4.17, sharpens resonance frequencies at 12 GHz and 17 GHz and shift them to 11 GHz and 14 GHz and. Consequently, resonance frequencies bandwidths at 11 GHz and 14 GHz increase. In addition to that, multiple resonance frequencies at low frequency range (at 3 GHz and 6 GHz) are obtained as shown figure 4.18.

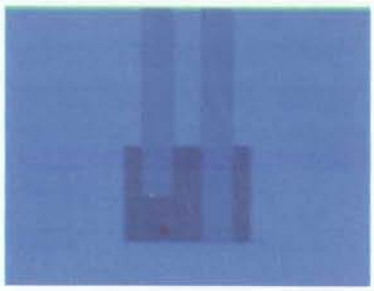

Figure 4.17: Patch antenna EBG case 8 layout

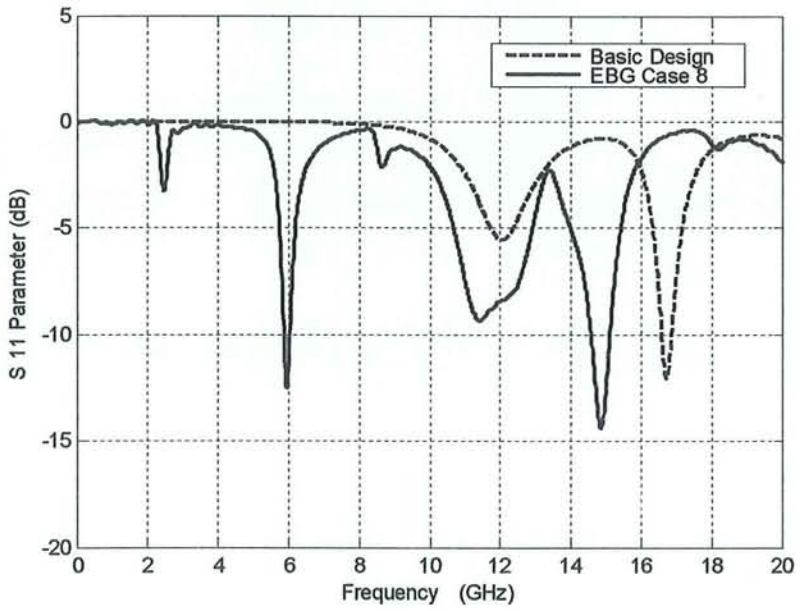

Figure 4.18: Patch antenna EBG case 8 S_{11} parameter

4.2 EBG ON PATCH RESULTS

If we change the way that EBG is placed and place it on the patch itself, different effects take place. A wide EBG line or EBG slot as shown in figure 4.19 was place and consequently one sharper resonance frequency at 9 GHz was obtained. The resonance frequencies at 12 GHz and 17 GHz were shifted to 11 GHz and 15 GHz as presented in figure 4.20. However, the resonance frequencies will be shifted to 11 GHz and 15 GHz and one sharper resonance frequency at lower frequency range (at 7 GHz) will be obtained as shown in figure 4.22, if the EBG with four wide slots are placed in the patch alone as in figure 4.21.

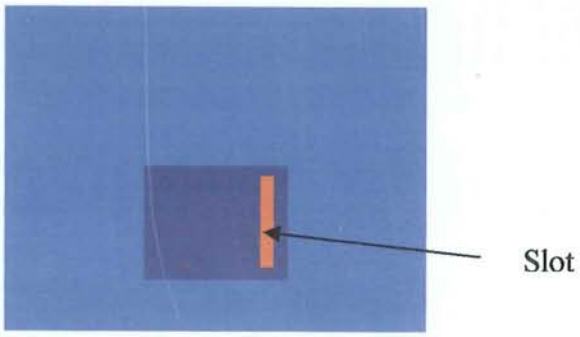

Figure 4.19: Patch antenna EBG case 9 layout

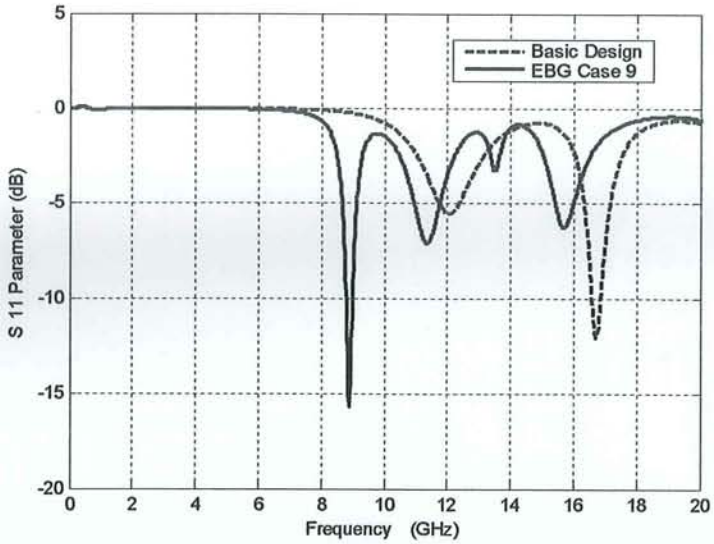

Figure 4.20: Patch antenna EBG case 9 S_{11} parameter

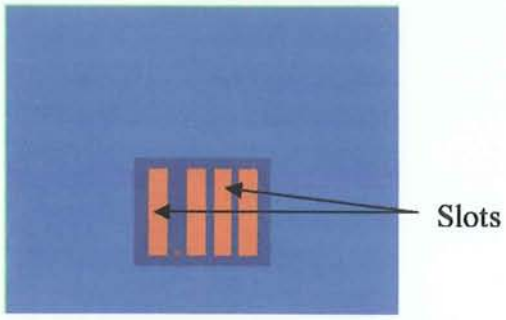

Figure 4.21: Patch antenna EBG case 10 layout

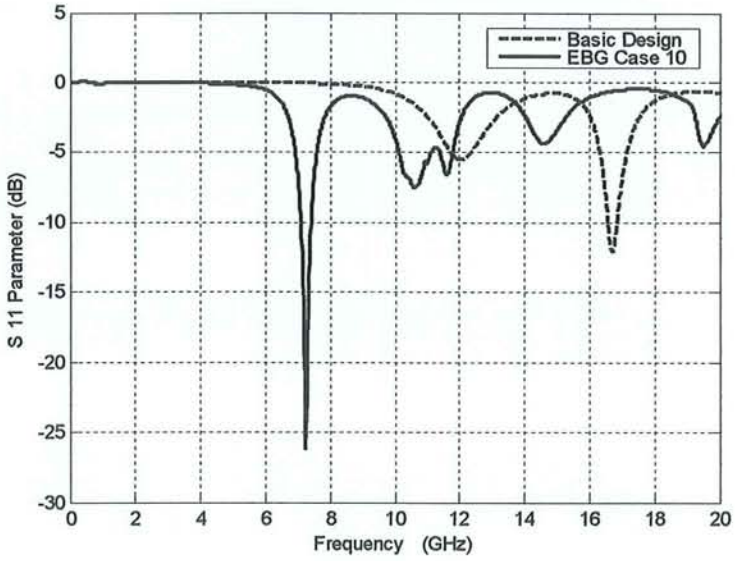

Figure 4.22: Patch antenna EBG case 10 S_{11} parameter

Moreover, if an EBG loading structure in the ground plane of the patch alone is inserted on the reference structure as illustrated in figure 4.23, multiple resonance frequencies (at 5 GHz, 8 GHz and 11 GHz and 17 GHz) will be obtained. The new resonance frequencies are shaper than the original ones and their bandwidths are better compared with the basic design bandwidths as shown in figure 4.24. Moreover, a resonance frequency for the structure can be obtained at the lower range also as presented in figure 4.26, if enhanced EBG loading structure is applied as in figure 4.25.

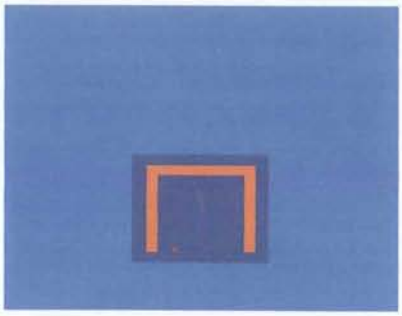

Figure 4.23: Patch antenna EBG case 11 layout

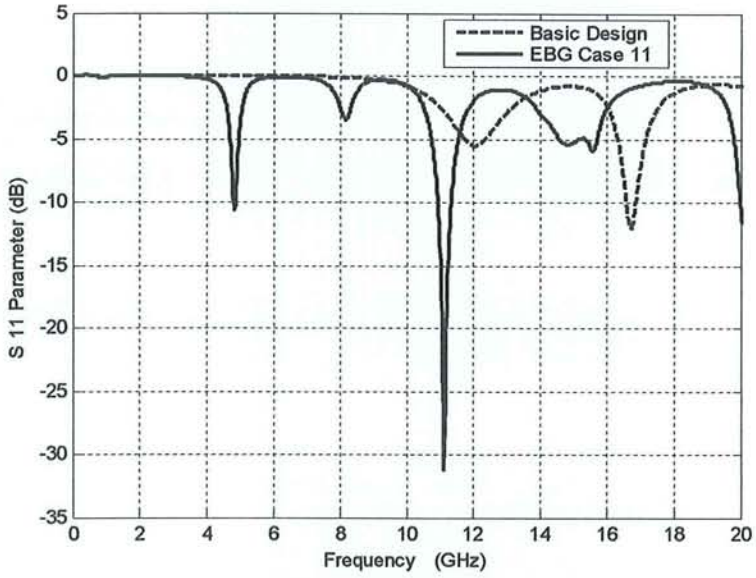

Figure 4.24: Patch antenna EBG case 11 S_{11} parameter

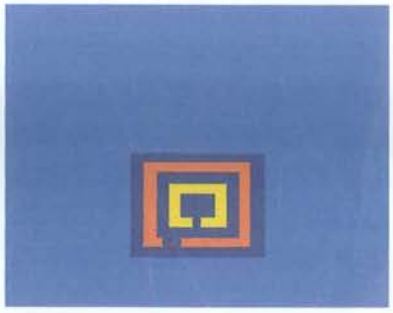

Figure 4.25: Patch antenna EBG case 12 layout

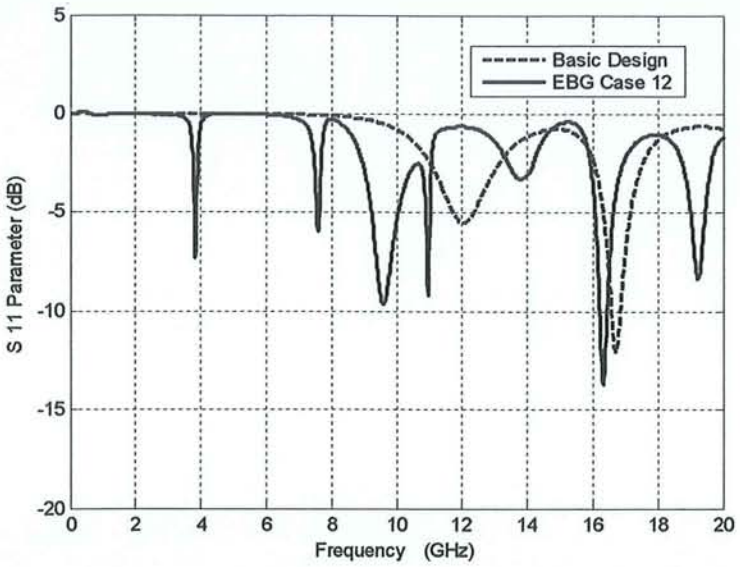

Figure 4.26: Patch antenna EBG case 12 S_{11} parameter

4.3 OBSERVATIONS

From the previous structures, we observed that EBG placement in the ground plane of the substrate and on the patch itself, can play positively or negatively with the structure resonance frequencies and bandwidth. This is because, EBG is able to sharpen the resonance frequencies, enlarge or shorten the bandwidth or even shift the resonance frequencies of the structure toward the low or high frequency range.

Keeping these observations in mind and referring to the thesis main objective to design an EBG-based low profile patch antenna that resonate at low frequency range for wireless communications applications, the design will be re-worked. To seek for this objective, another patch antenna with different dimensions will be used as a basic design or reference for the following cases. The basic design or reference patch antenna dimensions and parameters that suit desired thesis application, taking into account the electromagnetic fringing effect, were mathematically calculated. The below equations will be used to calculate the

effective substrate relative dielectric and patch antenna effective length (L) based on a resonance frequency at 1 GHz, relative dielectric that is equal to 2.2 and substrate thickness that is equal to 1.58 cm:

$$w = \frac{1}{2f_r\sqrt{\mu_o\varepsilon_o}}\sqrt{\frac{2}{\varepsilon_r+1}} \tag{4.1}$$

$$\varepsilon_r eff = \frac{\varepsilon_r+1}{2} + \frac{\varepsilon_r-1}{2}\left[1+12\frac{\mathrm{h}}{\mathrm{w}}\right]^{-\frac{1}{2}} \tag{4.2}$$

$$\Delta L = 0.412h\left[\frac{(\varepsilon_r eff+0.3)\left(\frac{w}{h}+0.264\right)}{(\varepsilon_r eff-0.258)\left(\frac{w}{h}+0.8\right)}\right] \tag{4.3}$$

$$L\ eff = \frac{\lambda}{2} - 2\Delta L \tag{4.4}$$

where, w is width , L is length of patch, ΔL is increase in patch length due to fringing effect, λ is wavelength and h is the substrata thickness, ε_r is dielectric constant or relative permittivity and ε_r eff is effective dielectric constant.

At the end, all needed dimensions for substrate and patch were respectively obtained as 110x140x1.58 mm and 90x118 mm for the new structure as shown in figure 4.27. The new basic structure as shown in figure 4.28 theoretically resonates at 1.1 GHz and 1.7 GHz.

Figure 4.27: New basic design Patch antenna layout

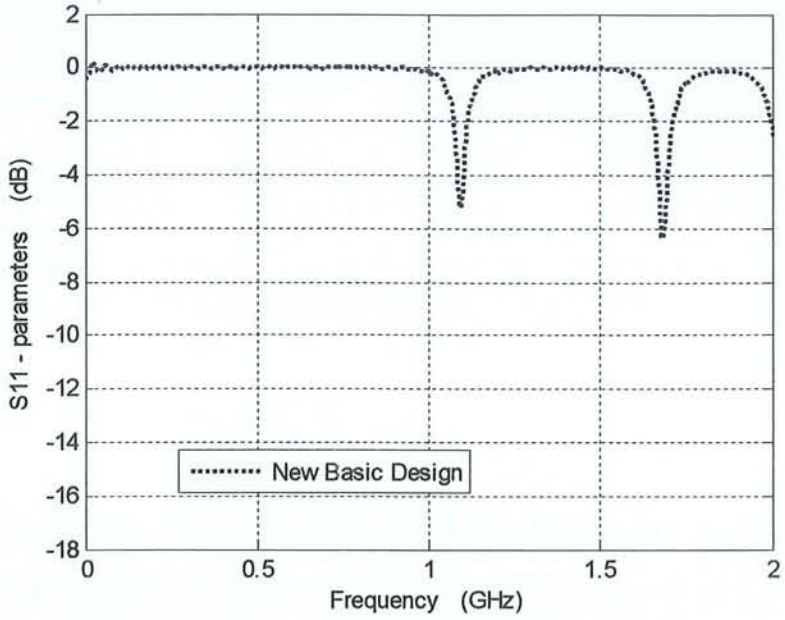

Figure 4.28: New Patch antenna design S_{11} parameter

Implementing the modified EBG loading structure on the patch alone on the reference design as illustrated in figure 4.29 and figure 4.31, results in having two new resonance frequencies below 1 GHz and shifting the original resonance frequencies to lower frequencies ranges maintaining the bandwidth as shown in figure 4.30 and in figure 4.32 . A better improvement in bandwidth and resonance frequencies is noticed when structure as in figure 4.31 is used.

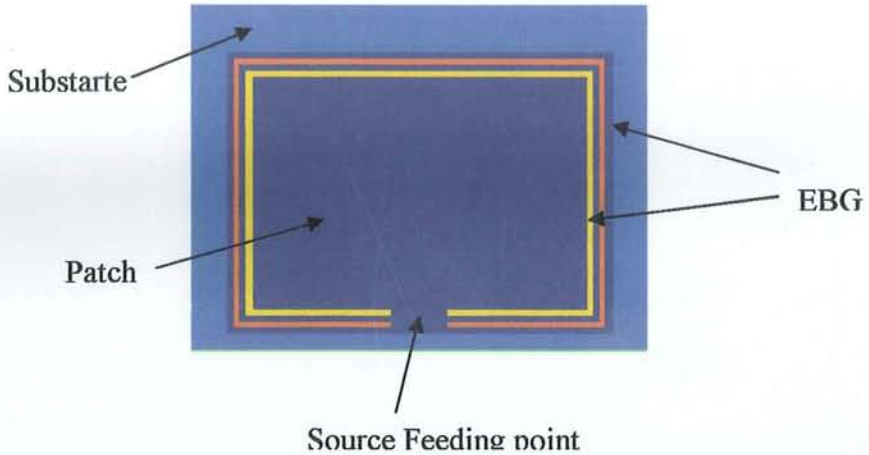

Figure 4.29: Patch antenna EBG case 13 layout

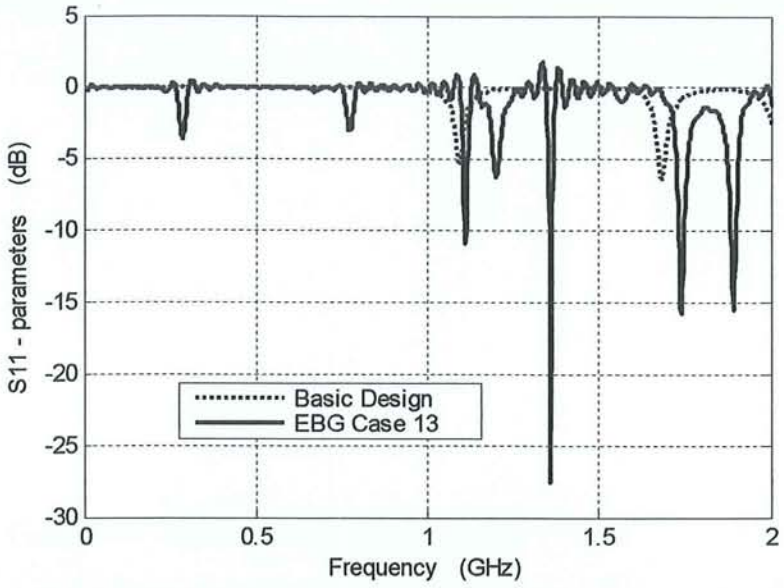

Figure 4.30: Patch antenna EBG case 13 S_{11} parameter

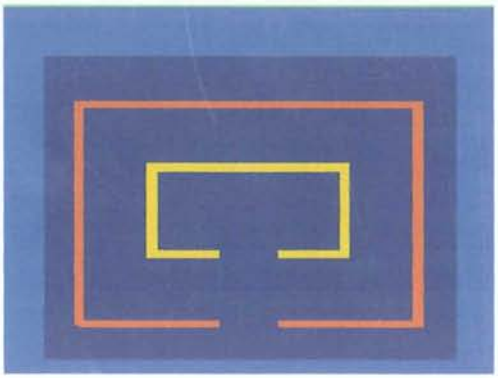

Figure 4.31: Patch antenna EBG case 14 layout

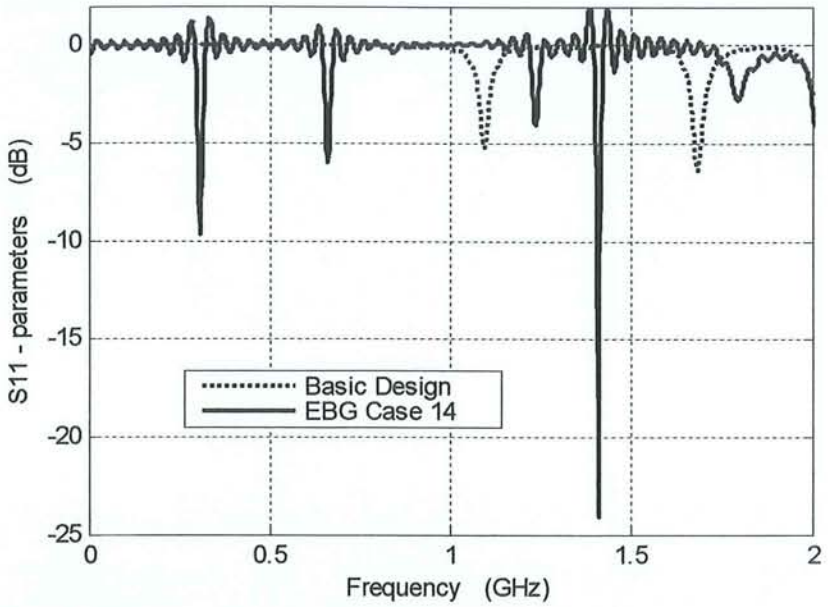

Figure 4.32: Patch antenna EBG case 14 S_{11} parameter

If EBG structure is designed with additional EBG as illustrated in figure 4.33, the resonance frequencies at lower frequencies range will be sharpened compared with the basic design resonance frequencies. On the other hand, the resonance frequencies at high frequencies range will be shifted to lower frequencies ranges as shown in figure 4.34.

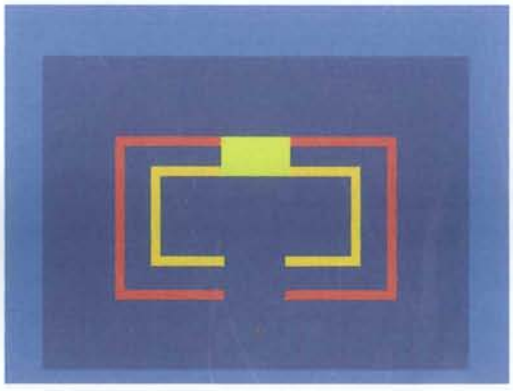

Figure 4.33: Patch antenna EBG case 15 layout

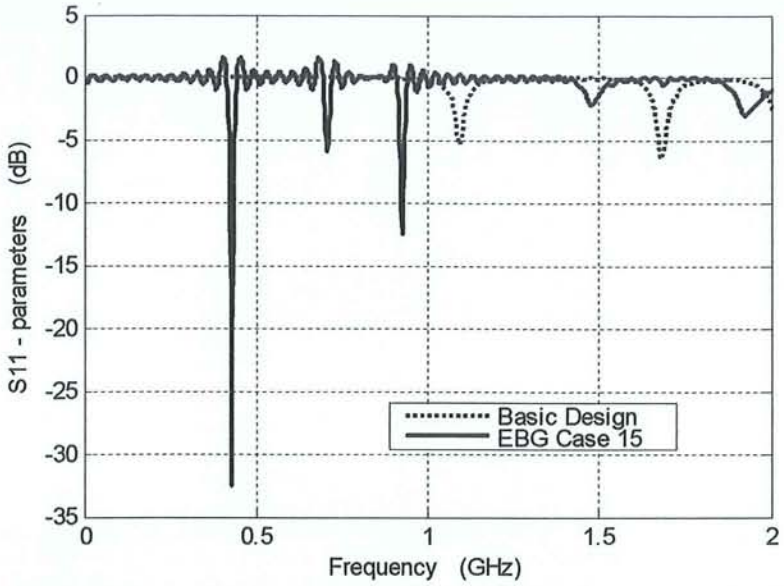

Figure 4.34: Patch antenna EBG case 15 S_{11} parameter

Better resonance performance and enhanced bandwidth are obtained as figure 4.36 shows when Spilt Ring Resonator (SRR) is utilized as depicted in figure 4.35 with proper selections of all SRR spaces and distances.

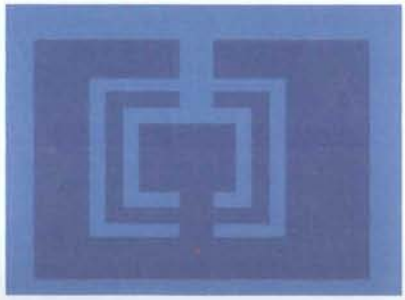

Figure 4.35: Patch antenna EBG case 16 layout

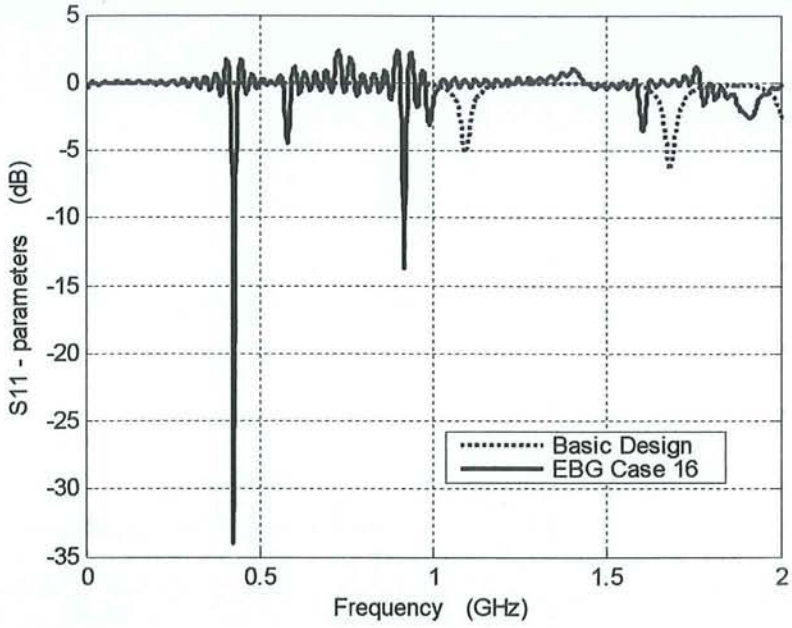

Figure 4.36: Patch antenna EBG case 16 S_{11} parameter

We have observed in this chapter that positioning EBG on the ground plane or on the patch gave us good improvement toward the patch antenna resonance frequency and bandwidth. The reference design that is supposed to resonate at 1 GHz can now radiate around 0.4 GHz after applying EBG concept. Therefore, patch antenna will be re-designed in which substrate and patch dimensions will be shortened so that it saves on patch size.

As a starting point, the new size of patch antenna substrate and patch dimensions will be chosen as half of the old dimensions. In another word, the substrate dimensions and patch dimensions will be selected to be 55x70x1.58 mm and 45x59 mm respectively as new design and we expect that, it will resonate at 1 GHz with a relative dielectric constant kept unchanged. Figure 4.37 proves the assumption and validates it.

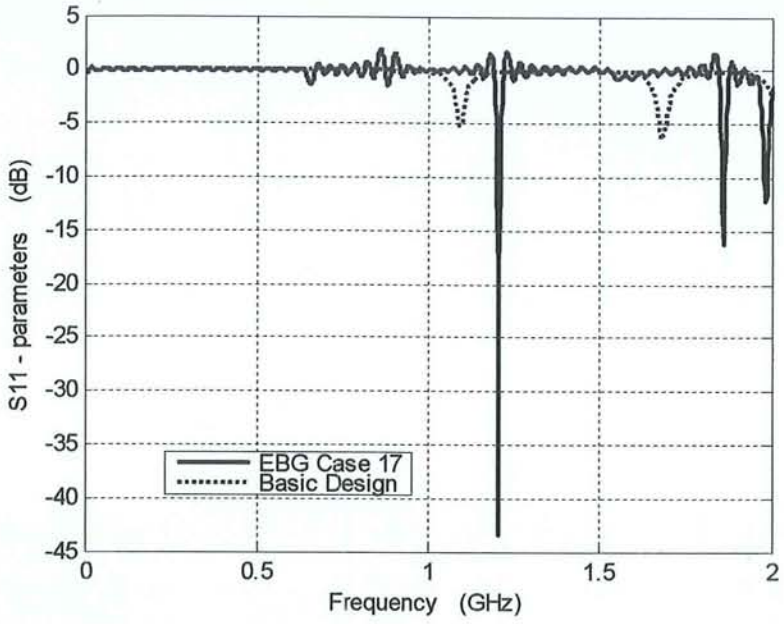

Figure 4.37: Patch antenna EBG case 17 S_{11} parameter

Moving forward for further patch antenna size reduction considering the last case (EBG case 17) as a reference. The S11 parameter of the reference structure is plotted in figure 4.38.

Several trials were made to come up with a good design, which satisfies the thesis objective. These designs were obtained from minimizing pre-defined FORTRAN program step size Δx and Δy (the step size of the reference design is 1 mm). Then, MATLAB software was used directly to visualize the S_{11} parameter for each suggested case (8 cases, were suggested. They are: $\Delta x=\Delta y=$: 0.95 mm, 0.85 mm, 0.78 mm, 0.75 mm, 0.72 mm, 0.70 mm, 0.65 mm, 0.60 mm). S_{11} parameters for these cases are plotted as shown in the following figures (from 4.39 to figure 4.46).

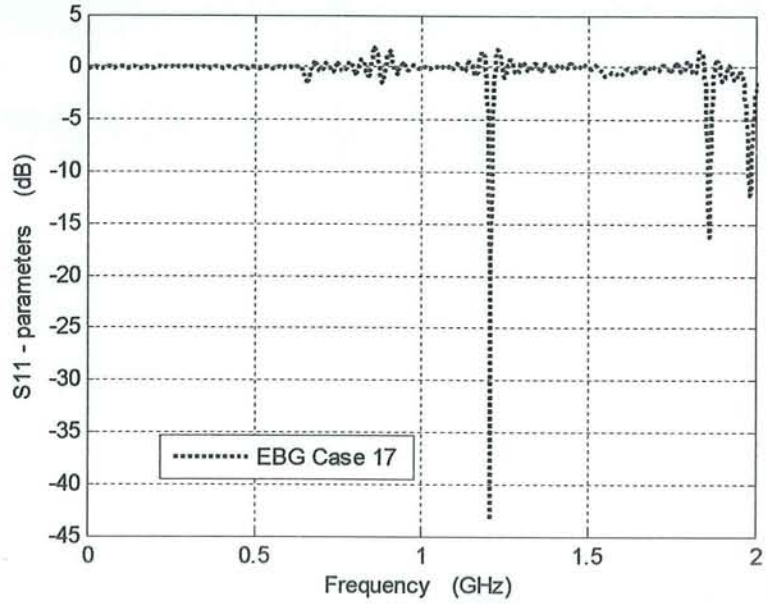

Figure 4.38: S_{11} parameter for new patch antenna reference design

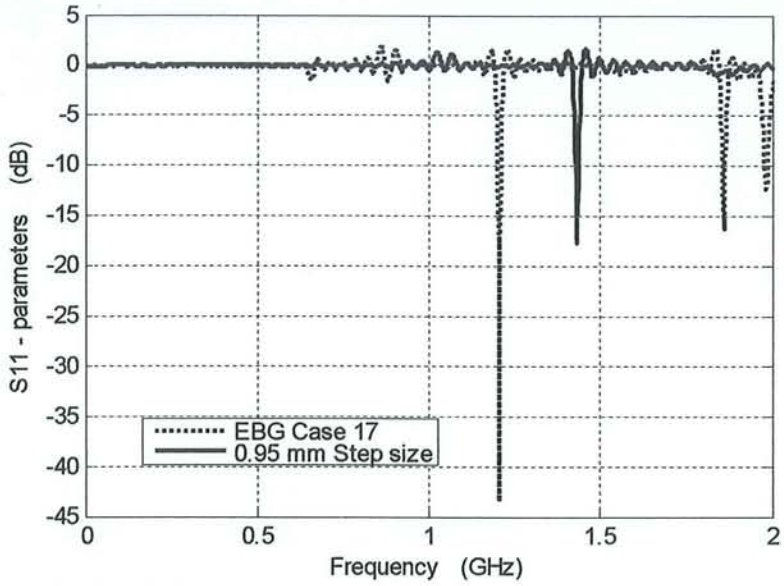

Figure 4.39: S_{11} parameter for the reference design with step size 0.95 mm

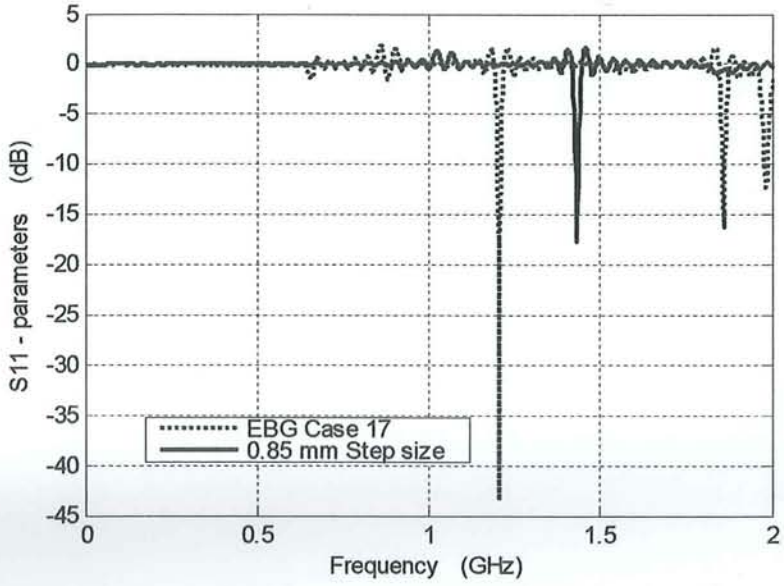

Figure 4.40: S_{11} parameter for the reference design with step size 0.85 mm

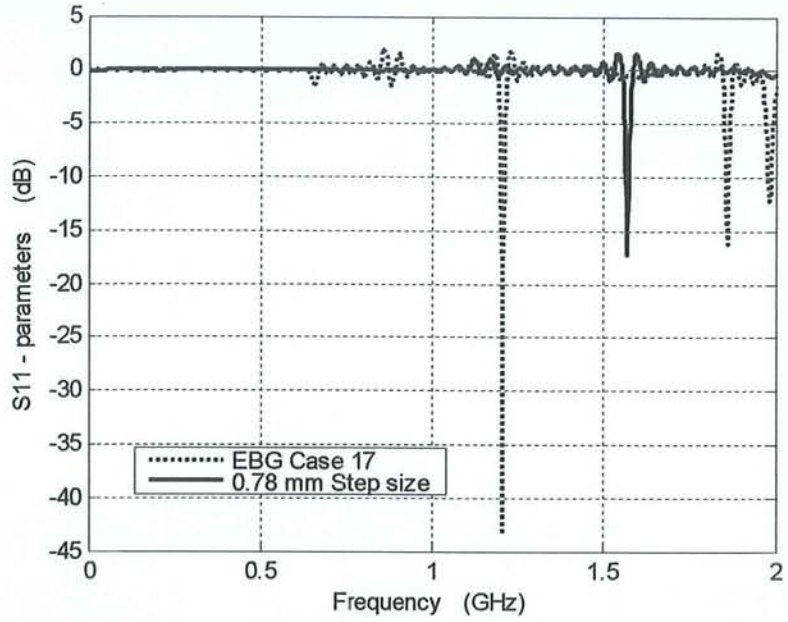

Figure 4.41: S_{11} parameter for the reference design with step size 0.78 mm

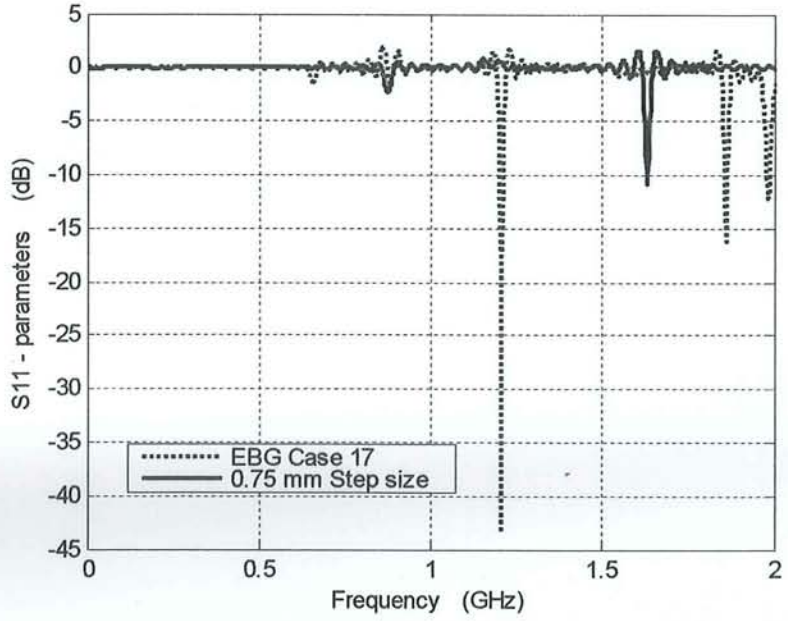

Figure 4.42: S_{11} parameter for the reference design with step size 0.75 mm

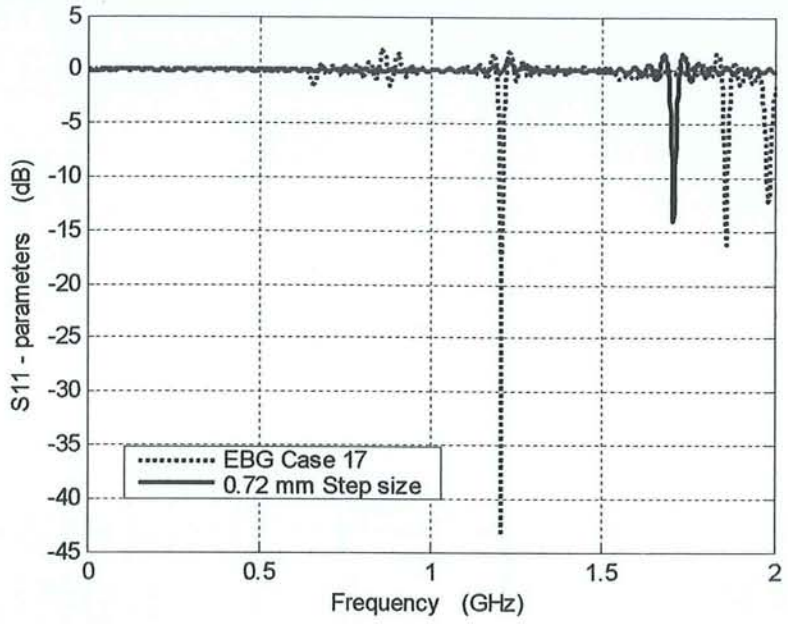

Figure 4.43: S_{11} parameter for the reference design with step size 0.72 mm

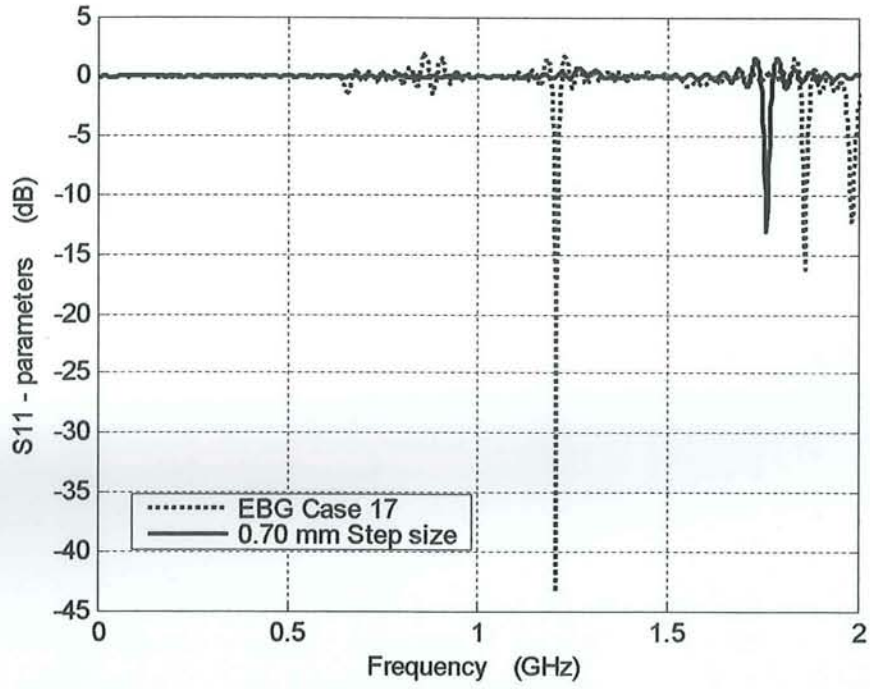

Figure 4.44: S_{11} parameter for the reference design with step size 0.70 mm

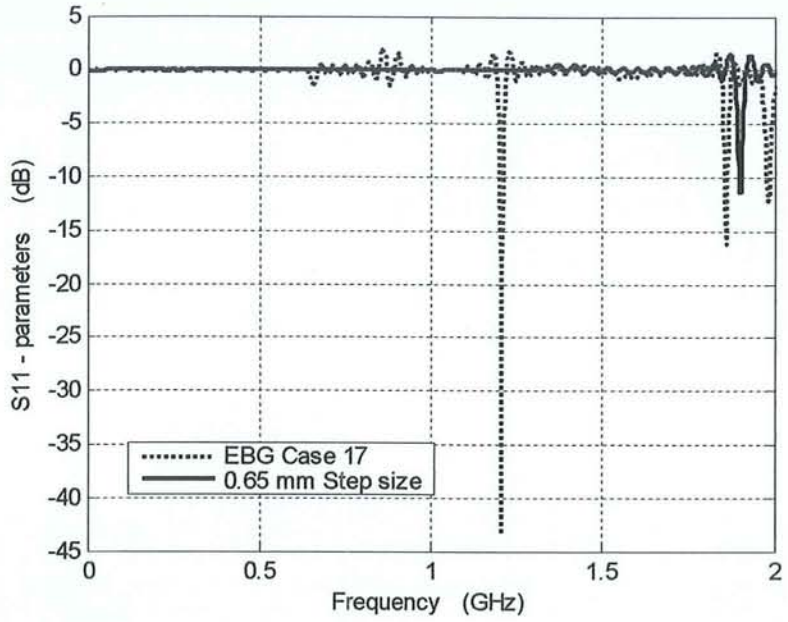

Figure 4.45: S_{11} parameter for the reference design with step size 0.65 mm

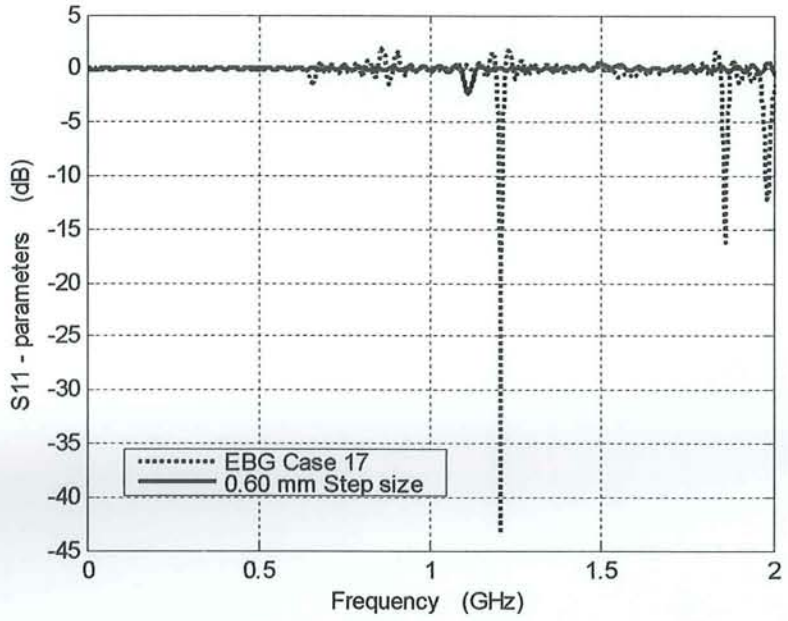

Figure 4.46: S_{11} parameter for the reference design with step size 0.60 mm

We observed, that the design that has step size $\Delta x=\Delta y$ equals 0.65 mm gives good performance for wireless communication among other designs. This is due to the fact that, it has a resonance frequency before 2 GHz (it is at 1.9 GHz with -11.5 dB) with an acceptable bandwidth (bandwidth 24 MHz) and allows for a high size reduction (92.7 % or 89.44 % patch area saving compared to the basic design structure as shown in table 4.1).

Table 4.1: Calculated Patch Size Reduction and Patch Area Saving.

Designs	**Patch Dimension (Width x Length in mm)**	**Patch Size Reduction (cm^2)**	**Patch Area Saving (%)**
Basic design structure	90 X 118 (or 106.20 cm^2)	**Reference**	**Reference**
New design (EBG case 5) as a reference design	45 X 59 (or 26.55 cm^2)	79.65	75.0
Design 1 with 0.95 mm step size	42.75 X 56.05 (or 23.96 cm^2)	82.24	77.43
Design 2 with 0.85 mm step size	38.25 X 50.15 (or 19.18 cm^2)	87.02	81.94
Design 3 with 0.78 mm step size	35.1 X 46.2 (or 16.21 cm^2)	89.99	84.74
Design 4 with 0.75 mm step size	33.75 X 44.25 (or 14.93 cm^2)	91.27	85.94
Design 5 with 0.72 mm step size	32.4 X 42.48 (or 13.76 cm^2)	92.44	87.04
Design 6 with 0.70 mm step size	31.5 X 41.3 (or 13.01 cm^2)	93.19	87.69
Design 7 with 0.65 mm step size	**29.25 X 38.35 (or 11.21 cm^2)**	**94.99**	**89.44**
Design 8 with 0.60 mm step size	27 X 35.4 (or 9.56 cm^2)	96.64	90.99

Seeking further for low profile microstrip patch antenna improvement, EBG concept will be employed on ground plane using several designs to come up with an effective EBG-based low profile patch antenna structure. This will be thoroughly explained in the coming chapter.

CHAPTER 5

ANAYLYSIS OF PROPOSED ANTENNAS MODLES

After several designs, some SRR models were selected and extensively studied theoretically and experimentally. This chapter explains these models and their obtained results and then compares the experimental results with theoretical (FDTD) results.

5.1 FDTD SOLUTIONS

This part of this chapter is devoted for the FDTD solution for some models and then it shows experimental results for best model structure among others.

At the beginning, the reference as figure 5.1 shows, was with substrate dimensions 40x49x1.58 mm and patch dimensions 29.25x38.35 mm while source feeds the patch on one third and one half of the patch x and y dimensions respectively for all following cases. This structure is resonating with three resonance frequencies at 3.2 GHz (with -7 dB and bandwidth 200 MHz), 5 GHz (with -15 dB and bandwidth 300 MHz) and 6.3 GHz (with -19 dB and bandwidth 700 MHz) as figure 5.2 shows.

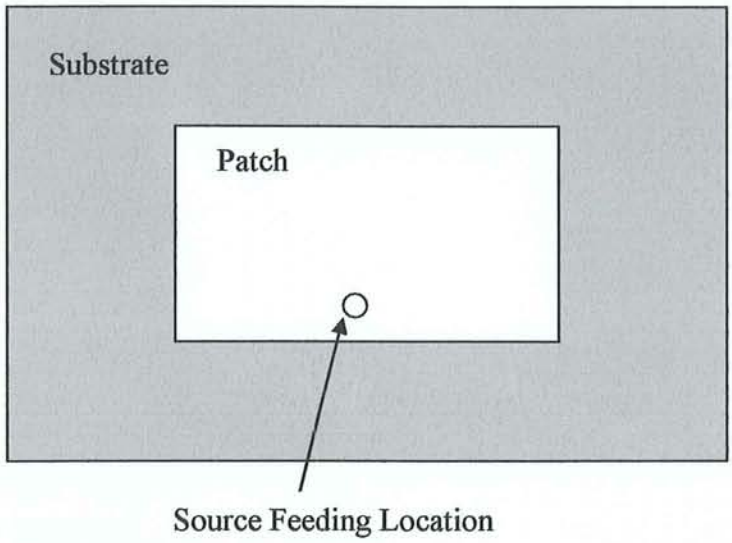

Figure 5.1: Basic Patch Antenna without EBG

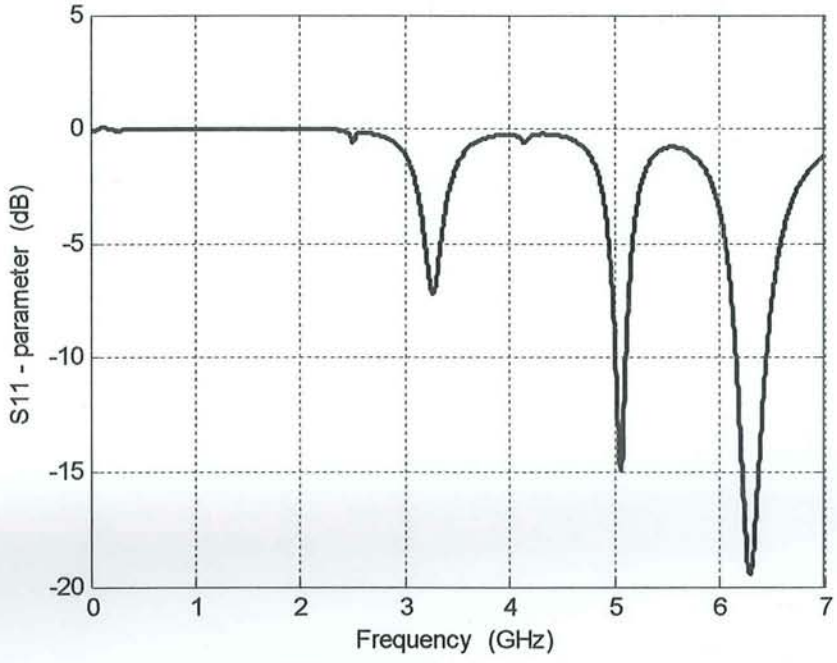

Figure 5.2: Reference Structure without EBG S_{11} Parameter

By introducing an SRR into the patch of the reference structure keeping the dimensions of the structure and feeding point unchanged as depicted in figure 5.3, this structure is able to resonate at 1.9 GHz (-11.5 dB and bandwidth 20 MHz) as in figure 5.4.

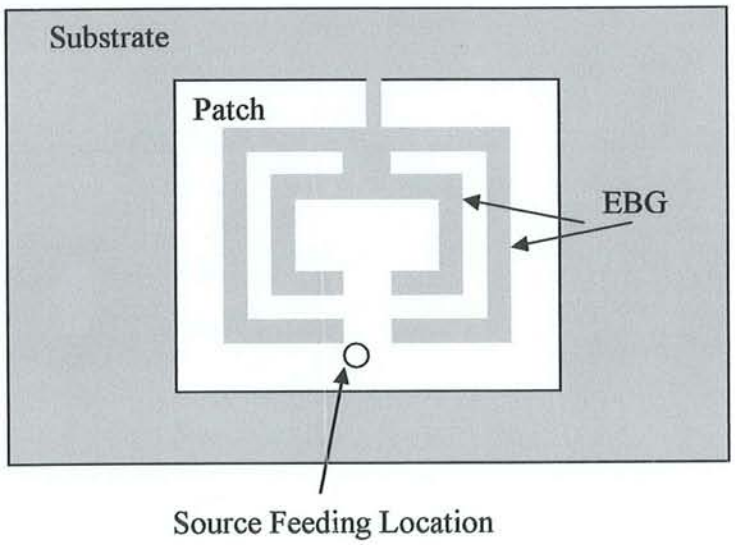

Figure 5.3: Patch Antenna with EBG (SRR on the patch)

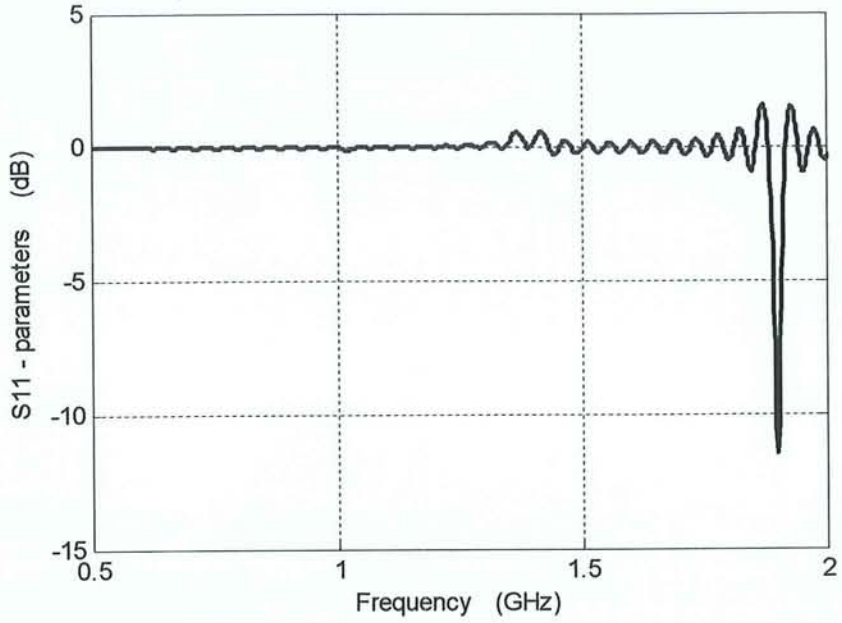

Figure 5.4: Reference Structure with EBG (SRR only)

Now, if same structure that has both reference structure as well as the SRR, maintaining same dimensions of the structure and feeding point location as illustrated in figure 5.5, has inserted EBG on the ground plane, this structure will have two resonance frequencies. One is at 0.9 GHz (- 15 dB and bandwidth 24 MHz) and second is at 1.9 GHz (with -7 dB and bandwidth 1 MHz) as shown in figure 5.6.

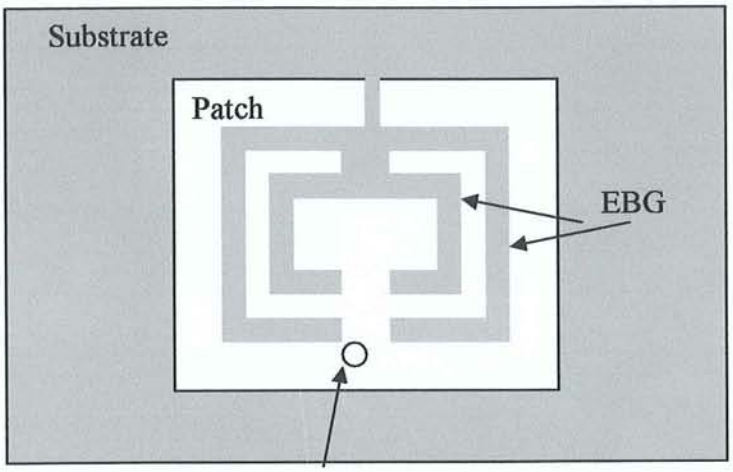

(a)

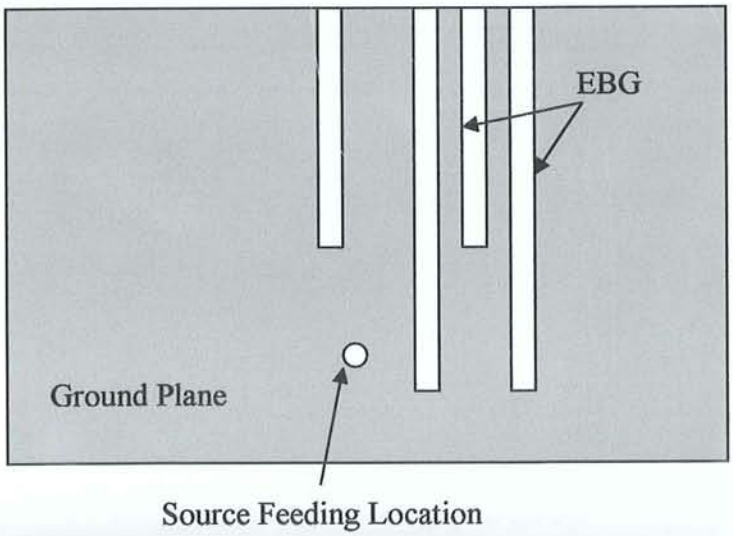

(b)

Figure 5.5: Design No.1, Patch Antenna with EBG (a) Top View and (b) Bottom View

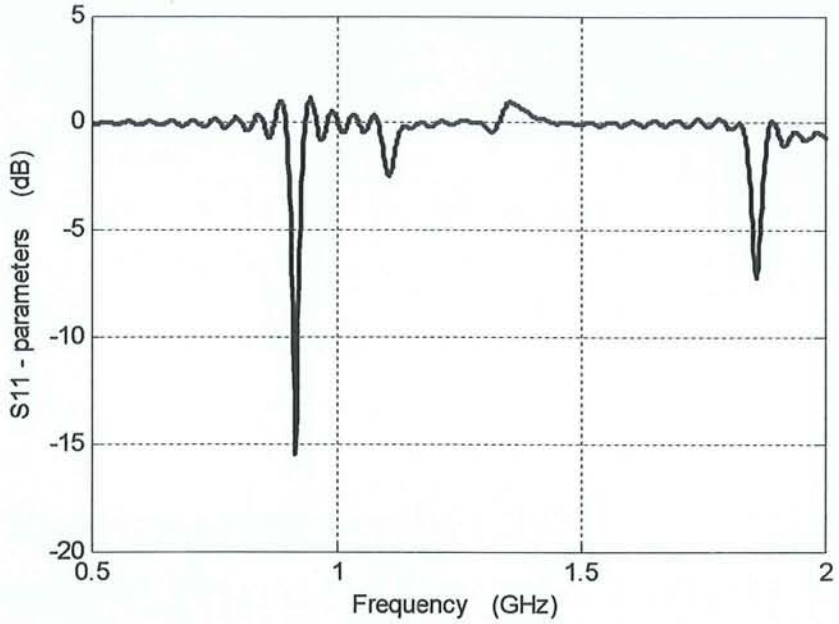

Figure 5.6: Design No. 1 S_{11} Parameter.

However, if the basic or reference structure that has an SRR plus (10 EBG slots or 10 lines) incorporated on the ground plane maintaining all dimensions same as the basic structure including the source feeding point location as illustrated in figure 5.7, this structure will resonate with two resonance frequencies. They are as follows: one is at 1.1 GHz (with -10.7 dB and bandwidth 20 MHz) and second is at 1.78 GHz (with -33 dB and bandwidth 40 MHz) as shown in figure 5.8.

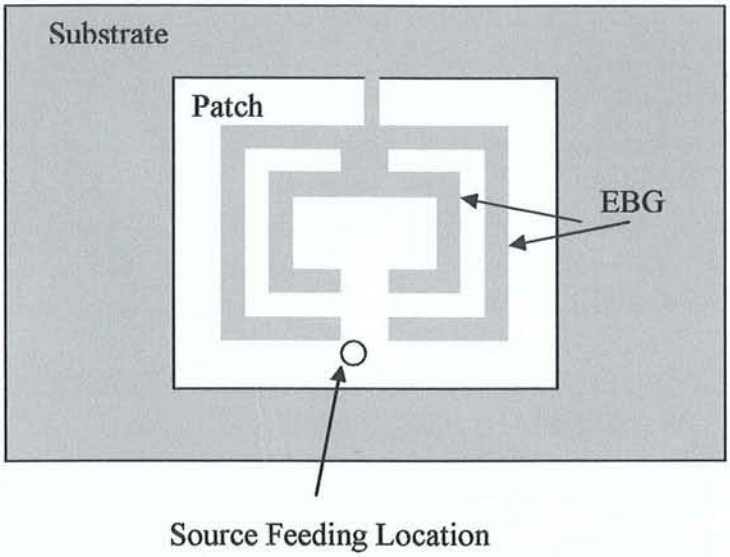

(a)

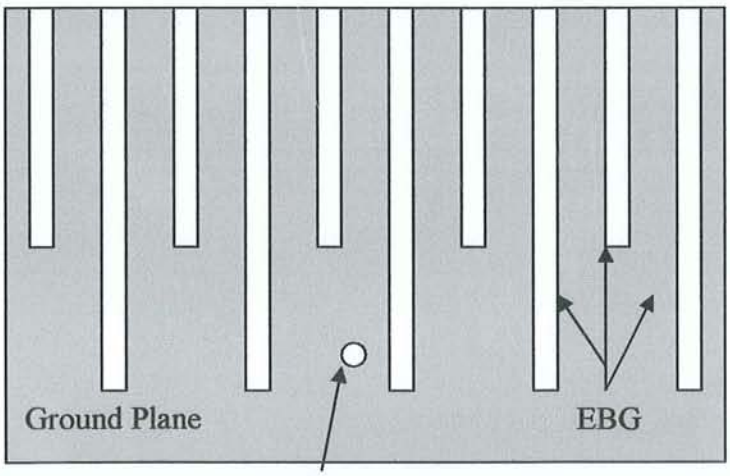

(b)

Figure 5.7: Design No. 2, Patch Antenna with EBG (a) Top View and (b) Bottom View

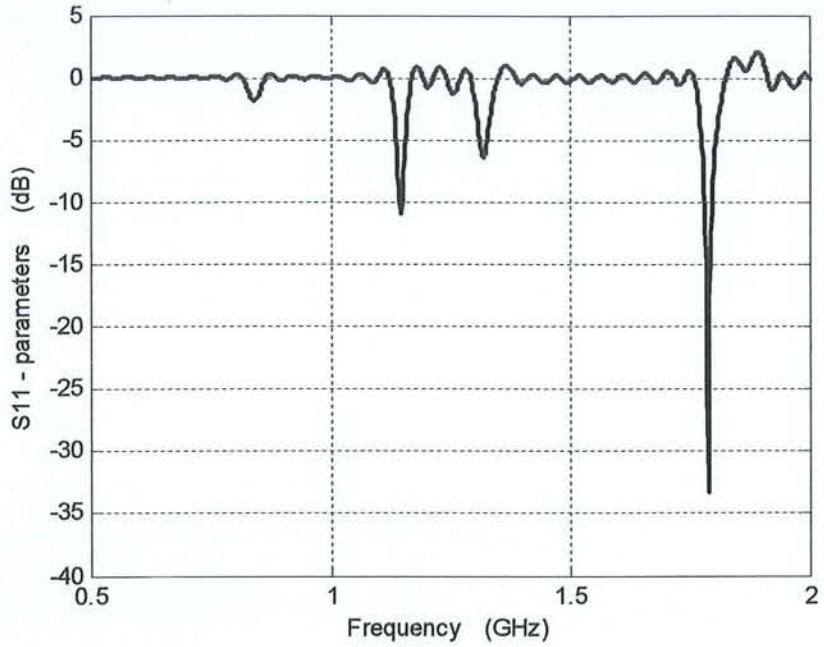

Figure 5.8: Design No. 2 S_{11} Parameter.

On the other hand, a different EBG structure as figure 5.9 shows is inserted on the ground plane of the basic structure that has both reference structure as well as the SRR maintaining the same dimensions of the structure and feeding point location. This structure found resonating with three resonance frequencies. One is at 0.79 GHz (with – 8.3 dB and bandwidth 27 MHz) and second is at 1 GHz (with – 6.4 dB and bandwidth 44 MHz) and the third one is at 1.9 GHz (with – 33.8 dB and bandwidth 33 MHz) as shown in figure 5.10.

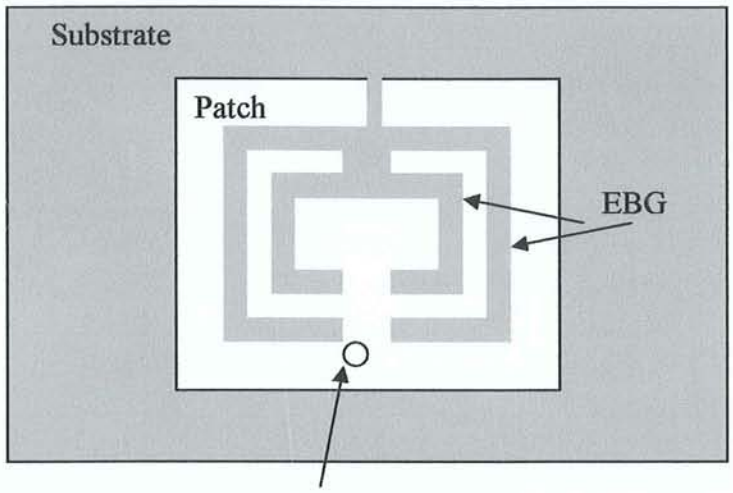

(a)

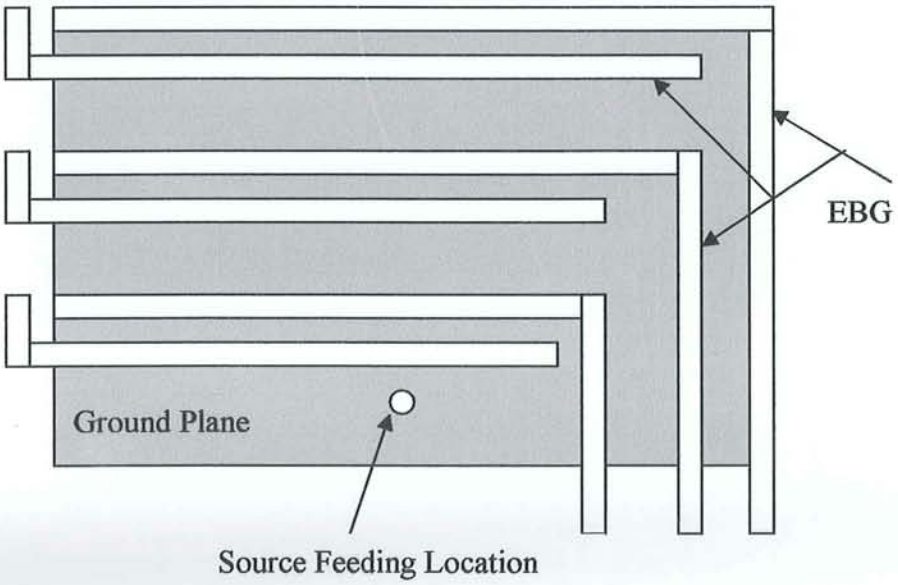

(b)

Figure 5.9: Design No. 3, Patch Antenna with EBG (a) Top View and (b) Bottom View

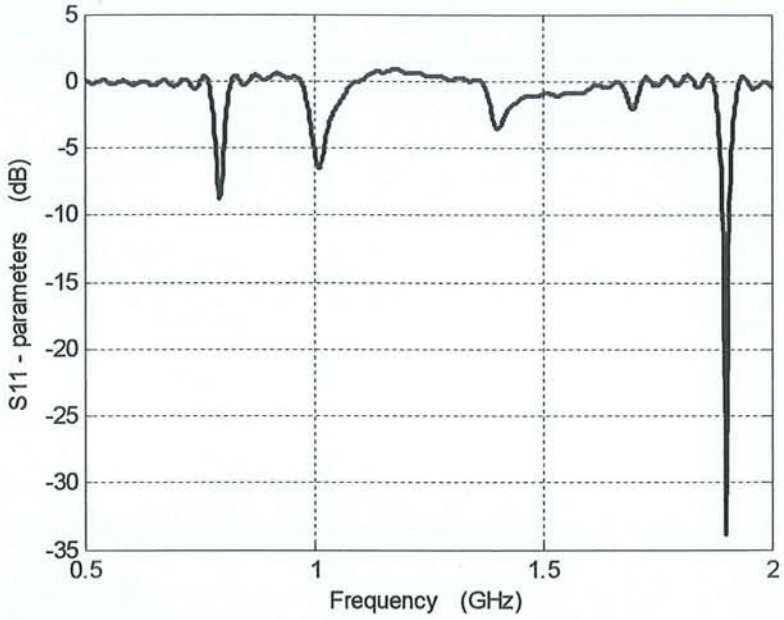

Figure 5.10: Design No. 3 S_{11} Parameter.

Figure 5.11 shows a basic structure with SRR but with different EBG configuration where six EBG slot or six lines were introduced on the ground plane. This structure is resonating with two resonance frequencies, one is at 1.15 GHz (- 11.9 dB and bandwidth 25 MHz) and second one is at 1.78 GHz (with - 36.2 dB and bandwidth 45 MHz) as shown in figure 5.12.

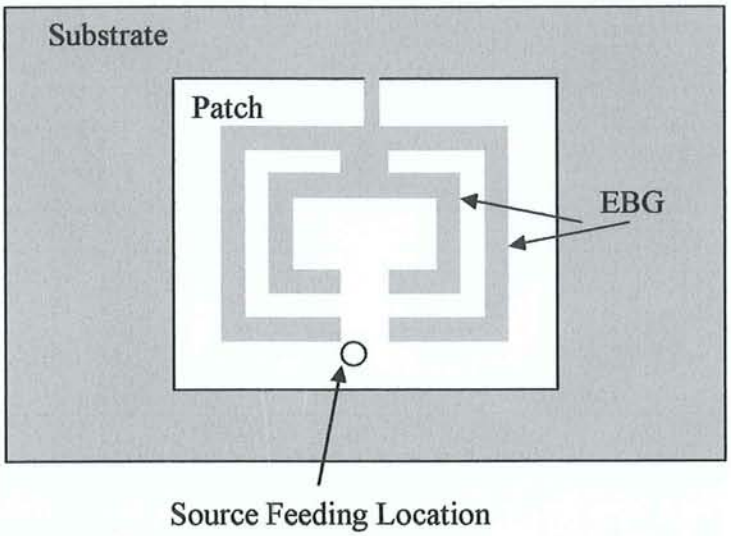

(a)

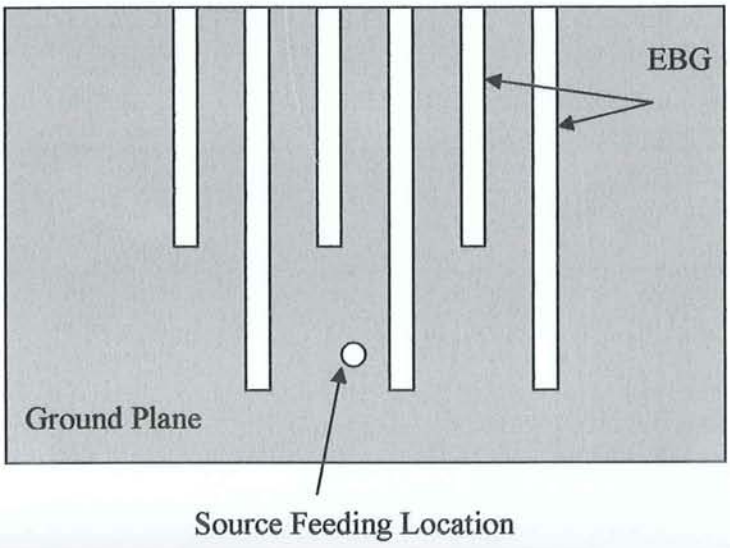

(b)

Figure 5.11: Design No.4, Patch Antenna with EBG (a) Top View and (b) Bottom View

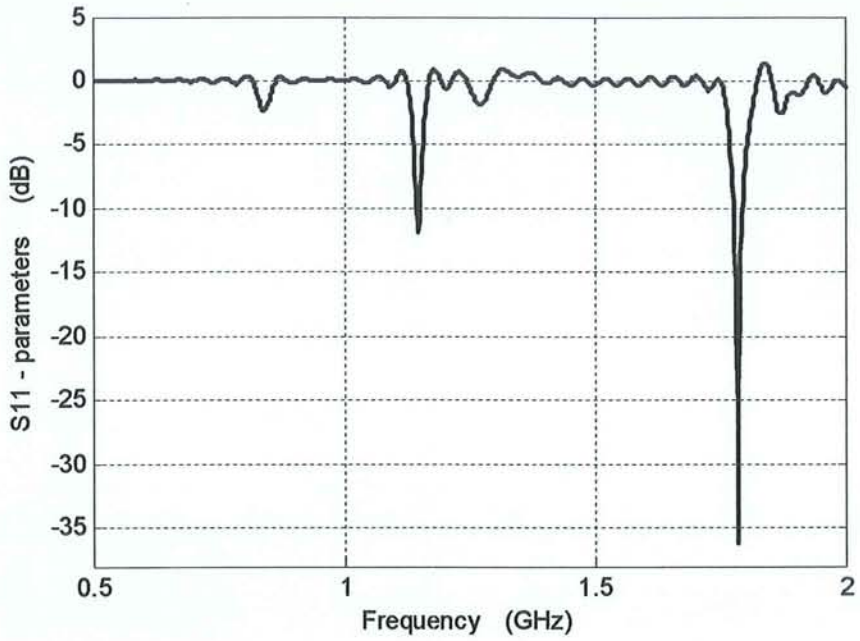

Figure 5.12: Design No. 4 S_{11} Parameter.

A different EBG structure consists of two parallel lines and connections with branches as in figure 5.13 was incorporated on the ground plane of reference structure having SRR and keeping dimensions of the structure and feeding point location unchanged. This structure will resonate with three resonance frequencies. One is at 0.69 GHz (with -24.9 dB and bandwidth 38 MHz) and second is at 1.56 GHz (with - 9.9 dB and bandwidth 27 MHz) and the third is at 1.84 GHz (with - 8.5 dB and bandwidth 33 MHz) as shown in figure 5.14.

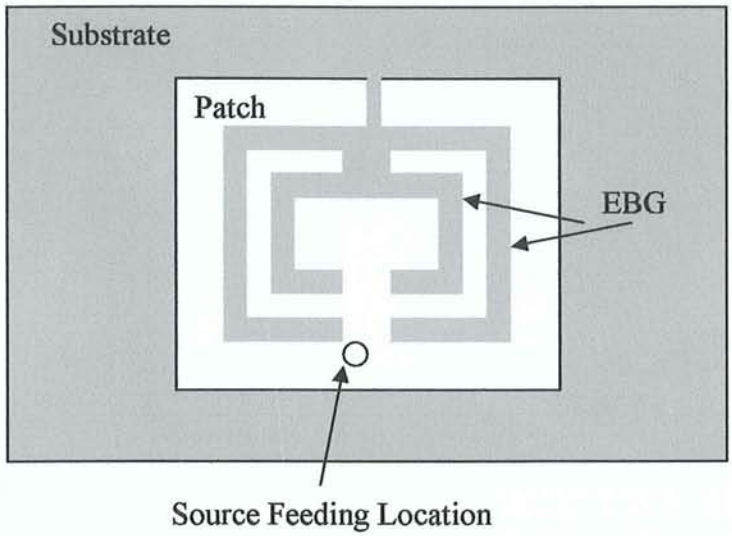

(a)

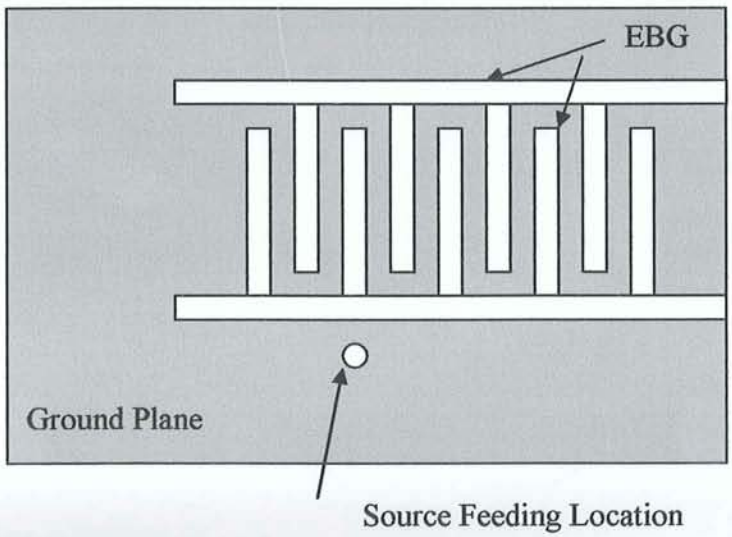

(b)

Figure 5.13: Design No.5, Patch Antenna with EBG (a) Top View and (b) Bottom View

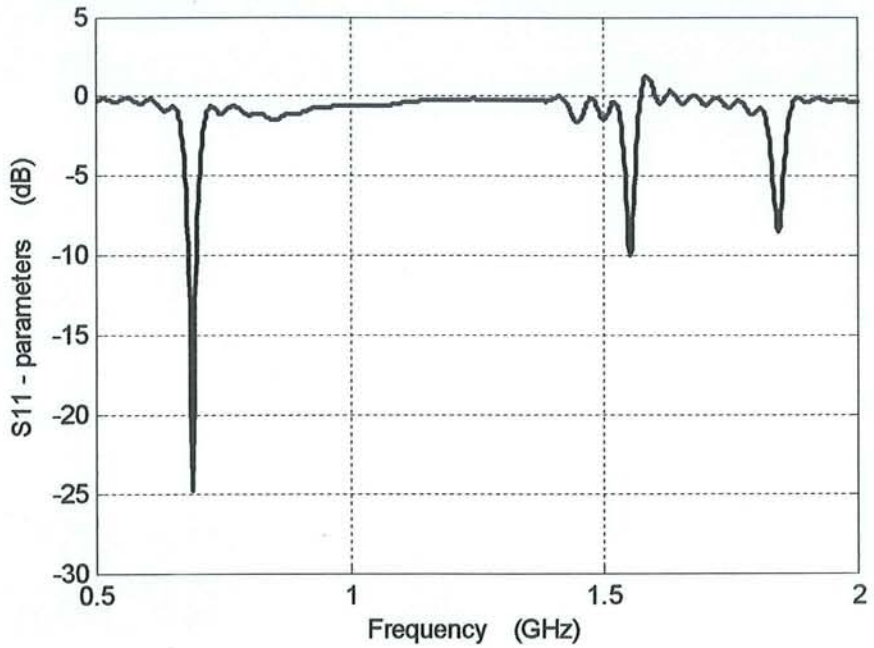

Figure 5.14: Design No. 5 S_{11} Parameter

The following table summarizes the previously mentioned five designs and list their features:

Table 5.1: A summary of the features of the five proposed designs.

Design No.	Resonance Frequencies (GHz) And Bandwidth (MHz)			Operating @
1	0.91 GHz (-15dB) bandwidth 24 MHz	1.86 GHz (-7 dB) bandwidth 1 MHz		0.9 GHz
2	1.15 GHz (-10.7 dB) bandwidth 20 MHz	1.32 GHz (-6.2 dB) bandwidth 30 35 MHz	1.79 GHz (-33 dB) bandwidth 40 MHz	1.15 GHz, 1.32 GHz and 1.79 GHz (multiple frequencies)
3	0.79 GHz (-10.7 dB) bandwidth 20 MHz	1.9 GHz (-33 dB) bandwidth 40 MHz		0.79 GHz and 1.9 GHz (dual frequency)
4	1.15 GHz (-11.9 dB) bandwidth 25 MHz	1.78 GHz (-36.2 dB) bandwidth 45 MHz		1.15 GHz and 1.78 GHz (dual frequency)
5	0.69 GHz (-24.9 dB) bandwidth 38 MHz	1.55 GHz (-9.9 dB) bandwidth 27 MHz	1.84 GHz (-8.5 dB) bandwidth 33 MHz	0.69 GHz, 1.55 GHz and 1.84 GHz (multiple frequencies)

5.2 EXPERIMENTAL RESULTS

At the beginning, the structure as in figure 5.1, that has substrate dimensions 40x49x1.58 mm and patch dimensions 29.25x38.35 mm and source that is fed into the patch on the one third and one half of the patch x and y dimensions respectively for all following cases was chosen as a reference. This structure resonates with three resonance frequencies. They are as follows. One is at 3.2 GHz (-7 dB and bandwidth 207 MHz), second is at 5 GHz (with -15 dB and bandwidth 314 MHz) and the third one at 6.3 GHz (with -19 dB and bandwidth 718 MHz) as figure 5.2 showed.

It was aimed to study deeply these five designs, choose one model design, and subject it for verification using network analyzer in the laboratory and get it compared with the theoretical data. The selection criteria were based on two factors. First factor is targeting for a design with a resonance frequency at 0.9 GHz and the second one is having a simple design to fabricate to reduce the source of error generated while fabrication as it will be done manually where error source might present. Design No. 1 has satisfied these two conditions as it is resonating at 0.915 GHz and when it is compared with other designs, considered as simplest structure to fabricate with a minimum possibility for a fabrication error. Therefore, design No. 1 as shown in figure 5.5 was chosen and subjected for an experimental for verification.

To re-call, this selected design, has theoretically two resonance frequencies one at 0.9 GHz (- 15 dB and bandwidth 24 MHz) and second at 1.9 GHz (with -7 dB and bandwidth 1 MHz) as it was shown in figure 5.6.

The laboratory simulations on the selected model were performed in three cascaded steps and experimental data were plotted at each step.

Step 1: Patch antenna was fabricated and made ready without inserting an EBG structure as illustrated in figure 5.15. It is noticed theoretically; that this structure has first resonance frequency at 3.6 GHz (with -7 dB) followed by another two-resonance frequency at 5.2 GHz (with -14 dB) and at 6.6 GHz (with -9.7 dB) as shown in figure 5.16.

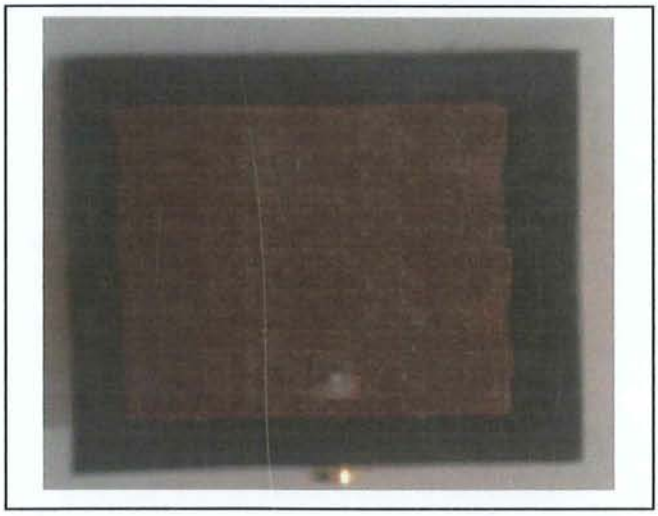

(a) Top view

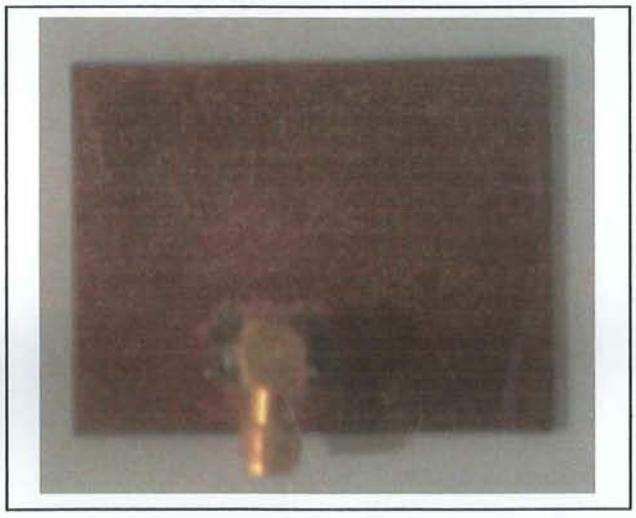

(b) Bottom view

Figure 5.15: Fabricated patch antenna before SRR and EBG etching (a) Top view and (b) Bottom view.

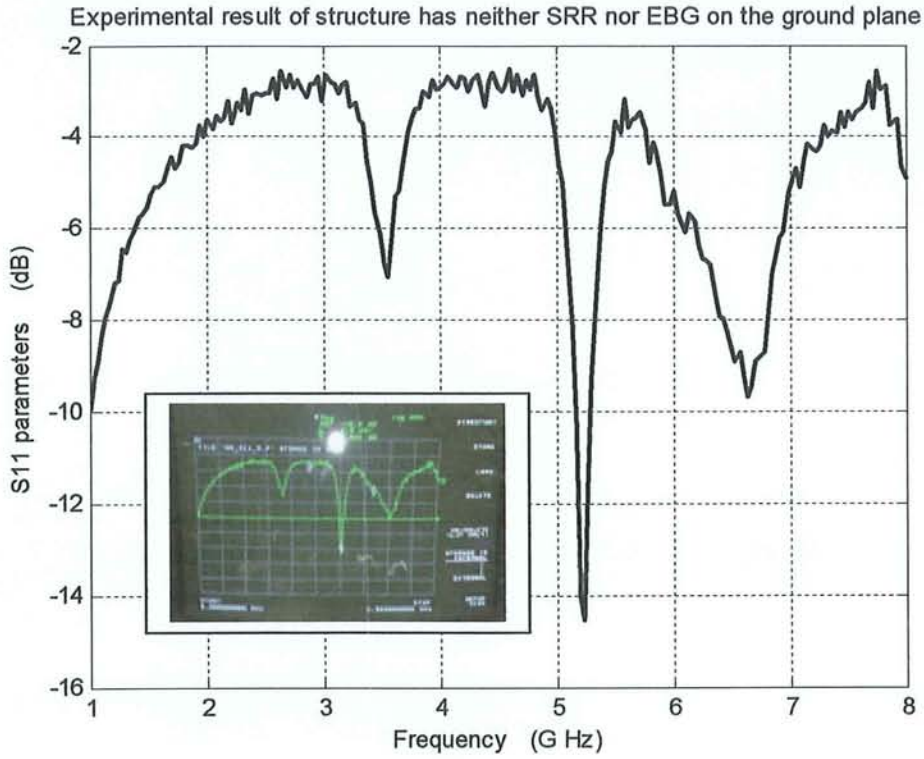

Figure 5.16: Experimental result of structure has neither SRR nor EBG on the ground plane

When the theoretical and experimental results are compared in this case, results were found almost in a good agreement as shown in figure 5.17.

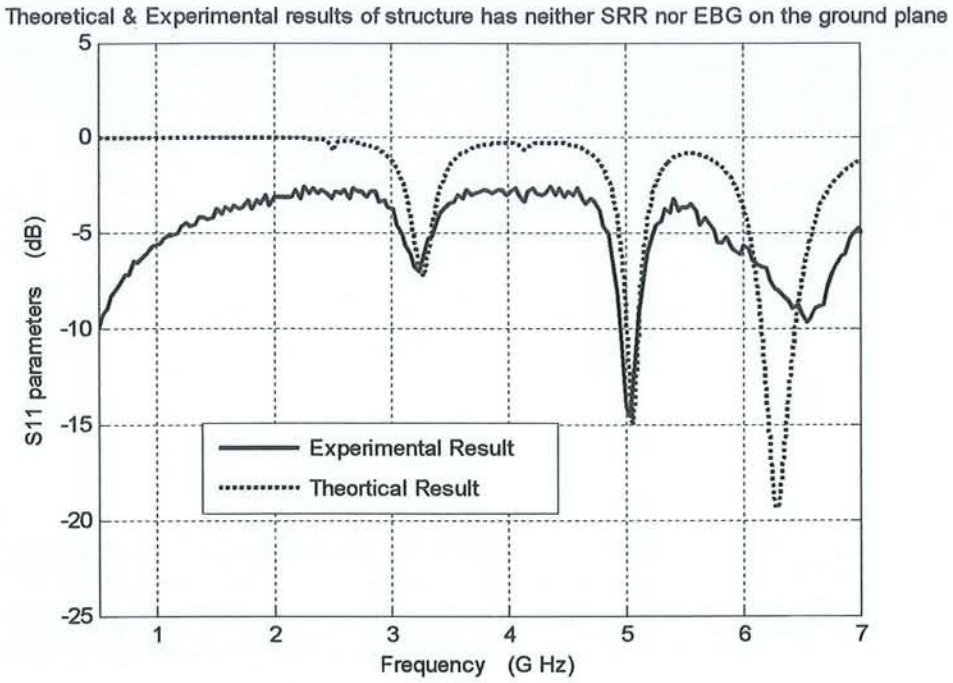

Figure 5.17: Theoretical & Experimental results of structure has neither SRR nor EBG on the ground plane.

Step 2: Same basic design or patch antenna reference structure was used in this step and SRR was inserted on the patch as illustrated in figure 5.18 and then the experiment was carried out. The structure was found resonating with two resonance frequencies, one at 2 GHz (-4.5 dB and bandwidth 150 MHz) and second at 2.6 GHz (with – 6 dB and bandwidth 150 MHz).

(a) Top view

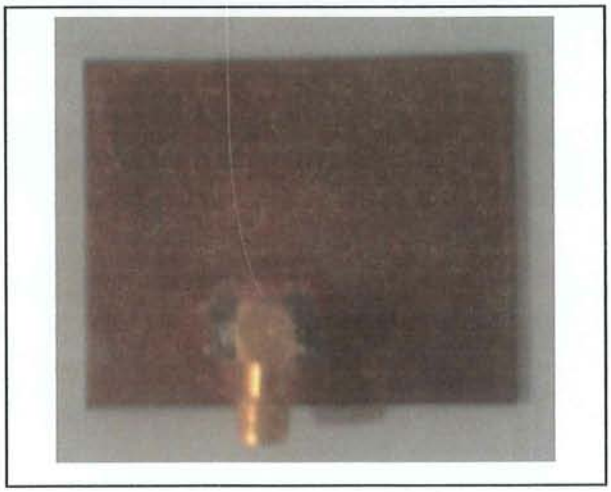

(b) Bottom view

Figure 5.18: Etched SRR only on the fabricated patch antenna without EBG on the ground plane (a) Top view and (b) Bottom view.

When the theoretical and experimental results are compared of a patch antenna that has only applied SRR on the patch, result are noticed matching at 1.6 G Hz resonance frequency as shown in figure 5.19.

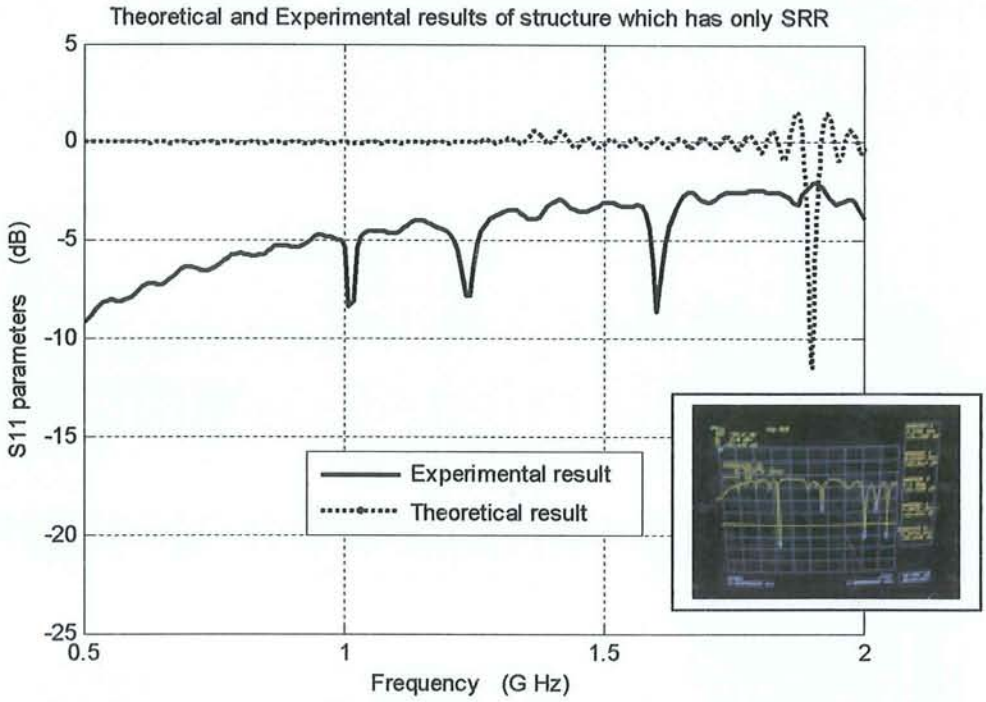

Figure 5.19: Theoretical & Experimental result of structure has only SRR.

On the other hand, structure resonating experimentally below 1.5 GHz with two resonance frequencies. This might be due to three factors. Firstly, fabrication error during EBG manufacturing and etching as manual method was used instead of Printed Circuit Board (PCB) machine that has been out of service before the experiment or due to network analyzer reliability because of over due calibration or insufficient experimental resolution because network analyzer frequency range was taken wide (from 0.5 GHz up to 8 GHz). Taking into account that, a study was made earlier on EBG case 5 set as a reference structure using 0.75 mm step size as it was shown in figure 4.42 and its S_{11} Parameter plot showed short resonance frequencies below 1 GHz do exist.

Step 3: After incorporating EBG on the patch antenna reference structure that has already SRR etched on the patch as well as EBG on the ground plane as shown in figure 5.20, the experiment was made.

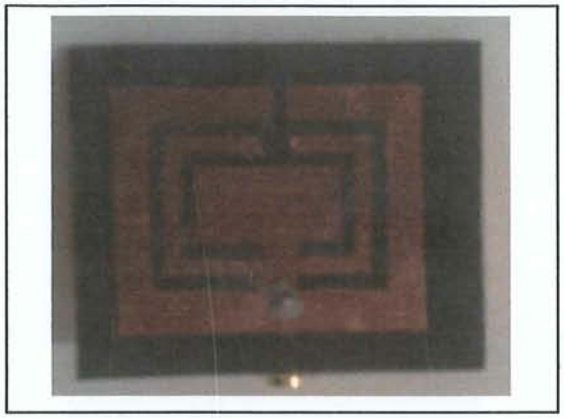

(a) Top view

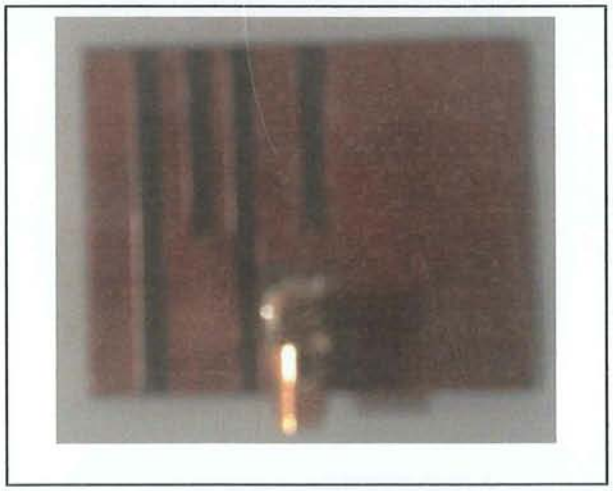

(b) Bottom view

Figure 5.20: Etched antenna with SRR and EBG on the ground plane (a) Top view and (b) Bottom view.

The theoretical and experimental results of EBG based-structure in this case was compared after plotting them as shown in figure 5.21.

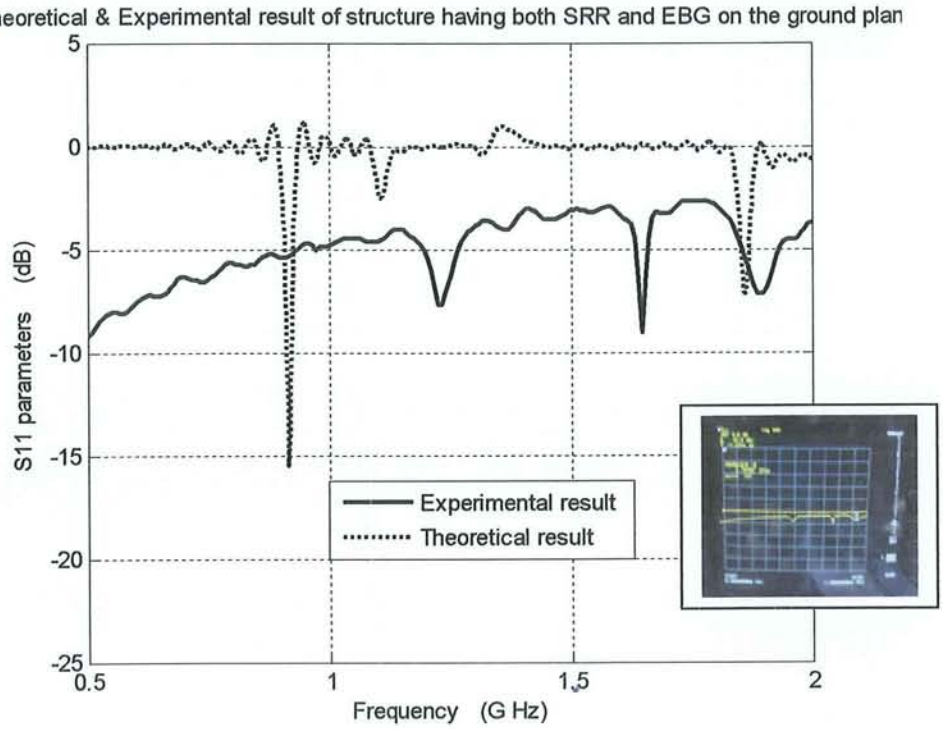

Figure 5.21: Theoretical & Experimental result of structure having both SRR as well as EBG on the ground plane.

This structure experimentally is observed resonating above 1 GHz and does not resonate below 1 GHz. This might be due to two factors as mentioned in the previous step (Step 2). Firstly, fabrication error during EBG manufacturing and etching as manual method was used instead of Printed Circuit Board (PCB) machine that has been out of service before the experiment or due to network analyzer reliability because of over due calibration or insufficient experimental resolution because network analyzer frequency range was taken wide (from 0.5 GHz up to 8 GHz).

To investigate the new proposed design radiation patterns before and after adopting SRR and EBG, the radiation patterns of azimuthal plane (H plane) and elevation plane (E plane) as shown in figure 5.22 and figure 5.23, were plotted. It

is observed that no loss in radiation pattern in the azimuthal plane (H plane) when the SRR and EBG on the ground plane are incorporated. Moreover, in radiation pattern elevation plane (E plane) does not have a null when SRR and EBG on the ground plane are etched.

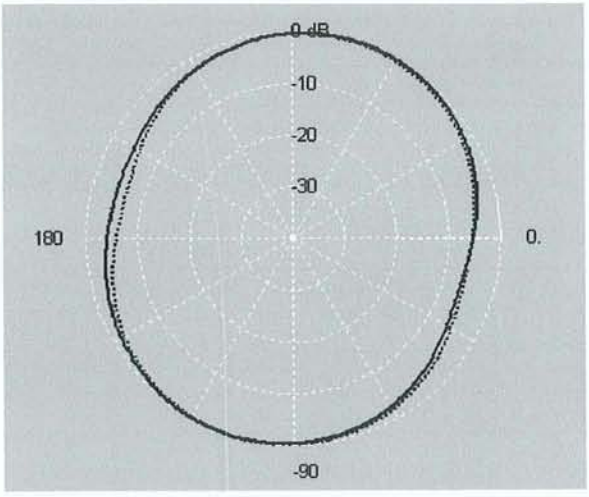

Figure 5.22: The Azimuthal radiation pattern (H plane) – Dashed line for structure without SRR and EBG on the ground plane while bold and continuous line is for the structure with SRR and EBG.

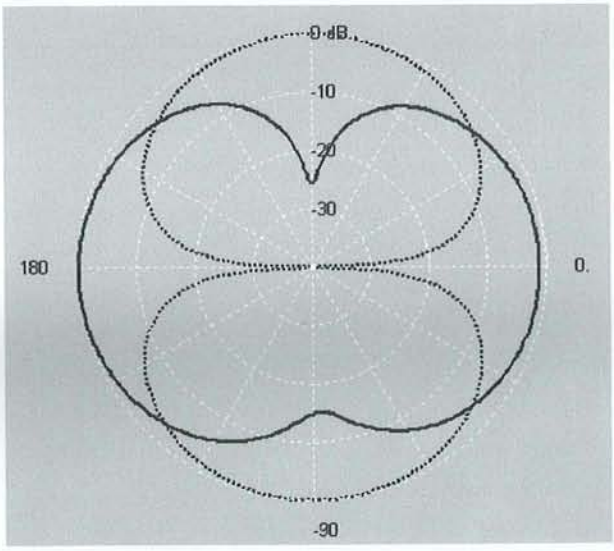

Figure 5.23: The elevation radiation pattern (E plane) – Dashed line for structure without SRR and EBG on the ground plane while bold and continuous line is for the structure with SRR and EBG.

CHAPTER 6

CONCLUSION AND FUTURE WORK

A summary and conclusion at the end of this work is given in this chapter followed by suggested future work.

6.1 SUMMARY AND CONCLUSION

In this thesis, we have studied application of Electromagnetic Band Gap (EBG) on the microstrip patch antenna; both on the ground plane and on the patch and we have briefly described their features. The work that has been completed in this thesis can be summarized as follows:

1. The full-wave theoretical model designing the EBG-based microstrip antennas for wireless communications problem has been formulated.
2. The simulation algorithm based on the FDTD methods has also been developed. The algorithm was equipped with the following a) PML absorbing boundaries b) visualization routines (in MATLAB).
3. The simulation results have verified the features of the novel designs of EBG-based microstrip antennas. It has been found, proper design of EBG concept on the ground plane and on the patch of the microstrip patch antenna has three merits. They are shifting the microstrip patch antenna resonance frequency to lower frequency range, having additional resonance frequencies or sharpen the structure resonance frequency.
4. One of the appreciated achievements of this thesis work is 94.99 cm^2 patch size reduction and consequently saving 89.44 % from patch area compared with the basic design. In addition to attaining a low profile, patch antenna that cost cheaper during fabrication.

5. One EBG-based antenna model was tested also experimentally to validate the theoretical results obtained using FDTD algorithm and comparison remarks were presented.

6.2 FUTURE WORK

The model developed in this thesis can be extended to the following:

1. Study and analyze the electromagnetic parameters such as radiation pattern, directivity and gain of the suggested designs of EBG-based low profile microstrip patch antenna and look for enhancement and improvement using High Impedance Surface (HIS) or other techniques.
2. Introducing a defect (or more defects) on the suggested periodic EBG-based models and evaluate it (their) effect.
3. Studying and analyzing EBG-based stacked microstrip patch or with multi-layers substrates having different relative dielectric.
4. Studying the coupling techniques for the proposed models of EBG-based low profile microstrip patch antenna.
5. The accuracy of the FDTD solution is expected to improve if a higher-order scheme is used. In this case, significant saving in computational time and memory can be achieved.
6. Proposing new structures that can apply EBG with ease of manufacturing.

REFERENCES

1. C. A. Balanis, Antenna Theory: Analysis and Design, John Wiley & Sins Inc., 2nd edition, pp.1-8, pp.28-100, pp.722-735, 1997.
2. D. Qu, L. Shafai and A. Foroozesh, "Improving Microstrip Patch Antenna performance Using EBG Substrate", IEE Pro-Microw. Antenna Propag.,Vol.153, No.6, pp. 558-563, December 2006.
3. Hsing-Yi Chen and Shu-Hsuan Chen, "Analysis of Characteristics of A U-Slot patch Antenna Using Finite-Difference Time Domain Method", Microwave and Optical Technology Letter, Vol. 48, No. 9, pp.1687-1694, September 2006.
4. O. Ayop, M.K.A Rahim, T.Masr, M.N.A Karim and M.Z.A. Abdual Aziz, "Modified Slotted Patch Electromagnetic Band Gap for Antenna Applications", Proceedings of Asia-Pacific Microwave Conference, pp. 1-4, 2007.
5. Hongmin Lee and Joong-kwan Kim, "Front-to-Back Ratio Improvement of a Microstrip Patch Antenna using an Isolated Soft Surface", Proceedings of the 39th European Microwave Conference, No.7, pp.385-388, 29 September ~ 1 October 2009.
6. K. Y. Hui and K. M.Luk, "Bandwidth of Small Dielectric Resonator Loaded Patch Antenna ", IEEE Transactions on antennas and propagation, Vol. 54, No. 6, pp.1882-1885, June 2006.
7. S.K. Palit, A. Hamadi and D. Tan, "Design of a wideband dual-frequency notched microstrip antenna", IEEE Antenna and propagation society international symposium, pp.2351-2354, 1998.
8. Annan Kaya and E.Yesim Yuksel, "Investigation of a Compensation Rectangular Microstrip Antenna With Negative Capacitor and Negative Inductor for Bandwidth Enhancement", IEEE Transaction on Antennas and Propagation,Vol. 55, No. 5, pp. 1275- 1282, May 2007.

9. Nabil Ghannay and Abdelaziz Samet, "E-Shaped Patch Antenna Modeling with MoM and RWG basis Functions", 16th IEEE electronic Circuits and Systems international conference, pp.199-202, 2009.
10. Hsing-Yi Chen and Shu-Hsuan Chen, "Analysis of Characteristics of A U-Slot patch Antenna Using Finite-Difference Time Domain Method", Microwave and Optical Technology Letter, Vol. 48, No.9, pp.1687-169,2006.
11. Hossein Mosallaei and Kamal Sarabandi, "A compact Wide-band EBG Structure Utilizing Embedded Resonant Circuits", IEEE Antenna and wireless propagation letters, Vol. 4, pp. 5-8, 2005.
12. Shao Ying HUANG, Yee Hui LEE, "A Small-Size Dual-Plane EBG Microstrip Lowpass Filter with a U-Shaped Microstrip Line Geometry", RFIT 2005- IEEE International Workshop on Radio-Frequency Integration Technology, Singapore, pp.195-197, Nov 30-Dec 02, 2005.
13. Yahya Rahmat-Samii, "Electromagnetic Band Gap (EBG) Structure in Antenna Engineering: From Fundamentals to Recent Advances", Microwave Asia Pacific conference APMC 2008, pp. 1-2, 2008.
14. N. Engheta and R. W. Ziolkowski, Metamaterials; Physics, Engineering, Explorations, IEEE Press Wiley Interscience, 2006.
15. Ning yian, Tat Soon Yeo, Xiao-Cun Nie and Le Eie Li, "A Fast Analysis of scattering and Radiation of Large Microstrip Arrays", IEEE Transaction on Antennas and Propagation, Vol. 51, No. 9, pp. 2218-2226, September 2003.
16. Mohammed S. Sharawi, and Daniel N. Aloi, "Design of Linearly Polarized Rectangular Patch Antenna Using MoM, FDTD and FEM", IEEE Antenna and propagation society international symposiums, pp.3916-3918, 2007.
17. Gordon Mayhew-Ridgers, Johann W. Odendaal, and Johan Joubert, "Entire-Domain Versus Subdomain Attachment Modes for the Spectral-Domain Method of Moment Analysis of Probe-Fed Microstrip Patch

Antennas", IEEE Transactions on Antennas and Propagation, Vol. 52, No. 6, pp 1616-1620, June 2004.

18. R. Alias, R. A. A. Ahammed, P.S. Excel, M. Z. Ismail, and A. H. Ali, "Dual Band Patch Antenna Design Using Modified Surface Boundary Hybird FEM-FDTD Technique, 2005 Asian-Pacific Conference on Applied Electromagnetic Proceedings ", pp. 21-25, December 20-21, 2005.
19. K.S. Yee, "Numerical Solution of Initial Boundary Value Problems Involving Maxwell's Equations in Isotropic Media," IEEE Transaction on antenna and propagation, Vol. AP-14, No.3, pp.302-307, May 1966.
20. Kurt L. Shlager and John B. Schneider, "A Selective Survey of the Finite-Difference Time-Domain Literature", IEEE Antennas and propagation Magazine, No. 4, pp. 39-56, Vol. 37,August 1995.
21. C.C. Chiau, X.Chen, C.G. Paini, "A Multi-Period EBG structure for Microstrip Antennas", IEEE Antenna and propagation twelfth international conference, pp.727-730, 2008.
22. T. Masri, M.K. A. Rahim, M.H. Jamaluddin and A. Asrokin , "Bandwidth Enhancement of a Narrow band Rectangular Microstrip Antenna on a Spiral Fan-Shape Electromagnetic Band-Gap (EBG) Patch Structure". 2006 International RF and Microwave Conference Proceedings, Putrajaya, Malaysia, pp. 225-227, September 12-14, 2006,
23. Osman Ayop, Mohammed Kamal A.Rahim and Thelaha Masri, " A Dual Band Gap Slotted Patch Electromagnetic Band Gap for Dual Band Microstrip Antenna", 2008 IEEE International RF and Microwave Conference Proceedings, Kuala Lumpur, Malaysia, pp. 322-325, December 2-4, 2008
24. X. Chen, C.H Liang, L. Liang and Z.J Su "A Low Profile Dual-Band Inverted L Antenna with Slotted Electromagnetic Band-Gap (EBG) Structures", IEEE International workshop on metamaterials, pp. 341-343, 2008.

25. Ang YU and Xuexia Zhang, "A Novel 2-D Electromagnetic Band-Gap Structure and its Application in Micro-strip Antenna Arrays", 3rd International Conference on Microwave and Millimeter Wave Technology Proceedings, pp.580-585, 2002.
26. Li Yang, Zhenghe Feng, Fanglu Chen and ingyan Fan, "A Novel Compact Electrometric Band-Gap (EBG) Structure and its Application in Microstrip Antenna Arrays", IEEE transactions on Microwave theory and techniques, pp.1635-1638, 2004.
27. Yan Wang, Jiawen Sun, and Zhenghe Feng, "Design of Suspended Patch Antenna with EBG Substrate", IEEE Microwave and Millimeter wave technology international conference, pp.1-3, 2007.
28. Rens Baggen, Marta Martinez-Vazquez, Jens LeiB and Sybille Holzwarth, "Comparison of EBG substrates with and without vias for GALILEO/GPS applications", , IEEE Antenna and propagation society international symposium, the second European conference, pp.1-5, 2007.
29. M. Fallah-Rad and L. Shafai, "Enhanced Performance of a Microstrip Patch Antenna Using a High Impedance EBG Structure", IEEE Antenna and propagation society international symposium, pp.982-985, 2003.
30. Sreedevi K Menon, B Lethakumary, C K Aanandan, K Vasudevan and P Mohanan, "A Novel EBG Structure Ground Plane for Microstrip Antennas", IEEE Antenna and propagation society international symposium, pp.578-581, 2005.
31. Kyungho Yoo, Raj Mittra and Nader Farahat, "A Novel Technique for Enhancing Directivity of Microstrip Patch Antennas Using an EBG Superstrate", IEEE Antenna and propagation society international symposium, pp.1-4, 2008.
32. Li Yang and Zhenghe Feng, "Advanced Methods to Improve Compactness in EBG Design and Utilization", IEEE Antenna and propagation society international symposium, pp.3585-3588, 2006.
33. Dan Sievenpiper, L. Zhang, R.F. Jimenez Broas, N. G. Alexopolous and E. Yablonovitch " High-Impedance Electromagnetic Surfaces with a

Forbidden Frequency Band", IEEE Transaction on Microwave Theory and Techniques, Vol. 47, No.11, pp. 2059-2074, November 1999.

34. Q. Wu, M.ing-Feng Wu, Fan-Yi Meng, Jian Wu, Le-Wei Li, "Modeling the Effect of an Individual SRR by Equivalent Circuit Method", An antenna and propagation society international symposium, pp 631-634, 2005.
35. Juan Baena, J. Bonache, F. Martin, R Sillero, F. Falcone, T. Lopetegi, M. Laso, J. Garcia-Garcia, I. Gill, M. Florers and M. Sorolla, "Equivalent-Circuit Models for Split-Ring Resonators and complementary Spilt-Ring Resonators Coupled to planar Transsioning Lines", IEEE Transactions on Microwave Theory and Techniques, Vol 33, No. 4, pp.1451-1497, 2005.
36. D. Mishra, G. Arun Kumar, D.R. Poddar and R.K. Mishra, "SRR and Patch Antenna", Proceedings of International Conference on Microwave, pp. 242-243, 2008.
37. C. Cheype, C. Serier, M. Thevenot, T. Monediere, A. Reineix and B. Jecko, "An Electromagnetic Bandgap Resonator Antenna", IEEE Transactions on Antenna and Propagation, Vol. 50, No. 9, pp, 1285-1290, September 2002.
38. Pirhadi, M. Hakkak, F. Keshmiri, R. Karimzadeh Baee, "Design of Compact Dual Band High Directive Electromagatic Bandgap (EBG) Resonator Antenna Using Artificial Magnetic Conductor", IEEE Transactions on antennas and propagation, Vol. 55, No. 6, pp. 1682-1690, June 2007.
39. L. Mustafa, M. Thevenot, T. Monediere and B. Jecko, "Design method of EBG material with wide defect band", IEEE Antenna and propagation EUCAP 2009, 3rd European conference, pp. 3235-3239, 2009.
40. Taflove A and M. E. Brodwin, "Numerical solution of steady-state electromagnetic scattering using time-dependent Maxwell's equations," IEEE Trans. Microwave Theory and Tech., Vol. 23, pp. 623-630, Aug. 1975.

41. J. P. Berenger, "Perfectly matched layers for the absorption of electromagnetic waves," Journal of Computational Physics, Vol.114, pp185-200, 1994.

42. H.AL-Mudhaffar, "Vectorial Analysis and Modeling of EM Wave Propagation in Second Order Nonlinear Optical Waveguide Structures", Thesis Master of Science in Electrical Engineering, KFUPM, May 2007.

43. B. Chen, D. G. Fang, and C. Gao, "The modified Berenger PML absorbing boundary condition for FD-TD meshes in anisotropic material,", Asia Pacific Microwave Conference, Hong Kong, pp. 257-260,1997.

Vitae

- Fahad Ahmed AL-Khuraish
- Born in Al-Kharj, South of Riyadh, Kingdom of Saudia Arabia Capital, on June 17th, 1977.
- Received Bachelor of Science (B.S) in Electrical Engineering from KING FAHD UNIVERSITY OF PETROLEUM & MINERALS in 2000.
- Joining Eastern Petrochemical Company, A Saudi Basic Industries Corporation (SABIC) affiliate in 2000 as maintenance and reliability instrument engineer and then plant operation superintendent until April 2010.
- Joining Saudia Arabian Mining Company (Ma'aden) in May 2010 as maintenance leader.
- Studying Master of Science (M.S) in Electrical Engineering as Part-time at KING FAHD UNIVERSITY OF PETROLEUM & MINERALS.
- Email: fahd239@gmail.com.